

For Reference

NOT TO BE TAKEN FROM THIS ROOM

Ex LIBRIS
UNIVERSITATIS
ALBERTAENSIS



THE UNIVERSITY OF ALBERTA

THE PREDICTION OF TRANSPORT PROCESSES OCCURRING
WITHIN UNCONSOLIDATED POROUS MEDIA

by



GRAHAM HENRY NEALE

A THESIS

SUBMITTED TO THE FACULTY OF GRADUATE STUDIES AND RESEARCH
IN PARTIAL FULFILMENT OF THE REQUIREMENTS FOR THE DEGREE
OF DOCTOR OF PHILOSOPHY

DEPARTMENT OF CHEMICAL AND PETROLEUM ENGINEERING

EDMONTON, ALBERTA

SPRING, 1972

Thesis
1972
451

UNIVERSITY OF ALBERTA

FACULTY OF GRADUATE STUDIES AND RESEARCH

The undersigned certify that they have read, and recommend to the Faculty of Graduate Studies and Research for acceptance, a thesis entitled "THE PREDICTION OF TRANSPORT PROCESSES OCCURRING WITHIN UNCONSOLIDATED POROUS MEDIA", submitted by GRAHAM HENRY NEALE, M.Sc., D.I.C., in partial fulfilment of the requirements for the degree of Doctor of Philosophy.

ABSTRACT

This work is aimed at developing a better theoretical understanding of the principal transport processes, namely diffusion and fluid flow, when occurring within unconsolidated porous media, in particular when occurring within an homogeneous swarm of spheres. The principal objective has been to develop an efficient geometric model to represent such a system, a model which can be employed to study diffusive *as well as* hydrodynamic flow processes when occurring therein.

The model proposed in this work satisfactorily fulfils the above specified objective; it permits a totally rigorous mathematical analysis of diffusive as well as hydrodynamic flow processes and it yields encouraging quantitative predictions in both instances. Moreover, this model may be extended to the study of transport processes occurring within a swarm of co-axially orientated spheroids. This extension has permitted an assessment of the important effects which particle shape and orientation can have in systems composed of non-spherical particles.

The solutions to some important, but hitherto unresolved, problems have incidentally been forthcoming in this work, of particular interest being the generalization of Stokes Law to the case of the *porous* sphere. In addition, an exact solution to the dual problem of creeping flow through a porous medium containing a spherical cavity has been effected.

ACKNOWLEDGEMENT

I remain indebted to Dr. Walter Nader for his continued interest, guidance and constructive suggestions whilst supervising this work.

I would like to extend thanks to Dr. R. A. Bentsen, Dr. F. A. Seyer, Dr. G. S. H. Lock and Dr. R. K. Wood for providing many useful suggestions whilst acting on the Thesis Committee, and to Dr. R. J. Nunge of Clarkson College of Technology, New York, for consenting to act in the capacity of External Examiner.

Respectfully acknowledged is Dr. H. C. Brinkman, whose invaluable foundation work concerning multi-particle systems inspired the author in this work.

Financial support from the National Research Council of Canada and the Pan Petroleum Corporation, which enabled this work to be completed, is gratefully acknowledged.

TABLE OF CONTENTS

<i>Abstract</i>	<i>page</i> i
<i>Acknowledgement</i>	ii
<i>List of Tables</i>	v
<i>List of Figures</i>	vi
<i>Nomenclature</i>	ix
 INTRODUCTION	 1
 THE PROPOSED MODEL FOR AN HOMOGENEOUS AND ISOTROPIC SWARM OF SPHERES	 5
 PART 1A: STEADY STATE DIFFUSION THROUGH AN HOMOGENEOUS AND ISOTROPIC SWARM OF SPHERES	 9
I.1 Objectives	10
I.2 The Defining Equations and Boundary Conditions	11
I.3 Solution of the Defining Equations	15
I.4 Discussion of Previous Work	26
I.5 Summary	31
 PART 1B: EXTENSION OF THE PROPOSED MODEL TO THE STUDY OF DIFFUSION WITHIN ANISOTROPIC UNCONSOLIDATED POROUS MEDIA	 32
I.6 Objectives	33
I.7 The Equations Governing Diffusion through Anisotropic Porous Media	34
I.8 Diffusion through an Homogeneous Swarm of Co-axially Orientated Oblate Spheroids	37
I.9 Diffusion through an Homogeneous Swarm of Co-axially Orientated Prolate Spheroids	42
I.10 Diffusion through a Swarm of Co-axially Orientated Spheroids at an Arbitrary Angle of Attack	47
I.11 Diffusion through an Homogeneous Swarm of Randomly Orientated Spheroids	48
I.12 Discussion of Previous Work	52

I.13	Summary	page 56
PART II:	STEADY STATE INCOMPRESSIBLE CREEPING FLOW THROUGH AN HOMOGENEOUS AND ISOTROPIC SWARM OF SPHERES	57
II.1	Objectives	58
II.2	The Equations Governing Incompressible Creeping Flow through Porous Media	59
II.3	The Modelled System for Fluid Flow through an Homogeneous Swarm of Spheres	64
II.4	The Defining Equations and Boundary Conditions	66
II.5	Solution of the Defining Equations	70
II.6	Discussion of Previous Work	82
II.7	The Effects of the Size Distribution	87
II.8	The Effects of the Reynolds Number	91
II.9	The Effects of Particle Porosity	93
II.10	The Effects of Particle Shape and Orientation	100
II.11	Summary	101
CONCLUSION		102
BIBLIOGRAPHY		104
APPENDIX A:	THE CALCULATION OF λ_x AND λ_y FOR CO-AXIALLY ORIENTATED OBLATE SPHEROIDS	108
APPENDIX B:	THE CALCULATION OF λ_x AND λ_y FOR CO-AXIALLY ORIENTATED PROLATE SPHEROIDS	124
APPENDIX C:	THE CALCULATION OF α AND W FOR AN HOMOGENEOUS SWARM OF SPHERES	128
APPENDIX D:	INCOMPRESSIBLE CREEPING FLOW THROUGH A FRACTURED POROUS MEDIUM	143
APPENDIX E:	INCOMPRESSIBLE CREEPING FLOW THROUGH AN ISOTROPIC POROUS MEDIUM CONTAINING A SPHERICAL CAVITY	154

LIST OF TABLES

TABLE 1.	EXPERIMENTAL CONDUCTIVITY FACTOR DATA FOR HOMOGENEOUS SWARMS OF SPHERES	<i>page</i> 23
TABLE 2.	PREDICTIONS FOR RANDOMLY ORIENTATED SPHEROIDS	52
TABLE 3.	THE PREDICTED DEPENDENCE OF α AND W ON ϵ FOR HOMOGENEOUS SWARMS OF MONOSIZED SPHERES	76
TABLE 4.	EXPERIMENTAL PERMEABILITY DATA FOR AN HOMOGENEOUS SWARM OF MONOSIZED SPHERES	79

LIST OF FIGURES

FIGURE 1.	AN HOMOGENEOUS AND ISOTROPIC SWARM OF SPHERES	<i>page</i> 7
FIGURE 2.	THE PROPOSED MODEL FOR AN HOMOGENEOUS AND ISOTROPIC SWARM OF SPHERES	8
FIGURE 3.	DESCRIPTION OF THE MODELLED SYSTEM FOR DIFFUSION THROUGH AN HOMOGENEOUS SWARM OF SPHERES	12
FIGURE 4.	THE PROPOSED MODEL FOR AN HOMOGENEOUS SWARM OF POROUS SPHERES	19
FIGURE 5.	EQUIPMENT USED FOR THE EXPERIMENTAL DETERMINATION OF THE CONDUCTIVITY FACTOR OF A PACK OF SPHERES	24
FIGURE 6.	THE PREDICTED DEPENDENCE OF λ ON ϵ FOR SPHERES: COMPARISON WITH EXPERIMENTAL DATA	25
FIGURE 7.	THE DEPENDENCE OF λ ON ϵ FOR SPHERES: COMPARISON WITH PREVIOUS WORK	30
FIGURE 8.	AN HOMOGENEOUS SWARM OF CO-AXIALLY ORIENTATED OBLATE SPHEROIDS	38
FIGURE 9.	THE PREDICTED DEPENDENCE OF λ_x AND λ_y ON ϵ FOR CO-AXIALLY ORIENTATED OBLATE SPHEROIDS	40
FIGURE 10.	AN HOMOGENEOUS SWARM OF CO-AXIALLY ORIENTATED PROLATE SPHEROIDS	43
FIGURE 11.	THE PREDICTED DEPENDENCE OF λ_x AND λ_y ON ϵ FOR CO-AXIALLY ORIENTATED PROLATE SPHEROIDS	45
FIGURE 12.	THE PREDICTED DEPENDENCE OF λ_Σ ON ϵ FOR RANDOMLY ORIENTATED OBLATE SPHEROIDS	49

FIGURE 13.	THE PREDICTED DEPENDENCE OF λ_{Σ} ON ϵ FOR RANDOMLY ORIENTATED PROLATE SPHEROIDS	<i>page</i> 50
FIGURE 14.	THE PREDICTED RESULTS FOR RANDOMLY ORIENTATED PROLATE SPHEROIDS: COMPARISON WITH EXPERIMENTAL DATA	55
FIGURE 15.	AN IDEALIZED TWO-REGION SYSTEM	60
FIGURE 16.	DESCRIPTION OF THE MODELLED SYSTEM FOR FLUID FLOW THROUGH AN HOMOGENEOUS SWARM OF SPHERES	65
FIGURE 17.	TYPICAL STREAMLINES FOR INCOMPRESSIBLE CREEPING FLOW THROUGH THE MODELLED SYSTEM	72
FIGURE 18.	EQUIPMENT USED FOR THE EXPERIMENTAL DETERMINATION OF THE PERMEABILITY OF A PACK OF SPHERES	80
FIGURE 19.	THE PREDICTED DEPENDENCE OF α ON ϵ FOR MONOSIZED SPHERES: COMPARISON WITH EXPERIMENTAL DATA	81
FIGURE 20.	THE DEPENDENCE OF W ON ϵ FOR MONOSIZED SPHERES: COMPARISON WITH PREVIOUS WORK	86
FIGURE 21.	THE EFFECTS OF THE SIZE DISTRIBUTION IN BINARY MIXTURES OF SPHERES (SIZE RATIO 5:1)	89
FIGURE 22.	THE EFFECTS OF THE SIZE DISTRIBUTION IN BINARY MIXTURES OF SPHERES (SIZE RATIO 2:1)	90
FIGURE 23.	THE DEPENDENCE OF α ON THE REYNOLDS NUMBER FOR MONOSIZED SPHERES: EXPERIMENTAL DATA	92
FIGURE 24.	THE GENERALIZED FORM OF STOKES LAW FOR A POROUS SPHERE	96
FIGURE 25.	TYPICAL STREAMLINES FOR INCOMPRESSIBLE CREEPING FLOW THROUGH AN ISOLATED POROUS SPHERE	99

FIGURE 26.	OBLATE SPHEROIDAL COORDINATES IN A MERIDIAN PLANE	<i>page</i> 110
FIGURE 27.	THE PROPOSED MODEL FOR AN HOMOGENEOUS SWARM OF CO-AXIALLY ORIENTATED OBLATE SPHEROIDS	114
FIGURE 28.	AN IDEALIZED FRACTURE WITHIN A PETROLEUM RESERVOIR	145
FIGURE 29.	THE APPROXIMATE AND RIGOROUS VELOCITY PROFILES FOR THE FRACTURED SYSTEM	152
FIGURE 30.	TYPICAL STREAMLINES FOR INCOMPRESSIBLE CREEPING FLOW THROUGH AN ISOTROPIC POROUS MEDIUM CONTAINING AN ISOLATED SPHERICAL CAVITY	160

NOMENCLATURE

I. SYMBOLS PERTAINING TO DIFFUSIVE FLOW PROCESSES

c	concentration of diffusing species
D	diffusivity of diffusing species
e	eccentricity of spheroid
K	specific conductivity
q	diffusive flux
Q	mainstream diffusive flux
R	radius of sphere
S	radius of unit (model) cell
$[x,y,z]$	Cartesian coordinates
$[r,\theta,\phi]$	spherical coordinates
$[\xi,\eta,\phi]$	spheroidal coordinates

Greek Symbols

ϵ	porosity of porous medium
τ	tortuosity of pore space
λ	diffusivity (conductivity) factor
∇	del (gradient) operator
∇^2	Laplacian operator

Subscripts

$\underline{\quad}$	designates vectorial quantities
$\underline{\underline{\quad}}$	designates tensorial quantities
Σ	designates randomly orientated spheroids
s	designates spheres which are porous

Superscript

$*$	designates macroscopically averaged quantities pertaining specifically to a porous medium
-----	--

II. SYMBOLS PERTAINING TO HYDRODYNAMIC FLOW PROCESSES

F	hydrodynamic resistance force
N	number of spheres within a swarm
p	pressure referred to a datum plane
R	radius of sphere
S	radius of unit (model) cell
u	velocity of flowing fluid
U	mainstream velocity
W	factor by which the resistance of a swarm of spheres differs from that predicted by Stokes Law
[x,y,z]	Cartesian coordinates
[r,θ,φ]	spherical coordinates
E^2	spherical harmonic operator

Greek Symbols

α	normalized radius of reference sphere, $R/\sqrt{\kappa}$
β	normalized radius of unit cell, $S/\sqrt{\kappa}$
ϵ	porosity of porous medium
κ	permeability of porous medium
μ	viscosity of fluid
ρ	density of fluid
ψ	streamfunction
τ	tangential shear stress
χ	normalized radial coordinate, $r/\sqrt{\kappa}$
ν	normalized radius of porous sphere, $R/\sqrt{\kappa}$
∇	del (gradient) operator
∇^2	Laplacian operator

Subscript

— designates vectorial quantities

Superscript

* designates macroscopically averaged quantities pertaining specifically to a porous medium

INTRODUCTION

Broadly speaking, the principal transport processes occurring within porous media may be classified as follows:

Molecular Transport	}	Diffusive Flow Processes
Ionic Transport		
Charge Transport		
Thermal Transport		
Momentum Transport	}	Hydrodynamic Flow Processes

The principal difference between these two major categories is that whilst diffusive flow processes are generally described by the Diffusion Equation (in the steady state by Laplace's Equation), hydrodynamic flow processes are governed by the Navier-Stokes Equation.

In engineering practice these fundamental transport processes often occur simultaneously. For example, the process of liquid evaporation within a porous medium would encompass molecular transport, thermal transport and momentum transport. However, in order to be able to make meaningful predictions concerning such complicated phenomena a fuller understanding must firstly be developed of the fundamental transport processes when occurring individually within porous media.

An appreciation of diffusive and hydrodynamic flow processes occurring within porous media (such as catalyst beds, sand beds, column packings, etc.) is of considerable importance in many fields of engineering. For example, in design work a prior knowledge of the permeability of various porous media is a great asset. Equally important is a knowledge of the effective diffusivity of molecules or ions diffusing through a porous medium, as well as a knowledge of the

specific conductivity of the medium when saturated with a conducting fluid.

It is well known that the accurate measurement of absolute diffusivities is excessively difficult on account of the inevitable presence of interfering convection. However, measurements of the effective diffusivity within a porous medium (for example, a randomly packed bed of spheres) are usually simpler to execute since convection effects can be arbitrarily reduced by a judicious choice of particle size. A knowledge of the relationship between this effective diffusivity and the absolute diffusivity in unobstructed space therefore permits an indirect determination of this latter quantity.

However, transport processes occurring within porous media rank amongst the most complex phenomena encountered in engineering practice. This is because the internal geometry of most porous media is not sufficiently well understood to afford more than a loose statistical description. Exact analytical studies are, therefore, usually out of the question and a mathematical model must be developed to predict, and to yield physical insight into, such phenomena. That is, certain approximations regarding the internal geometry must be introduced such that a mathematical solution can be effected.

Several models have been proposed and presented in the literature to study specific transport processes occurring within specific porous media. However, there does not appear to be available at present any one model which can be used to predict successfully diffusive as well as hydrodynamic flow processes within even the simplest homogeneous and isotropic medium, viz. within a randomly packed bed of spheres.

This is disappointing because such models are introduced only to simplify the complex pore structure of the medium in question and, *ideally*, their overall success should not depend on which particular transport process is being studied. The specific system of an homogeneous and isotropic swarm of spheres is of particular interest because many porous media, particularly those of a granular nature, may be well approximated thereby and such systems can be readily prepared in the laboratory for experimental investigation; moreover, such a system can be defined by a minimum of parameters, viz. the porosity and the particle size distribution.

A considerable number of models aimed at predicting transport processes within porous media have been based on reasonably well developed theories for these processes when occurring in capillaries. However, all such capillary models are inherently anisotropic in constitution and without exception their final predictions incorporate at least one adjustable parameter which must be determined by experiment. In this sense, therefore, approaches based on the capillary model can only be partially predictive and can often be misleading. Moreover, such models are not productive in the study of diffusive processes. On account of the extreme geometric simplifications inherent in the capillary model this representation requires but a minimum of mathematical sophistication during its application. In contrast, the model proposed later in this work will contain significantly fewer simplifications; this will necessarily lead to far more complicated mathematics.

The principal objective of this analysis is to develop an improved generalized model for an homogeneous and isotropic swarm of spheres

which can be used to predict successfully diffusive as well as hydrodynamic flow processes occurring therein. A secondary objective will be to extend this model to the study of anisotropic systems composed of non-spherical particles.

THE PROPOSED MODEL FOR AN HOMOGENEOUS AND ISOTROPIC SWARM OF SPHERES

Figure 1 depicts an unbounded, homogeneous and isotropic swarm of solid spheres possessing a porosity ϵ and an arbitrary size distribution. Choosing any *reference sphere* (of radius R) within the swarm it is postulated that this sphere, together with its associated pore space (here approximated by a concentric annulus having an outer radius S) sees the remainder of the system as an homogeneous and isotropic porous mass of porosity ϵ ; this is illustrated in Figure 2.

In other words the portion of the complicated pore space fairly attributable to our reference sphere has been replaced by a uniform annulus, the outer radius of which must be specified such that the porosity of the *unit cell* (comprising the reference sphere and its associated annulus) is identical to that prevailing throughout the original system. This necessitates that

$$S/R = (1-\epsilon)^{-1/3} \qquad 0 \leq \epsilon < 1.0 \quad . \qquad (1)$$

This relation ensures that the uniform porosity ϵ is not locally disturbed by the modelling procedure. An inherent advantage of the proposed model is that the macroscopically homogeneous and isotropic characteristics of the original system remain unchanged, i.e. the modelled system is indistinguishable from the original system when viewed from the outside.

To summarize then, the modelled system consists of our reference sphere and two adjoining concentric regions, viz. an *annular region* of void space and an *exterior region* of homogeneous and isotropic porous

material. In essence, the technique of solution will be to solve the differential equations which describe the transport process of interest within each of these regions and to properly connect these solutions at the interface between them. It is important to note that subsequent to the above indicated modelling of the porous medium the mathematical developments for both diffusion and fluid flow are rigorous in their entirety.

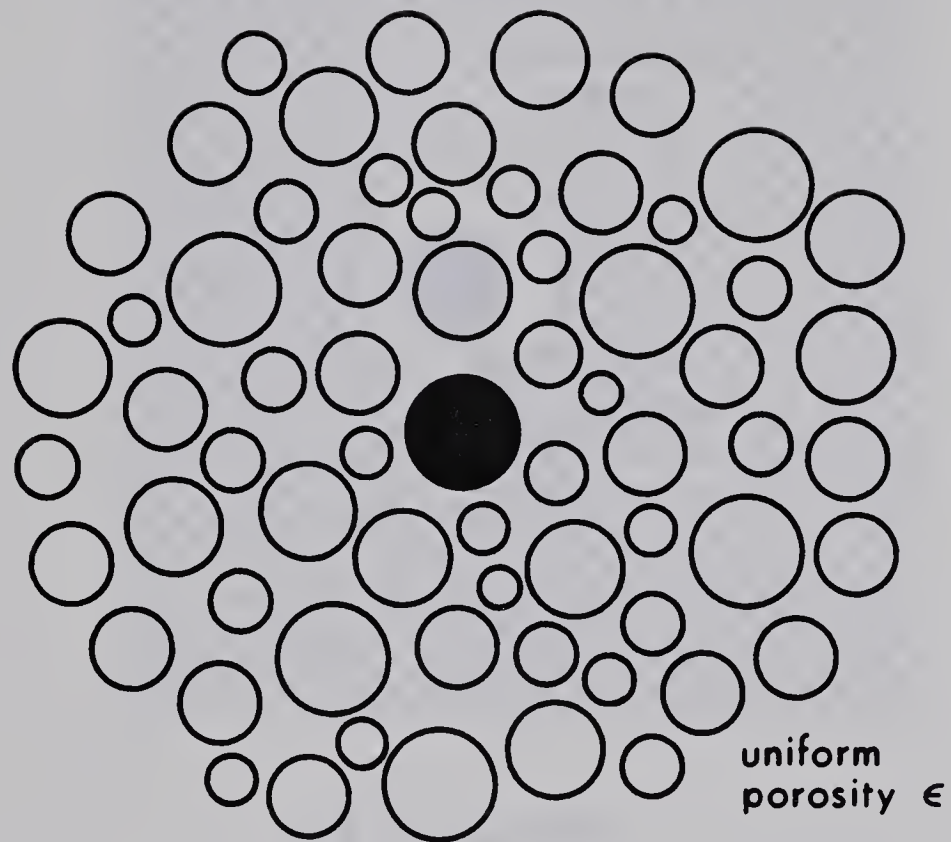
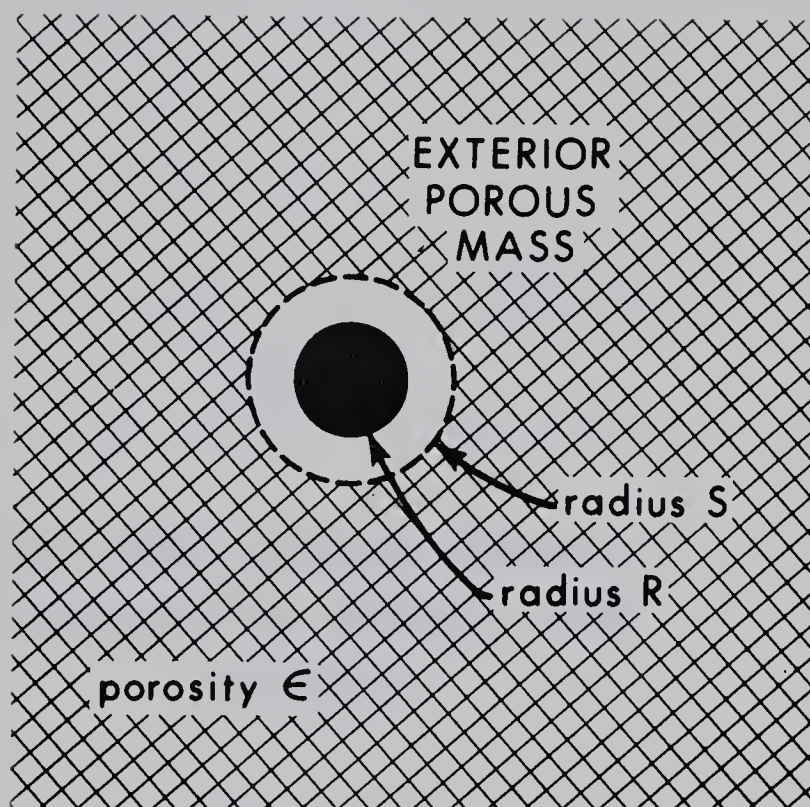


FIGURE 1. AN HOMOGENEOUS AND ISOTROPIC SWARM
OF SPHERES
(Cross-Section Through Centre of
Reference Sphere)



$$\frac{S}{R} = (1 - \epsilon)^{-1/3}$$

FIGURE 2. THE PROPOSED MODEL FOR AN HOMOGENEOUS AND ISOTROPIC SWARM OF SPHERES (Cross-Section Through Centre of Reference Sphere)

PART IA

STEADY STATE DIFFUSION THROUGH AN
HOMOGENEOUS AND ISOTROPIC SWARM
OF SPHERES

I.1 OBJECTIVES

The purpose of the following analysis is to develop a fuller understanding of diffusion taking place within an homogeneous and isotropic porous medium composed of spherical particles possessing an arbitrary size distribution; in particular to predict the *diffusivity factor*, λ , which is defined to be:

$$\lambda = \frac{\text{Effective diffusivity within porous medium}}{\text{Absolute diffusivity in unobstructed space}} = \frac{D^*}{D} . \quad (2)$$

This will be accomplished forthwith by application of the proposed cell model.

I.2 THE DEFINING EQUATIONS AND BOUNDARY CONDITIONS

I.2.1 FUNDAMENTAL DIFFERENTIAL EQUATIONS

The modelled system for diffusion through an homogeneous swarm of spheres is depicted in Figure 3. The validity of Fick's Law of diffusion² within the annular region of this system will be acknowledged, viz.

$$\underline{q} = -D \underline{\nabla} c \quad R < r < S . \quad (3)$$

Furthermore, Fick's Law in its *macroscopic* form^{2,27} will be postulated as a description of conditions within the exterior region, viz.

$$\underline{q}^* = -D^* \underline{\nabla} c^* \quad S < r < \infty . \quad (4)$$

The symbol * will be employed throughout this study to designate macroscopically averaged quantities pertaining specifically to a porous medium.

In the steady state there can prevail no net build-up of the diffusing material; this implies that

$$\underline{\nabla} \cdot \underline{q} = 0 , \quad (5)$$

$$\underline{\nabla} \cdot \underline{q}^* = 0 . \quad (6)$$

Since D and D* are independent of location, the application of these continuity conditions to Equations (3) and (4) yields:

$$\text{annular region:} \quad \nabla^2 c = 0 \quad R < r < S , \quad (7)$$

$$\text{exterior region:} \quad \nabla^2 c^* = 0 \quad S < r < \infty . \quad (8)$$

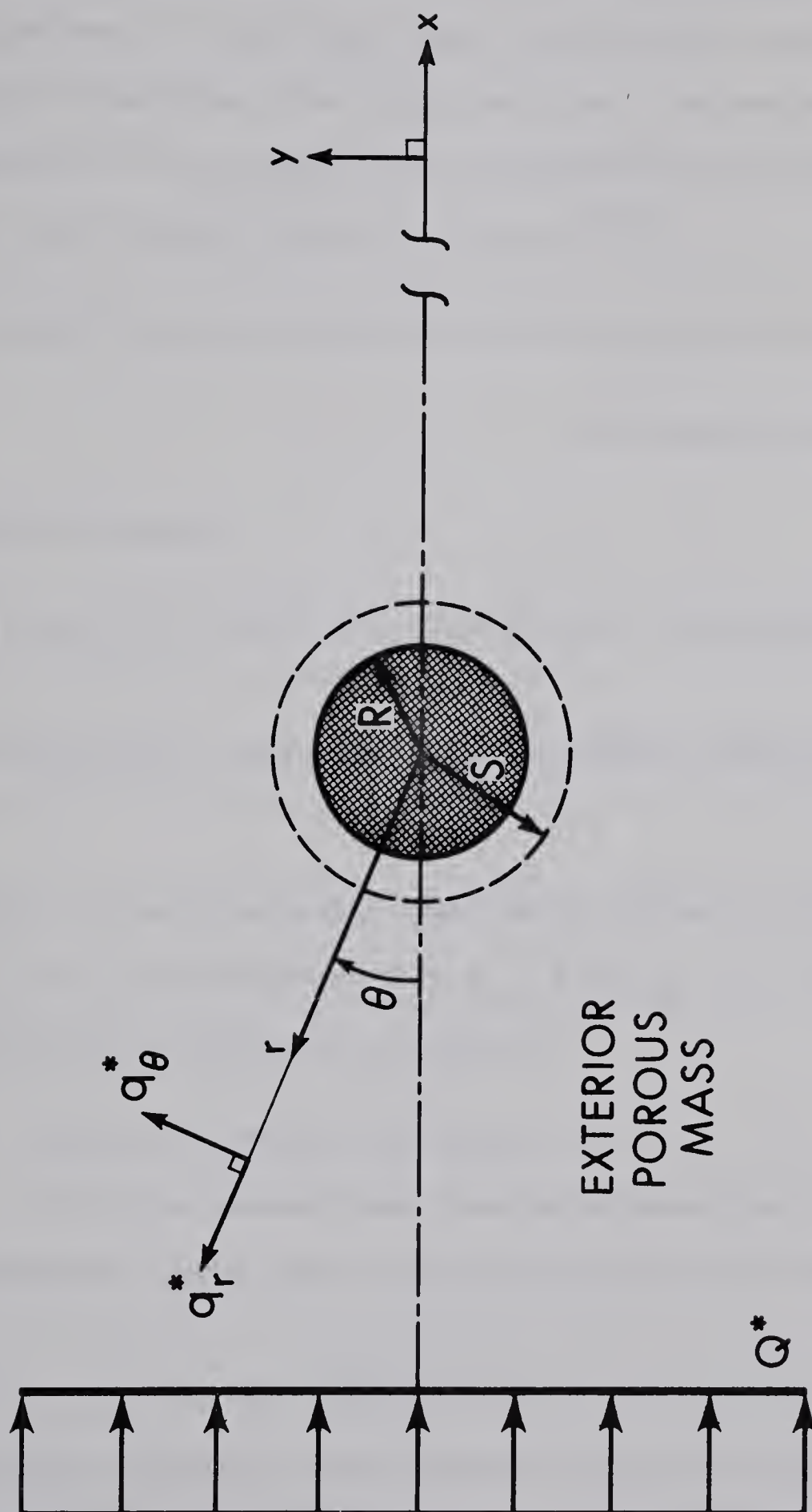


FIGURE 3. DESCRIPTION OF THE MODELLED SYSTEM FOR DIFFUSION THROUGH AN HOMOGENEOUS SWARM OF SPHERES (Cross-Section Through Centre of Reference Sphere)

In order to determine the global concentration distribution, solutions of Equations (7) and (8) are sought which satisfy physically rational boundary conditions to be stipulated later. The system of coordinates convenient to this analysis will be spherical coordinates $[r, \theta, \phi]$, in which the Laplacian operator is given by^{2,22}:

$$\nabla^2 \equiv (\partial^2/\partial r^2) + (2/r)(\partial/\partial r) + (1/r^2)(\partial^2/\partial \theta^2) + (\cot \theta/r^2)(\partial/\partial \theta) + (1/r^2 \sin^2 \theta)(\partial^2/\partial \phi^2) , \quad (9)$$

and Fick's Laws by:

$$\underline{q} = [q_r, q_\theta, q_\phi] = [-D(\partial c/\partial r), -D(1/r)(\partial c/\partial \theta), -D(1/r \sin \theta)(\partial c/\partial \phi)] , \quad (10)$$

$$\underline{q}^* = [q_r^*, q_\theta^*, q_\phi^*] = [-D^*(\partial c^*/\partial r), -D^*(1/r)(\partial c^*/\partial \theta), -D^*(1/r \sin \theta)(\partial c^*/\partial \phi)] . \quad (11)$$

However, for macroscopically rectilinear diffusion in the x-direction there is no ϕ -dependence so that $q_\phi = 0$ and $q_\phi^* = 0$. Consequently the ϕ variable may hereafter be suppressed.

I.2.2 STIPULATED BOUNDARY CONDITIONS

It will be assumed that there is no deposition of material on the reference sphere and no dissolution thereof; this implies that

$$q_r(R^+, \theta) = 0 . \quad (12)$$

From considerations of equilibrium and continuity at the interface separating the annular and exterior regions it is necessary that the concentration and radial flux distributions within these regions match

identically in the limit, viz.

$$c(S^-, \theta) = c^*(S^+, \theta) , \quad (13)$$

$$q_r(S^-, \theta) = q_r^*(S^+, \theta) . \quad (14)$$

Moreover, the flux vector at any station far removed from the reference sphere must approach that of the mainstream, $\underline{Q^*}$, viz.

$$\lim_{r \rightarrow \infty} q^*(r, \theta) = \underline{Q^*} , \quad (15)$$

where $\underline{Q^*} = [Q^*, 0, 0]$ in Cartesian coordinates $[x, y, z]$.

It is not possible to stipulate any boundary conditions concerning q_θ and q_θ^* (the tangential components of the flux vectors) owing to the poorly understood phenomenon of surface diffusion, that is the migration of molecules or ions over the solid surfaces^{9,27}. It is certainly dangerous to write $q_\theta(R, \theta) = 0$ by direct analogy with the viscous flow problem because *viscous flow* is a relative motion of the adjacent elements of a fluid whereas *diffusive flow* is a relative motion of its several constituents.

However, it transpires that Equations (12) - (15) constitute an exact set of physically realistic and consistent boundary conditions, thereby permitting unique solutions of Equations (7) and (8). Subsequently, the tangential component $q_\theta(R, \theta)$ may be calculated and, moreover, it does purport to the existence of surface diffusion over the solid surfaces (see Equation (27) to follow).

I.3 SOLUTION OF THE DEFINING EQUATIONS

I.3.1 THE GENERAL SOLUTIONS

The general solutions of Equations (7) and (8) for the case of rectilinear diffusion may be extracted from fundamental solutions of Laplace's Equation in spherical coordinates discussed by Sneddon²², viz.

$$c(r, \theta) = \sum_n [A_n r^n + B_n r^{-n-1}] [P_n(\cos \theta) + C_n Q_n(\cos \theta)] \quad R < r < S, \quad (16)$$

$$c^*(r, \theta) = \sum_n [A_n^* r^n + B_n^* r^{-n-1}] [P_n(\cos \theta) + C_n^* Q_n(\cos \theta)] \quad S < r < \infty, \quad (17)$$

where A_n , B_n , C_n , A_n^* , B_n^* , C_n^* represent arbitrary constants and $P_n(\cos \theta)$ and $Q_n(\cos \theta)$ denote n th order Legendre functions of the 1st and 2nd kind respectively. The particular solutions which satisfy the four stipulated boundary conditions can then be shown to be:

$$c(r, \theta) = c^*(r, \pi/2) + A(RQ^*/D^*) [(r/R) + (1/2)(r/R)^{-2}] \cos \theta, \quad (18)$$

$$c^*(r, \theta) = c^*(r, \pi/2) + (RQ^*/D^*) [(r/R) + (A^*/2)(r/R)^{-2}] \cos \theta, \quad (19)$$

where A and A^* are given by:

$$A = 3\lambda / (3\lambda - \lambda\epsilon + \epsilon), \quad (20)$$

$$A^* = (3\lambda - \lambda\epsilon - 2\epsilon) / \{(1 - \epsilon)(3\lambda - \lambda\epsilon + \epsilon)\}^\dagger. \quad (21)$$

In developing these composite expressions for A and A^* it was necessary to substitute for the ratio (S/R) according to Equation (1).

[†] Refer to Section I.3.4 for further information regarding the numerical value of A^* .

I.3.2 QUANTITATIVE CONSISTENCY OF THE MODELLED SYSTEM

The solution developed above represents the exact solution for the physically realizeable system of a single sphere concentrically suspended inside a spherical cavity within an isotropic porous medium. Therefore, if this simpler system is to be *quantitatively* representative of the original swarm of spheres it is necessary that within the unit cell the average flux in the mainstream direction be equal to that of the mainstream itself. In particular, this implies that

$$(1/\pi S^2) \int_R^S q_\theta(r, \pi/2) 2\pi r dr = Q^* . \quad (22)$$

The flux component $q_\theta(r, \pi/2)$ may be evaluated from Equations (10), (18) and (20), thus:

$$q_\theta(r, \pi/2) = \left\{ -D(1/r) (\partial c / \partial \theta) \right\}_{@ \pi/2} = 3Q^* \{ 1 + (1/2)(r/R)^{-3} \} / (3\lambda - \lambda\epsilon + \epsilon) . \quad (23)$$

Evaluating the integral and substituting for (S/R) from Equation (1) yields the ultimate expression

$$\lambda = D^*/D = 2\epsilon / (3 - \epsilon) \quad 0 \leq \epsilon \leq 1.0 . \quad (24)$$

I.3.3 PHYSICAL INSIGHT PROVIDED BY THE SOLUTION

It is immediately apparent that the predictions of Equation (24) are physically consistent at both porosity limits, viz. as $\epsilon \rightarrow 0$, $\lambda \rightarrow 0$ and as $\epsilon \rightarrow 1$, $\lambda \rightarrow 1$. Furthermore, this equation implies that λ is invariant with the size distribution for systems composed entirely of spheres and possessing a macroscopically uniform spatial distribution. In view of this fact it is clear that diffusivity measurements should

not be expected to provide quantitative information relating to pore sizes, pore size distributions and consequently to specific surface areas of porous media in general.

I.3.4 DISTURBANCE INTRODUCED BY THE MODELLING PROCEDURE

It is particularly elucidating to calculate the extent of any disturbance of the mainstream flowfield introduced by the modelling procedure.

Firstly, from Equations (21) and (24) it may in fact be noted that $A^* = 0$. In view of this it follows from Equations (11) and (19) that $q_r^*(r, \theta) = -Q^* \cos \theta$ and $q_\theta^*(r, \theta) = Q^* \sin \theta$. The flux vector, $\underline{q}^*(r, \theta)$, at *any* station within the exterior region will therefore be characterized by:

$$|\underline{q}^*(r, \theta)| = \sqrt{\{q_r^*(r, \theta)\}^2 + \{q_\theta^*(r, \theta)\}^2} = Q^* . \quad (25)$$

Hence, the flowfield everywhere within the exterior region remains *totally undisturbed* by the modelling procedure. In other words any disturbance introduced by the modelling procedure is wholly confined to within the unit cell, an observation which lends heavy support to the realistic nature of the proposed model.

I.3.5 EVALUATION OF THE SURFACE DIFFUSION

As noted previously the formulation of boundary conditions concerning the tangential components of the flux vector was avoided owing to the insufficiently understood phenomenon of surface diffusion. However, the magnitude of the surface flux, $q_\theta(R, \theta)$, over the reference sphere may now be evaluated by means of Equations (10) and (18), viz.

$$q_{\theta}(R, \theta) = \left\{ -D(1/r) \left(\frac{\partial c}{\partial \theta} \right) \right\}_{@R} = (9/2)Q^* \sin \theta / (3\lambda - \lambda \epsilon + \epsilon) . \quad (26)$$

Substituting for λ from Equation (24) then yields the ultimate expression

$$q_{\theta}(R, \theta) / Q^* = (3/2) \sin \theta / \epsilon . \quad (27)$$

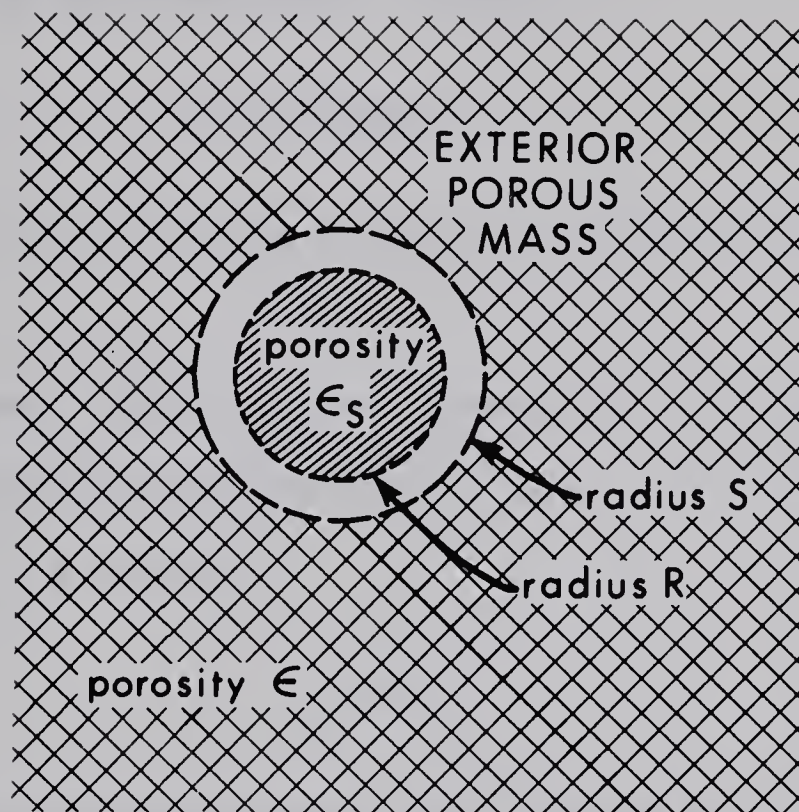
This result suggests, as intuitively expected, that the contribution of surface diffusion to the mainstream flux will be most significant for very low porosities.

I.3.6 CONSIDERATIONS WHEN THE SPHERES THEMSELVES ARE POROUS

Frequently the system under consideration is composed of porous particles, for example a bed of spherical catalyst pellets in which each pellet possesses the same porosity, ϵ_s , and the same diffusivity factor, λ_s . For such a system the model representation assumes the form depicted in Figure 4. To ensure that the porosity of the unit cell again remains equal to that of the original system, ϵ , it is here necessary that

$$S/R = \{(1-\epsilon)/(1-\epsilon_s)\}^{-1/3} . \quad (28)$$

The calculations for this system, although much more complicated, are entirely analogous to those of the preceding derivation for solid spheres. However, it now becomes necessary to solve Laplace's equation within three regions, viz. the exterior region, the annular region and the reference sphere itself, and to connect these solutions at the appropriate interfaces by means of boundary conditions analogous to those stipulated in Equations (12) - (15). The ultimate result is:



$$\frac{S}{R} = \left(\frac{1 - \epsilon}{1 - \epsilon_s} \right)^{-1/3}$$

FIGURE 4. THE PROPOSED MODEL FOR AN HOMOGENEOUS SWARM OF POROUS SPHERES

$$\lambda = \frac{(2+\lambda_s) - 2(1-\lambda_s)(1-\epsilon)/(1-\epsilon_s)}{(2+\lambda_s) + (1-\lambda_s)(1-\epsilon)/(1-\epsilon_s)} . \quad (29)$$

For the particular case of diffusion through *solid* spheres ($\epsilon_s = 0$, $\lambda_s = 0$) the above expression reduces to:

$$\lambda = 2\epsilon/(3-\epsilon) . \quad (30)$$

This is identical with Equation (24) for solid spheres as would be expected.

If, moreover, each individual sphere may be visualized as being composed of considerably smaller spheres then λ_s may be evaluated from Equation (30) above, viz.

$$\lambda_s = 2\epsilon_s/(3-\epsilon_s) . \quad (31)$$

The substitution of this expression into Equation (29) for porous spheres surprisingly yields the original expression for solid spheres, viz.

$$\lambda = 2\epsilon/(3-\epsilon) . \quad (32)$$

This analysis therefore suggests that λ is independent of ϵ_s for the special case of porous spheres themselves composed of much smaller spheres. Once again the inference is that λ is invariant with the size distribution for any system composed entirely of spheres and possessing a 'macroscopically' uniform spatial distribution.

I.3.7 ELECTRICAL CONDUCTION THROUGH AN HOMOGENEOUS SWARM OF SPHERES

The electrical analogue of Equation (32) for conduction through an homogeneous swarm of solid, non-conducting spheres, saturated with a conducting fluid of specific conductivity K , is

$$\lambda = K^*/K = 2\epsilon/(3-\epsilon) , \quad (33)$$

where λ here denotes the *conductivity factor* of the porous medium.

That this identification between diffusion and electrical conduction can be made is formally apparent from the similarity in structure of the underlying boundary value problems, namely the *partial differential equations* (based upon Fick's Law and Ohm's Law respectively) and the *stipulated boundary conditions*[†]. Moreover, Schofield and Dakshinamurti¹⁹ have actually measured the diffusivity and conductivity factors of a wide range of sands and clays and have obtained agreement to within the limits of experimental error (Klinkenberg¹⁰ has further confirmed this equivalence from similar observations). Throughout this work, therefore, λ will be understood to be synonymous with the diffusivity factor *and* the electrical conductivity factor.

† The boundary conditions stipulated for diffusion may be interpreted as follows for *electrical conduction*. Thus, Equation (12) expresses the non-conducting characteristics of the reference sphere, Equations (13) and (14) imply respectively potential continuity and radial-current continuity across the outer surface of the unit cell, and Equation (15) again reflects the finite nature of the disturbance created by the modelling procedure.

It should be emphasized that the expression $\lambda = 2\epsilon/(3-\epsilon)$ will not, in general, apply to the case of *thermal conduction* because no allowance has been made in the presented derivation for either a finite film resistance between the spheres and the fluid, or for the inevitable presence of convection.

I.3.8 COMPARISON OF PREDICTED RESULTS WITH EXPERIMENTAL DATA

There exists a great deal of electrical conductivity data^{4,6,26} supporting Equation (33) for $\epsilon > 0.4$; for lower porosities the predictions of this equation are somewhat higher than observed values (Figure 6).

As regards the effects of the size distribution of the component spheres, the consensus of opinion^{7,12,26} is that λ is essentially invariant with this parameter provided the spatial distribution of the spheres is macroscopically uniform; these observations are in accord with the conclusions of the present analysis.

However, it is appropriate at this juncture to stress that the experimental measurement of the conductivity factor, although significantly easier than that of the diffusivity factor, is by no means trivial. Such electrical measurements are often hampered by polarization at the electrodes⁷ whilst, for dispersions in particular, certain additional circumstances can interfere with the homogeneity of the system¹⁴, notable amongst these being sedimentation of the dispersed phase, adherence of the dispersed phase and chain formation in the presence of electric fields. The very small effects attributed by certain workers¹⁴ to the size distribution in systems of spheres should, therefore, be viewed with some caution.

Present Experimental Work

In order to confirm the trend of existing experimental data in the lower porosity range, a number of conductivity factor measurements were carried out using a cylindrical plexiglass cell packed

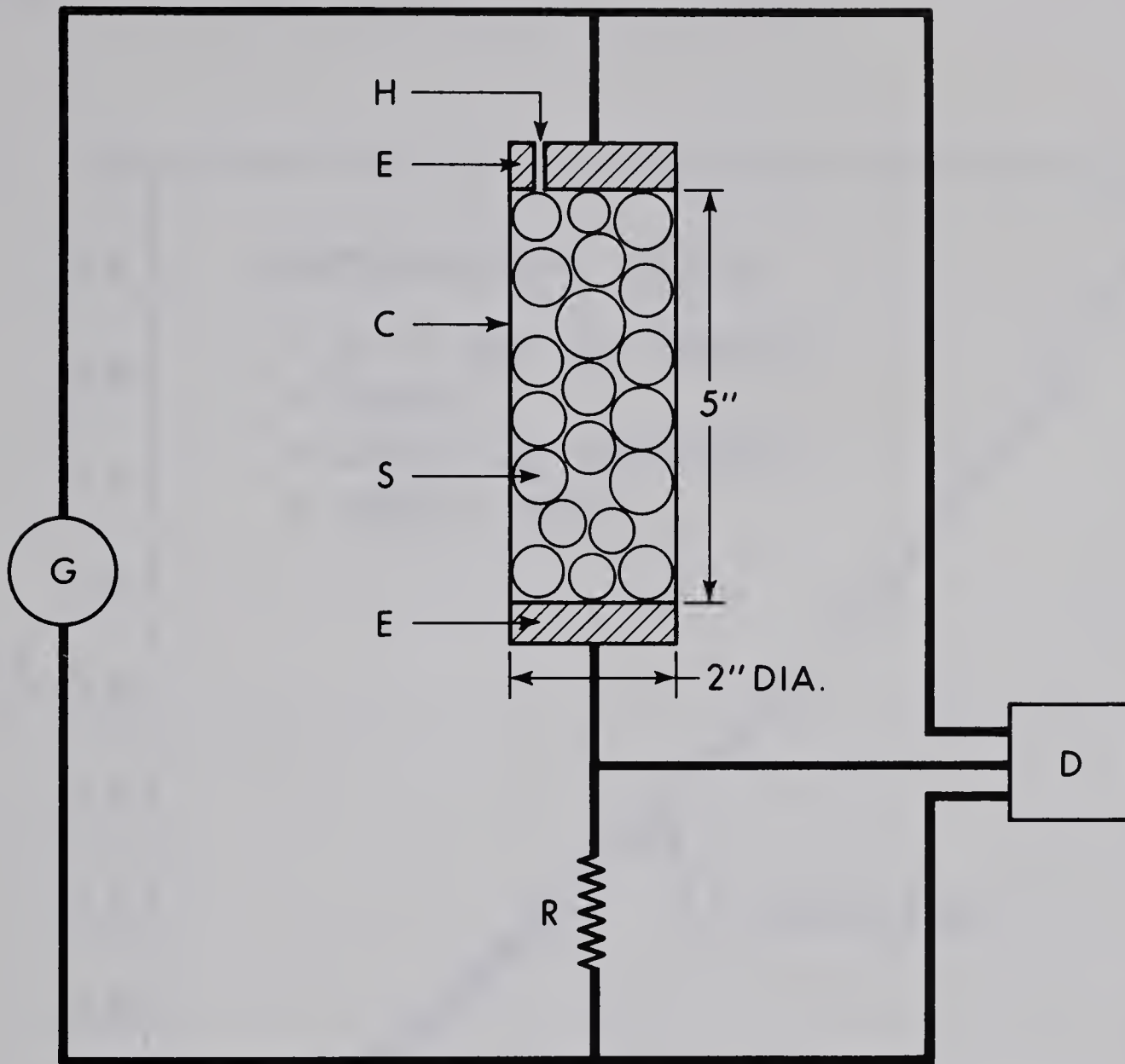
with various arbitrary mixtures of glass spheres (Figure 5). Solid copper electrodes were placed at both ends of the cell and an acidified aqueous copper sulphate solution was employed as the electrolyte in order to effectively eliminate surface effects at these electrodes¹³. All subsequent electrical measurements were made using audio-frequency alternating current in order to avoid polarization effects. In order to further avoid any effects due to packing discrepancies at the cell walls it was necessary to ensure a minimum cell to particle diameter of at least twenty-five to one²⁶.

The electrical resistance of the cell when filled with the electrolyte alone was firstly measured, followed by the resistance of the cell when packed with spheres and saturated with this same electrolyte, both measurements being taken at the same temperature. The ratio of these two resistances gave the conductivity factor directly. The porosity of the system was finally determined by a weighing technique. Representative data so obtained is tabulated below.

TABLE 1
EXPERIMENTAL CONDUCTIVITY FACTOR DATA
FOR HOMOGENEOUS SWARMS OF SPHERES

ϵ	λ
0.261	0.174
0.296	0.198
0.309	0.214
0.348	0.248
0.380	0.278

This data is also displayed in Figure 6; it can be seen to conform closely with the trend of previously reported experimental data.



KEY:

C CYLINDRICAL PLEXIGLASS CELL

E SOLID COPPER ELECTRODES

S PACK OF GLASS SPHERES SATURATED WITH ELECTROLYTE

H HOLE FOR LIQUID EXPANSION

R STANDARD RESISTANCE $100\ \Omega$

G AUDIO OSCILLATOR 1000 Hz (General Radio Co. type 1311-A)

D DIGITAL MULTI-FUNCTION METER
(Hewlett Packard, model 3450A)

FIGURE 5. EQUIPMENT USED FOR THE EXPERIMENTAL DETERMINATION
OF THE CONDUCTIVITY FACTOR OF A PACK OF SPHERES

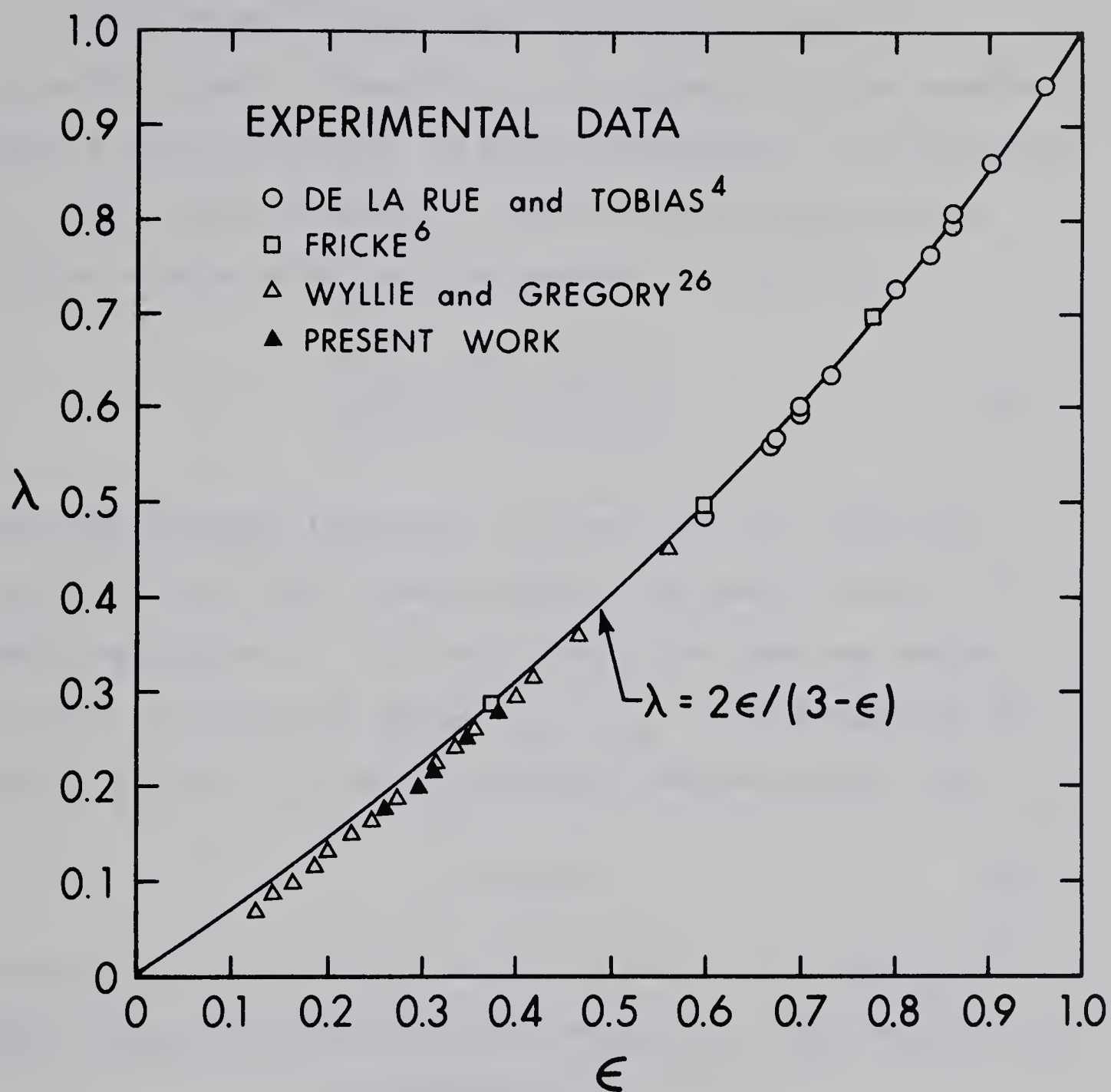


FIGURE 6. THE PREDICTED DEPENDENCE OF λ ON ϵ FOR SPHERES:
COMPARISON WITH EXPERIMENTAL DATA

I.4 DISCUSSION OF PREVIOUS WORK

Clerk Maxwell¹² investigated the problem of electrical conduction through a dispersion of solid conducting spheres embedded within a conducting medium. In essence he considered the limiting case of a single sphere in space ($\epsilon \rightarrow 1.0$) and proposed the following solution as being valid for dilute systems ($\epsilon \approx 1.0$), viz.

$$\lambda = \frac{(2+\lambda_s) - 2(1-\lambda_s)(1-\epsilon)}{(2+\lambda_s) + (1-\lambda_s)(1-\epsilon)} . \quad (34)$$

This equation agrees identically with the electrical conductivity analogue of the derived Equation (29) for the specific case of *solid* conducting spheres ($\epsilon_s = 0, \lambda_s \neq 0$) which do not touch one another. For solid non-conducting spheres ($\epsilon_s = 0, \lambda_s = 0$) both Equations (29) and (34) reduce to the familiar expression derived earlier, viz.

$$\lambda = 2\epsilon/(3-\epsilon) . \quad (35)$$

The above solution is closely related in form to Lord Rayleigh's¹⁷ exact solution for monosized spheres arranged in a cubic pattern, viz.

$$\lambda = \frac{2\epsilon - 0.3919(1-\epsilon)^{10/3} \dots\dots\dots}{3-\epsilon - 0.3919(1-\epsilon)^{10/3} \dots\dots\dots} \quad \epsilon \geq 0.4764. \quad (36)$$

This result is in good agreement with the derived Equation (35), differing nowhere by more than 3.02% (Figure 7). Lord Rayleigh himself questioned whether the orientation of the spheres could appreciably affect λ and stated that "an irregular isotropic arrangement would, doubtless, give the same result".

Slawinski²¹ studied the relationship between λ and ϵ for aggregates of non-conducting monosized spheres in several lattice orders. However, his approach was based on merely geometric concepts and thereby disregarded the fundamental principles of potential theory according to which the potential distribution throughout the conducting medium must satisfy Laplace's Equation (7). Despite this deficiency Slawinski was able to develop an expression which is in good agreement with experimental data for $\epsilon < 0.4$, viz.

$$\lambda = \epsilon / (1.3219 - 0.3219\epsilon)^2 . \quad (37)$$

Bruggemann³ examined the system in which one relatively large sphere is surrounded by a swarm of much smaller spheres. He considered the region exterior to this large sphere to be a continuum and subsequently applied Maxwell's result on the premise that the system is 'dilute' with respect to the large sphere. He derived the expression

$$\lambda = \epsilon^{3/2} . \quad (38)$$

However, for single sizes or narrow size fractions the physical conditions necessary for justifying the Bruggemann approximation are not satisfied, and this is reflected in the less satisfactory overall agreement of his formula with experimental data (Figure 7).

Archie¹ examined contemporary conductivity data for spheres and unconsolidated sands and suggested the following correlation:

$$\lambda = \epsilon^{1.3} . \quad (39)$$

This empirical result represents the data well for $\varepsilon < 0.4$. It is interesting to note the similarity in form of Archie's Equation (39) and Bruggemann's Equation (38).

Of particular interest is the work of Prager¹⁶ who applied the principle of minimum entropy generation to obtain bounds on the diffusion factor for an homogeneous suspension of solid particles of arbitrary shape. He showed that

$$\lambda < \varepsilon\{1-(1-\varepsilon)/3\} , \quad (40)$$

and stated this inequality to be valid for particles of any shape and at any porosity, the only stipulation being that the suspension be isotropic. For spheres in particular he suggested that

$$\lambda = \varepsilon\{1-(1-\varepsilon)/2\} . \quad (41)$$

This formula gives good agreement with experimental data over the entire porosity range (Figure 7).

It is instructive to note that Equation (41) constitutes the first two terms of each series obtained when Equations (38) and (35) are expanded in terms of $(1-\varepsilon)$, viz.

$$\lambda = \varepsilon^{3/2} = \varepsilon\{1-(1-\varepsilon)\}^{1/2} = \varepsilon\{1-(1-\varepsilon)/2-(1-\varepsilon)^2/8-(1-\varepsilon)^3/16-\cdots\} , \quad (42)$$

$$\lambda = 2\varepsilon/(3-\varepsilon) = \varepsilon\{1+(1-\varepsilon)/2\}^{-1} = \varepsilon\{1-(1-\varepsilon)/2+(1-\varepsilon)^2/4-(1-\varepsilon)^3/8+\cdots\} . \quad (43)$$

These expressions therefore exhibit an increasing agreement as $\varepsilon \rightarrow 1.0$ (Figure 7).

Arguments based on the classical capillary model^{15,24} have yielded expressions of the form

$$\lambda = \epsilon / \tau^n \quad n = 1 \text{ or } 2 . \quad (44)$$

The parameter τ denotes the so-called tortuosity of the pore space^{23,25}; this quantity must be measured experimentally. Clearly, such approaches are impractical since the determination of τ requires a prior measurement of λ itself.

It has recently been brought to my attention that a cell-type model, fundamentally related to that proposed in this work, has been employed by Hashin⁸ to study the conductive, magnetic and elastic properties of polycrystalline aggregates and bi-metallic composites. This serves to illustrate the fundamental significance of the proposed model in representing both porous *and* non-porous heterogeneous media.

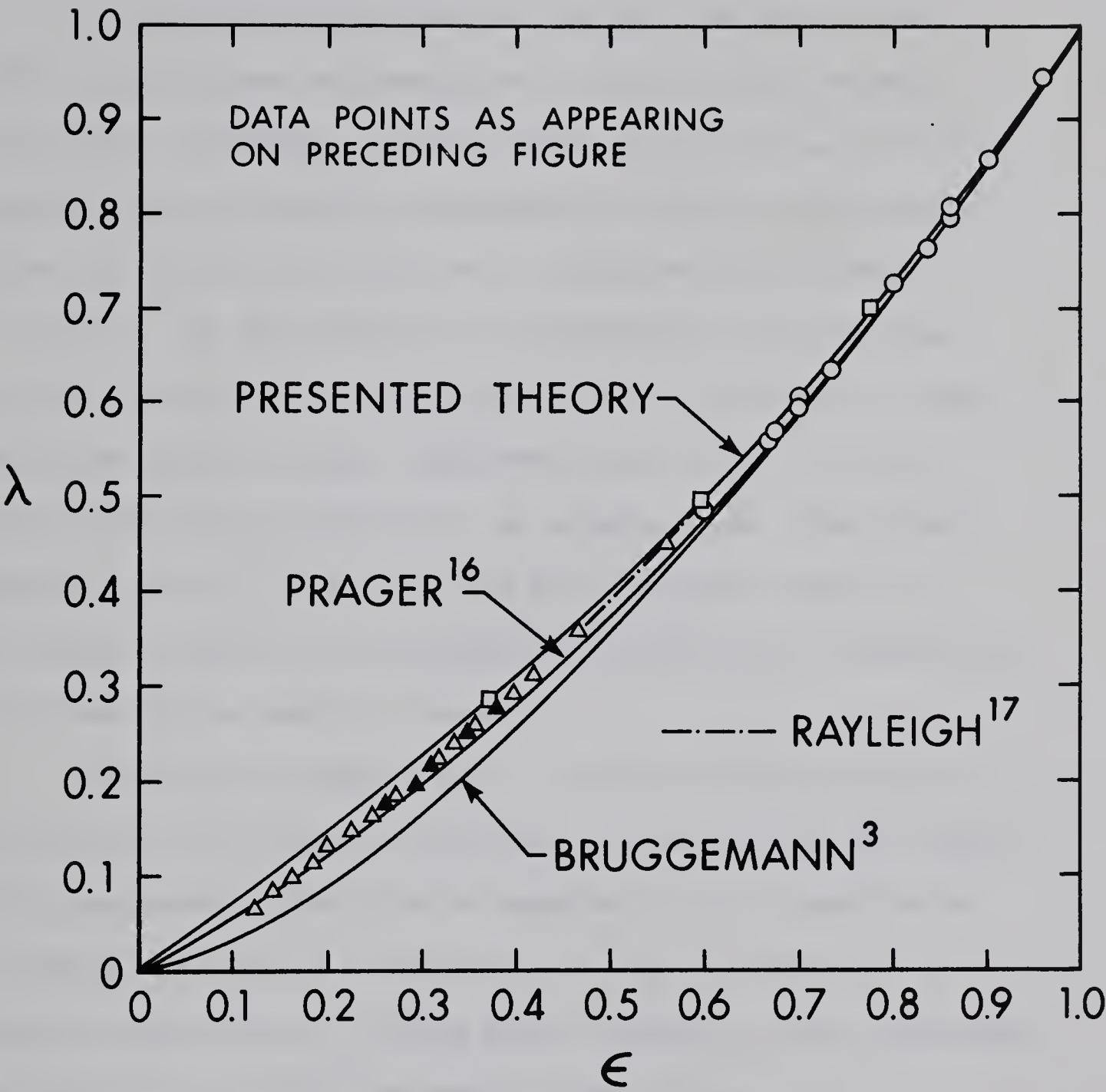


FIGURE 7. THE DEPENDENCE OF λ ON ϵ FOR SPHERES: COMPARISON WITH PREVIOUS WORK

I.5 SUMMARY

The presented results demonstrate that the proposed model offers a satisfactory representation of, and provides valuable insight into, diffusion occurring within an homogeneous swarm of spheres. For solid spheres possessing an arbitrary size distribution the diffusivity factor may be evaluated by the formula $\lambda = 2\epsilon/(3-\epsilon)$. If the spheres are non-conducting, the electrical conductivity factor also may be evaluated by this formula. These predictions agree well with experimental data for $\epsilon > 0.4$; for lower porosities the predictions are somewhat high. The overall agreement, however, is satisfactory and lends heavy support to the realistic nature of the proposed model and to the acceptability of the assumptions implicit therein.

This analysis suggests that λ is invariant with the size distribution of the spheres, inferring that diffusivity and conductivity measurements should not be expected to yield quantitative information relating to pore sizes, pore size distributions or specific surface areas of porous media in general; these conclusions are also in accord with experimental observations.

In view of these encouraging results attempts will now be made to apply the proposed model to the study of diffusion (conduction) occurring within certain *anisotropic* porous media. This will provide valuable insight into the important effects which particle shape and orientation have on the diffusivity (conductivity) factor of unconsolidated porous media.

PART IB

EXTENSION OF THE PROPOSED MODEL
TO THE STUDY OF DIFFUSION WITHIN
ANISOTROPIC UNCONSOLIDATED POROUS MEDIA

I.6 OBJECTIVES

The principal objective of this analysis is to assess the effects which particle shape and orientation have on the diffusivity factor of unconsolidated porous media.

In practice many such porous media are composed of preferentially orientated particles far removed in shape from the spherical geometry, for example a filter cake consisting of flattish or fibrous particles. An excellent representation of such an anisotropic system is often provided by an homogeneous swarm of co-axially orientated oblate or prolate spheroids respectively. This analysis seeks to achieve the above mentioned objectives by extending the geometric model proposed in Part IA for spheres to the case of co-axially orientated spheroids.

However, before proceeding further with the problem of interest it will firstly be elucidating to examine the nature of the differential equations which describe diffusion within anisotropic porous media in general.

I.7 THE EQUATIONS GOVERNING DIFFUSION THROUGH ANISOTROPIC POROUS MEDIA

I.7.1 POROUS MEDIA IN GENERAL

It is widely acknowledged that the appropriate form of Fick's Law describing steady state diffusion within anisotropic porous media (corresponding to Equation (4) for isotropic media) is

$$\underline{q}^* = -\underline{D}^* \underline{\nabla} c^* , \quad (45)$$

where \underline{D}^* denotes a symmetric, second-order tensor¹⁸; in a Cartesian frame of reference [x,y,z] the associated matrix would be represented by:

$$\begin{bmatrix} D_{xx}^* & D_{xy}^* & D_{xz}^* \\ D_{xy}^* & D_{yy}^* & D_{yz}^* \\ D_{xz}^* & D_{yz}^* & D_{zz}^* \end{bmatrix} . \quad (46)$$

Corresponding to the diffusivity factor for isotropic media, λ , it here becomes necessary to define a tensor, $\underline{\lambda}$, thus:

$$\underline{\lambda} = (1/D) \underline{D}^* = \begin{bmatrix} \lambda_{xx} & \lambda_{xy} & \lambda_{xz} \\ \lambda_{xy} & \lambda_{yy} & \lambda_{yz} \\ \lambda_{xz} & \lambda_{yz} & \lambda_{zz} \end{bmatrix} , \quad (47)$$

in which

$$\lambda_{ij} = (1/D) D_{ij}^* . \quad (48)$$

The diffusivity D again refers to that within unobstructed space.

The matrix representation in Equation (47) will be diagonalized by selecting a Cartesian frame of reference which is collinear with

the three principal directions of the porous medium in question¹⁸, thus:

$$\begin{bmatrix} \lambda_x & 0 & 0 \\ 0 & \lambda_y & 0 \\ 0 & 0 & \lambda_z \end{bmatrix} . \quad (49)$$

I.7.2 POROUS MEDIA COMPOSED OF CO-AXIALLY ORIENTATED SPHEROIDS

Having resolved matters concerning the nature of the tensor $\underline{\lambda}$ it is now in order to return to the original problem of interest, viz. the study of diffusion within an homogeneous swarm of co-axially orientated spheroids. In such a system one preferred direction of symmetry will be observed; thus, if the x-axis is taken to be collinear with this preferred direction (i.e. collinear with the axes of revolution of the individual spheroids), then it follows from symmetry that

$$\lambda_z = \lambda_y , \quad (50)$$

so that the diffusivity factor matrix here assumes the more specific form

$$\begin{bmatrix} \lambda_x & 0 & 0 \\ 0 & \lambda_y & 0 \\ 0 & 0 & \lambda_y \end{bmatrix} . \quad (51)$$

Hence, in order to extract meaningful information concerning diffusion through such an anisotropic system it will suffice to investigate the following two principal cases, viz.

Case 1: Diffusion collinear with the axes of revolution of the spheroids;

Case 2: Diffusion orthogonal to the axes of revolution of the spheroids.

The spheroid appears to be the most appropriate generalized geometry to study because (1) it approximates a vast range of physically important shapes (ranging between flat circular discs, spheres and circular cylinders), and (2) it lends itself to a rigorous mathematical analysis. Moreover, the oblate spheroid is now regarded to be a somewhat idealized shape in many mass transfer operations²⁰.

I.8 DIFFUSION THROUGH AN HOMOGENEOUS SWARM OF CO-AXIALLY ORIENTATED OBLATE SPHEROIDS

I.8.1 THE DERIVED SOLUTIONS

An *oblate spheroid* is generated when an ellipse is rotated about its minor axis; such a geometry may be visualized as a sphere which has undergone a flattening process. Figure 8 depicts an homogeneous swarm of oblate spheroids of identical eccentricity, e , possessing an arbitrary size distribution and orientated such that the axis of revolution of each particle is collinear with the x-direction. As before, λ_x denotes the diffusivity factor of the medium collinear with this principal direction whilst λ_y denotes the diffusivity factor in *any* orthogonal direction (i.e. in the y-z plane).

The modelled system for co-axially orientated oblate spheroids (Appendix A, Figure 27) is closely related to that for spheres (Figure 3); however, the eccentricity of the outer surface of the unit cell will now, in general, be different from that of the reference particle. The calculations involved are analagous to those for spheres but are necessarily much more tedious. As detailed in Appendix A the following important results are obtained for co-axially orientated oblate spheroids:

$$\lambda_x = \{g(\xi_0) - g(\xi_1)\} / \{g(\xi_0) - f(\xi_1)\} \quad , \quad (52)$$

$$\lambda_y = \{h(\xi_0) - h(\xi_1)\} / \{h(\xi_0) - g(\xi_1)\} \quad , \quad (53)$$

in which the functions $f(\xi)$, $g(\xi)$ and $h(\xi)$ are given by:

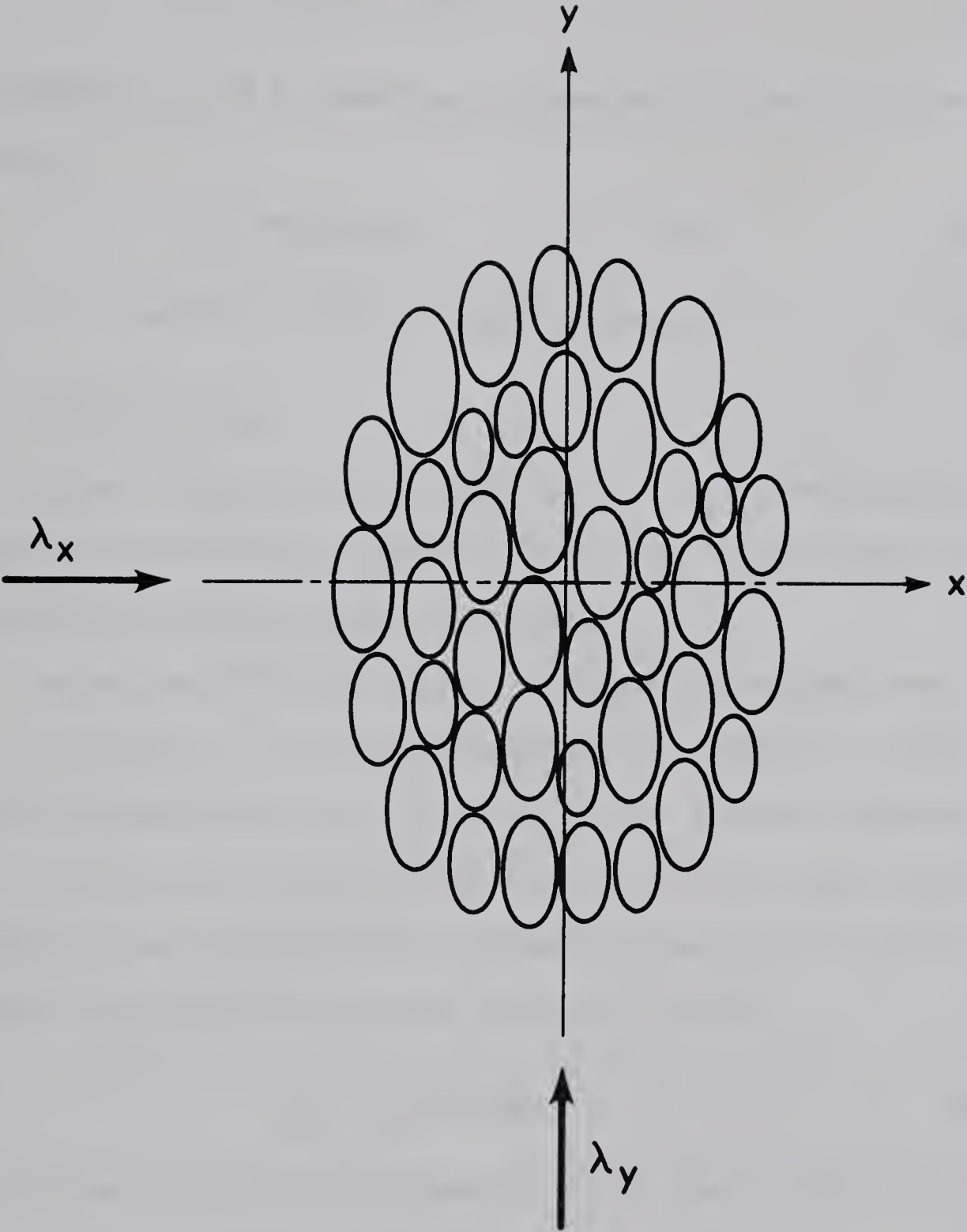


FIGURE 8. AN HOMOGENEOUS SWARM OF CO-AXIALLY ORIENTATED OBLATE SPHEROIDS (Cross-Section)

$$f(\xi) = 1/\sinh\xi - \operatorname{arccot}(\sinh\xi) , \quad (54)$$

$$g(\xi) = \sinh\xi/\cosh^2\xi - \operatorname{arccot}(\sinh\xi) , \quad (55)$$

$$h(\xi) = 2f(\xi) - g(\xi) . \quad (56)$$

The parameters ξ_0 and ξ_1 appearing in Equations (52) and (53) are defined by:

$$\xi_0 = \operatorname{areatanh}(e) \quad 0 < e < 1.0 , \quad (57)$$

$$\sinh^3\xi_1 + \sinh\xi_1 - (\cosh^2\xi_0 \sinh\xi_0)/(1-\epsilon) = 0 . \quad (58)$$

I.8.2 COMPUTED RESULTS

Figure 9 records the $\lambda_x = \lambda_x(\epsilon)$ and $\lambda_y = \lambda_y(\epsilon)$ relationships predicted by the preceding equations for several representative systems of co-axially orientated oblate spheroids.

For any specific eccentricity, e , it may be observed that $\lambda_x \leq \lambda_y$, also that λ_x is far more dependent on e than is λ_y ; this is especially significant for $e < 0.5$, that is for flattish particles.

For the particular case defined by $e = 1.0$ the oblate spheroids are spherical and the predictions offered here are in accord with those developed specifically for spheres (Section I.3), viz.

$$\lambda_x = \lambda_y = 2\epsilon/(3-\epsilon) . \quad (59)$$

For the specific case defined by $e \rightarrow 0$, that is for a co-axially orientated swarm of very thin circular discs, the present predictions are:

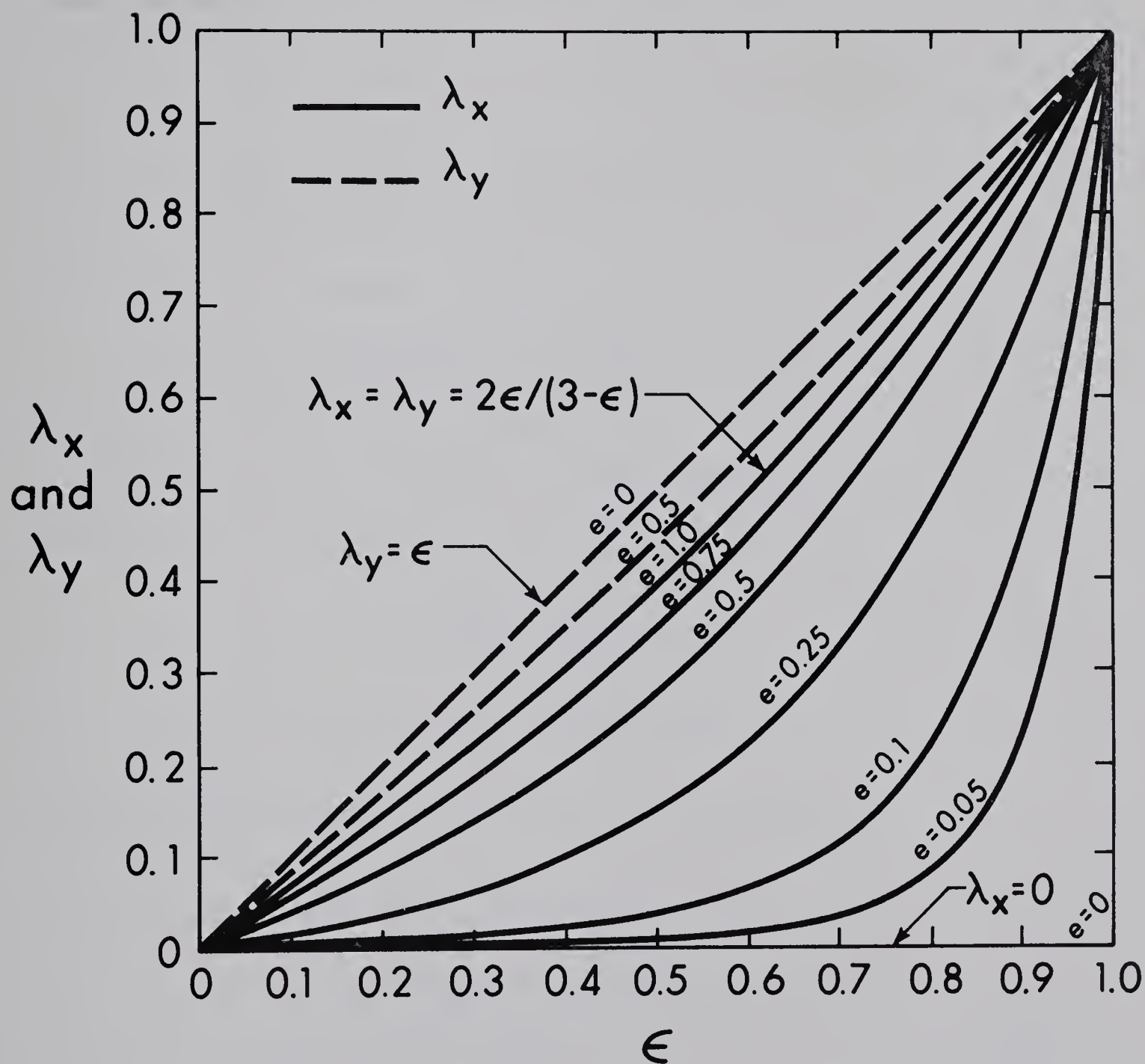


FIGURE 9. THE PREDICTED DEPENDENCE OF λ_x AND λ_y ON ϵ FOR CO-AXIALLY ORIENTATED OBLATE SPHEROIDS

$$\lambda_{\mathbf{x}} \rightarrow 0 \ , \quad (60)$$

$$\lambda_{\mathbf{y}} \rightarrow \varepsilon \ . \quad (61)$$

This representation of a porous medium constitutes, in the limit, a plate-type model.

I.9 DIFFUSION THROUGH AN HOMOGENEOUS SWARM OF CO-AXIALLY ORIENTATED PROLATE SPHEROIDS

I.9.1 THE DERIVED SOLUTIONS

A *prolate spheroid* is generated when an ellipse is rotated about its major axis; such a geometry may be visualized as a sphere which has undergone an elongating process. Figure 10 depicts an homogeneous swarm of prolate spheroids of identical eccentricity, e , possessing an arbitrary size distribution and orientated such that the axis of revolution of each particle is collinear with the x -direction.

As detailed in Appendix B the following results are obtained for co-axially orientated prolate spheroids; they can be seen to be closely related in form to those for oblate spheroids presented in Equations (52) - (58), viz.

$$\lambda_x = \{G(\xi_0) - G(\xi_1)\} / \{G(\xi_0) - F(\xi_1)\} , \quad (62)$$

$$\lambda_y = \{H(\xi_0) - H(\xi_1)\} / \{H(\xi_0) - G(\xi_1)\} , \quad (63)$$

in which the functions $F(\xi)$, $G(\xi)$ and $H(\xi)$ are given by:

$$F(\xi) = 1/\cosh\xi - \operatorname{arccoth}(\cosh\xi) , \quad (64)$$

$$G(\xi) = \cosh\xi/\sinh^2\xi - \operatorname{arccoth}(\cosh\xi) , \quad (65)$$

$$H(\xi) = 2F(\xi) - G(\xi) . \quad (66)$$

The parameters ξ_0 and ξ_1 appearing in Equations (62) and (63) are here defined by:

$$\xi_0 = \operatorname{arctanh}(e) \quad 0 < e < 1.0 , \quad (67)$$

$$\cosh^3\xi_1 - \cosh\xi_1 - (\sinh^2\xi_0 \cosh\xi_0)/(1-e) = 0 . \quad (68)$$

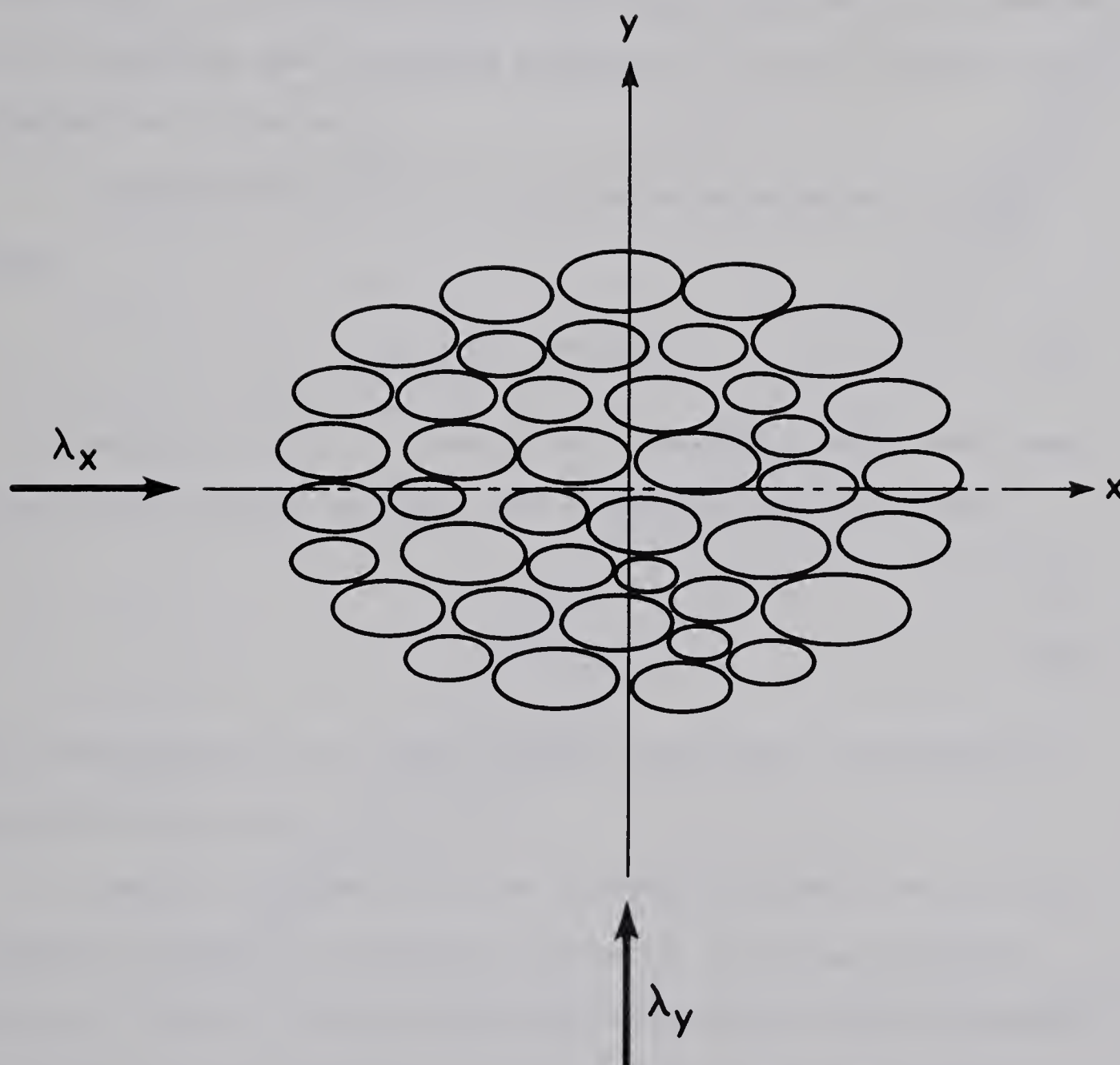


FIGURE 10. AN HOMOGENEOUS SWARM OF CO-AXIALLY ORIENTATED PROLATE SPHEROIDS (Cross-Section)

I.9.2 COMPUTED RESULTS

Figure 11 records the $\lambda_x = \lambda_x(\epsilon)$ and $\lambda_y = \lambda_y(\epsilon)$ relationships predicted by the preceding equations for several representative systems of co-axially orientated prolate spheroids. For any specific eccentricity, e , it may be observed that $\lambda_x \geq \lambda_y$; however, in contrast to the preceding case for oblate spheroids, λ_x is only slightly more dependent on e than is λ_y .

The predictions for $e = 1.0$, that is for spheres, are once again:

$$\lambda_x = \lambda_y = 2\epsilon/(3-\epsilon) . \quad (69)$$

However, for $\epsilon \rightarrow 0$, that is for a co-axially orientated swarm of very thin circular cylinders the predictions are as follows:

$$\lambda_x \rightarrow \epsilon , \quad (70)$$

$$\lambda_y \rightarrow \epsilon/(2-\epsilon) . \quad (71)$$

This representation of a porous medium constitutes, in the limit, a capillary-type model.

Equation (70) does of course represent the exact solution for diffusion parallel to co-axially orientated, very long cylinders. Moreover, Equation (71) constitutes a truncation of Lord Rayleigh's¹⁷ exact solution for conduction perpendicular to monosized circular cylinders arranged in a square pattern, viz.

$$\lambda_y = \frac{\epsilon - 0.3058(1-\epsilon)^4 - 0.0134(1-\epsilon)^8 - \dots}{2 - \epsilon - 0.3058(1-\epsilon)^4 - 0.0134(1-\epsilon)^8 - \dots} \quad \epsilon > 0.2146 . \quad (72)$$

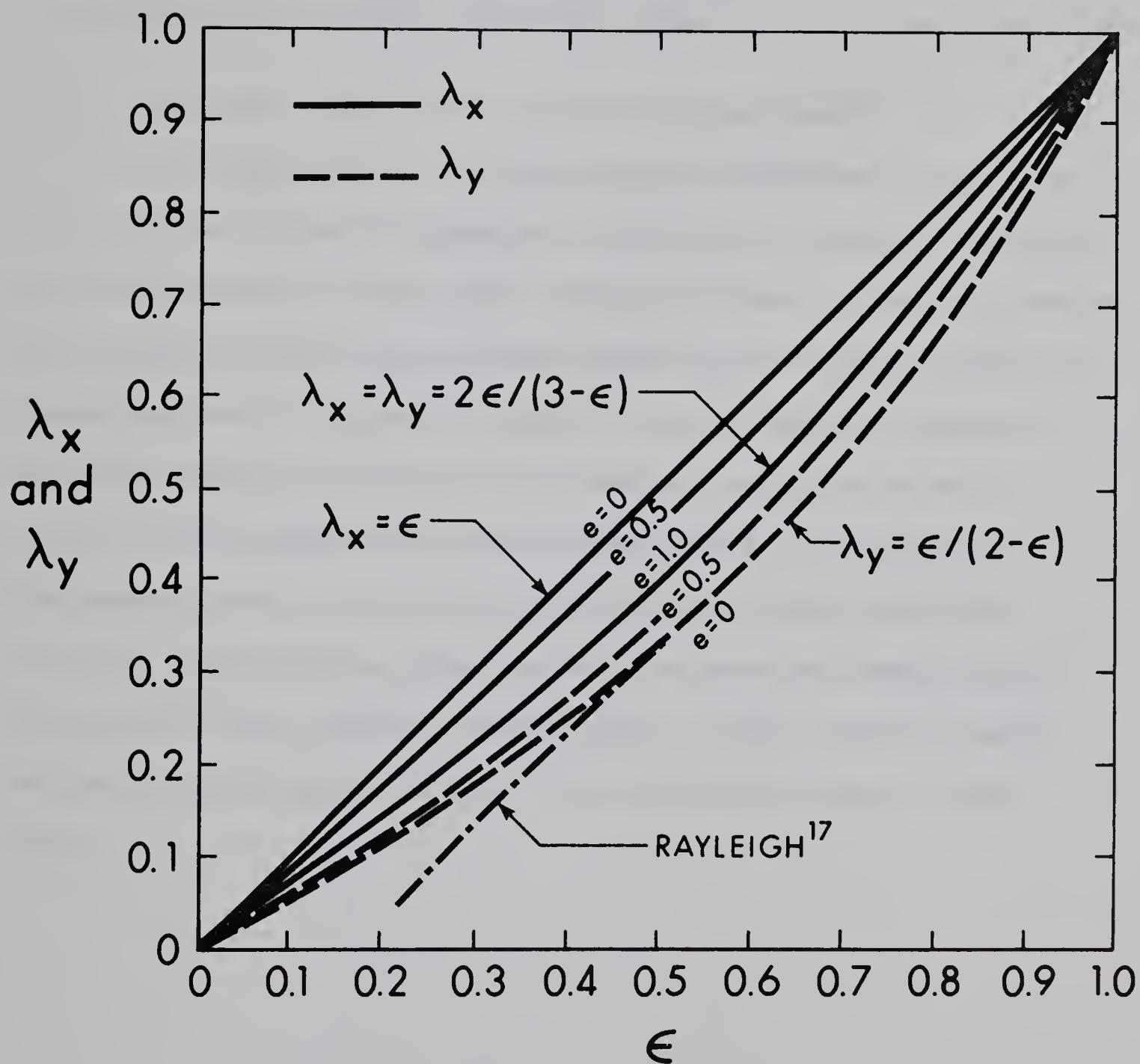


FIGURE 11. THE PREDICTED DEPENDENCE OF λ_x AND λ_y ON ϵ FOR CO-AXIALLY ORIENTATED PROLATE SPHEROIDS

This prediction is displayed in Figure 11. It should be emphasized that Rayleigh's solution applies only to monosized cylinders occupying a square array, for which 0.2146 represents the minimum obtainable porosity. However, for co-axially orientated cylinders possessing a wide distribution of radii, arbitrarily lower porosities are attainable.

Practical Significance of the Predicted Results

It is appropriate to mention here that knowledge of the ratio λ_x/λ_y provides valuable information concerning the extent of anisotropy in systems composed of co-axially orientated oblate or prolate spheroids. The predicted results have important significance because it sometimes becomes necessary to actually construct a porous medium possessing a specified degree of anisotropy (for example a specified value of λ_x/λ_y). Such a system may often be approximated by preparing an homogeneous swarm of co-axially orientated disc-like or rod-like particles (approximating oblate and prolate spheroids respectively), an estimate of the required 'eccentricity' of these particles being obtained by inspection of Figure 9 (for discs) and Figure 11 (for rods).

I.10 DIFFUSION THROUGH A SWARM OF CO-AXIALLY ORIENTATED SPHEROIDS AT AN ARBITRARY ANGLE OF ATTACK

The law describing diffusion through an anisotropic porous medium composed of co-axially orientated spheroids was discussed earlier in context with Equations (45) - (51). In the preferred frame of reference [x,y,z] it assumes the specific form:

$$\underline{q}^* = -D \begin{bmatrix} \lambda_x & 0 & 0 \\ 0 & \lambda_y & 0 \\ 0 & 0 & \lambda_y \end{bmatrix} \underline{\nabla c}^* . \quad (73)$$

It is clear that the predictions for λ_x and λ_y offered in Sections I.8 and I.9 may be used to construct the diffusivity factor matrix appearing in Equation (73) above. Moreover, this matrix provides a knowledge of the tensor $\underline{\lambda}$ which, in turn, permits a full description of the diffusion (conduction) occurring as a result of a concentration (potential) gradient in *any* arbitrary direction, within *any* chosen frame of reference.

I.11 DIFFUSION THROUGH AN HOMOGENEOUS SWARM OF RANDOMLY ORIENTATED SPHEROIDS

I.11.1 DISCUSSION OF THE SYSTEM

Under certain circumstances the system under consideration may be better approximated by a swarm of *randomly orientated* spheroids (which in consequence will be isotropic) than by a swarm of co-axially orientated spheroids. This is frequently true of particulate suspensions. Seldom would it apply to sedimented media, as in such systems the individual particles would usually have settled with some definite bias as regards preferential orientation.

The solution for such a system of randomly orientated spheroids may be constructed by a weighted superposition of the three principal solutions for the co-axial case. Now, by comparing Fick's Law with Ohm's Law² it becomes apparent that λ^{-1} is a direct measure of the resistance of a porous medium to diffusion. The following estimate may therefore be made for the diffusivity (conductivity) factor, λ_{Σ} , of a system of randomly orientated spheroids of identical eccentricity, possessing an arbitrary size distribution:

$$\lambda_{\Sigma}^{-1} = (1/3) \lambda_x^{-1} + (2/3) \lambda_y^{-1} , \quad (74)$$

where λ_x and λ_y are defined by Equations (52) and (53) for oblate spheroids, and by Equations (62) and (63) for prolate spheroids.

I.11.2 COMPUTED RESULTS

Figures 12 and 13 display the predicted $\lambda_{\Sigma} = \lambda_{\Sigma}(\epsilon)$ relationships for several representative systems of randomly orientated oblate and

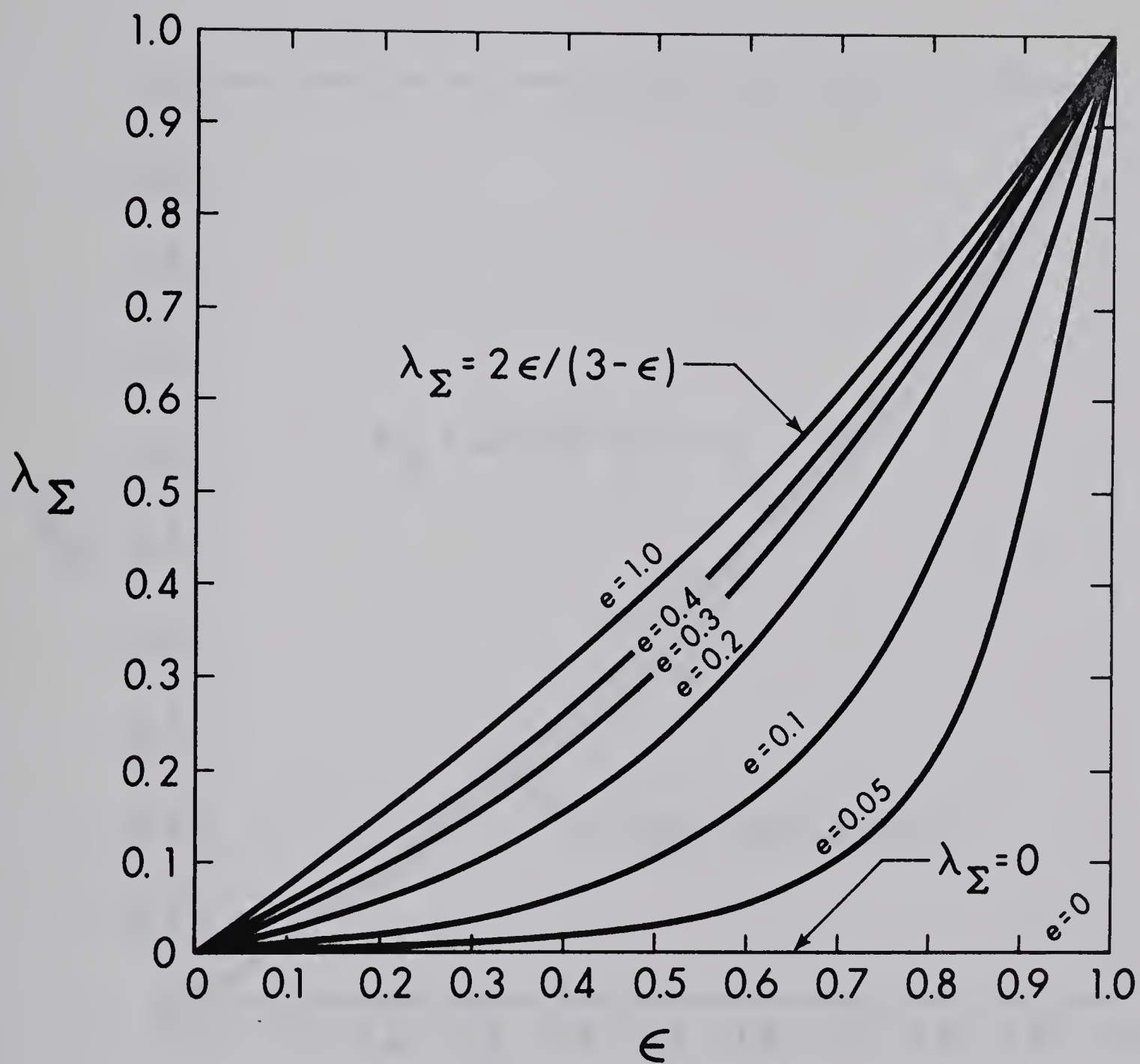


FIGURE 12. THE PREDICTED DEPENDENCE OF λ_{Σ} ON ϵ FOR RANDOMLY ORIENTATED OBLATE SPHEROIDS

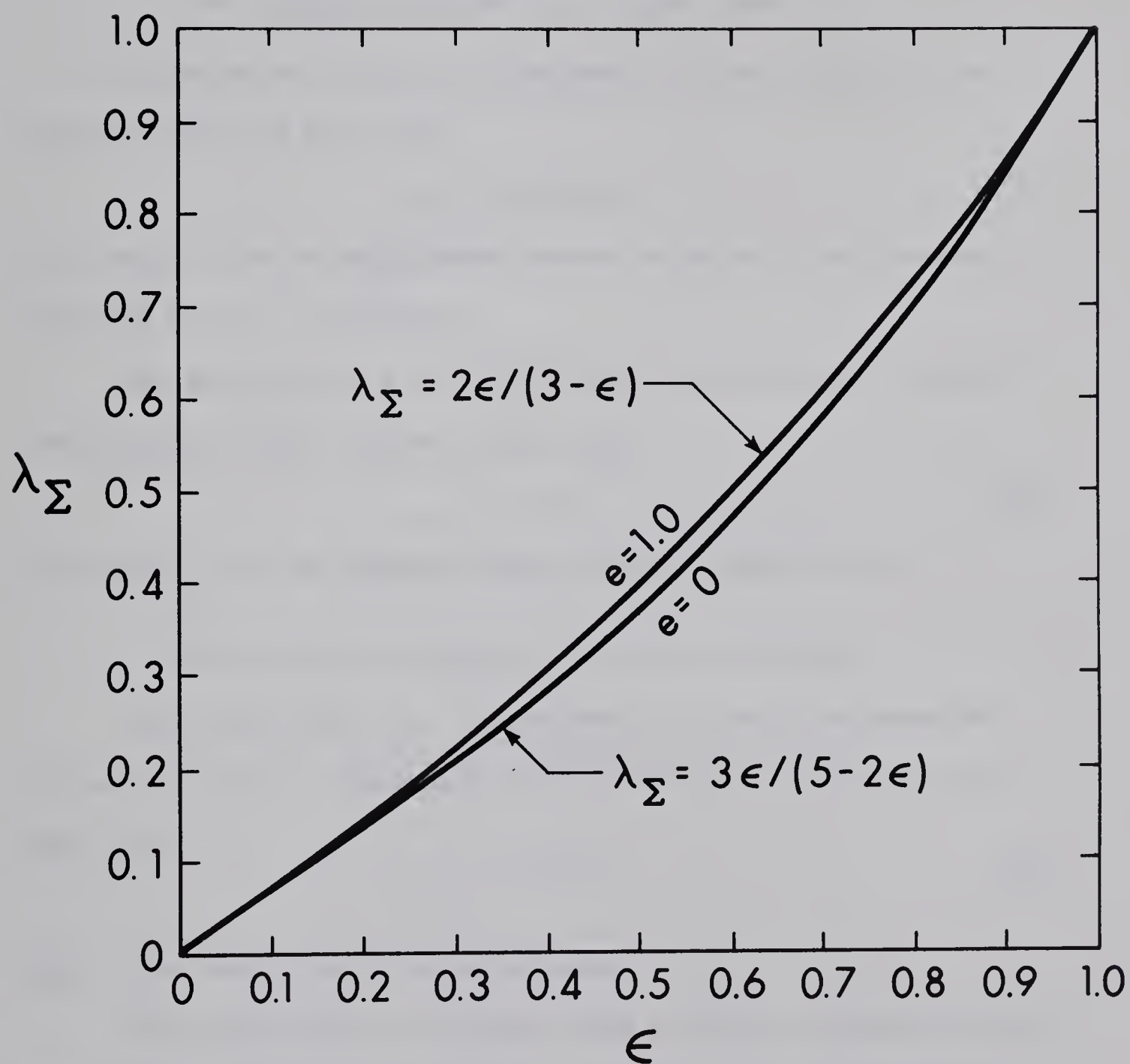


FIGURE 13. THE PREDICTED DEPENDENCE OF λ_{Σ} ON ϵ FOR RANDOMLY ORIENTATED PROLATE SPHEROIDS

prolate spheroids respectively. It is immediately apparent that for oblate spheroids λ_{Σ} is strongly dependent on the eccentricity, whereas for prolate spheroids this dependence is surprisingly mild.

The Limiting Solutions for Oblate Spheroids

The solution for $e = 1.0$ (spheres) follows directly from Equations (59) and (74), viz.

$$\lambda_{\Sigma} = 2\epsilon/(3-\epsilon) . \quad (75)$$

This result is to be anticipated because spheres do not possess a preferred axis of orientation.

The solution for $e \rightarrow 0$ (very thin circular discs) follows from Equations (60), (61) and (74), viz.

$$\lambda_{\Sigma} \rightarrow 0 . \quad (76)$$

This result is to be expected from physical considerations.

The Limiting Solutions for Prolate Spheroids

The solution for $e = 1.0$ (spheres) follows from Equations (69) and (74) and is identical to the prediction of Equation (75) above, viz.

$$\lambda_{\Sigma} = 2\epsilon/(3-\epsilon) . \quad (77)$$

Again, this result is to be anticipated.

The solution for $e \rightarrow 0$ (very thin circular cylinders) follows from Equations (70), (71) and (74), but cannot be anticipated, viz.

$$\lambda_{\Sigma} \rightarrow 3\epsilon/(5-2\epsilon) . \quad (78)$$

It is interesting to observe the similarity in structure of Equations (77) and (78).

I.12 DISCUSSION OF PREVIOUS WORK

No work has been reported to date concerning diffusion or conduction through a swarm of *co-axially orientated* spheroids. However, Fricke⁵ did extend Maxwell's¹² theory (concerning conduction through a dispersion of spheres) to the case of *randomly orientated* spheroids. From considerations of the potential of a single spheroid in space he developed the following formula for a low concentration dispersion of non-conducting spheroids within a conducting medium:

$$\lambda_{\Sigma} = A\epsilon / (A+1-\epsilon) , \quad (79)$$

the parameter A being a function of eccentricity alone. Some specific values of A for different shapes, as computed from Fricke's complicated formulae, are tabulated below for reference.

TABLE 2

PREDICTIONS FOR RANDOMLY ORIENTATED SPHEROIDS
(after Fricke⁵)

e	A	
	Oblate	Prolate
1.0	2.000	2.000
0.9	1.994	1.995
0.8	1.974	1.979
0.7	1.931	1.950
0.6	1.854	1.909
0.5	1.730	1.854
0.4	1.541	1.786
0.3	1.271	1.707
0.2	0.911	1.623
0.1	0.474	1.545
0.0	0.000	1.500

Fricke himself was of the opinion that his predictions were rather high, considerably so for oblate spheroids^{5,7}.

It is interesting to note that the predictions offered here agree identically with those of Fricke in the limit $\epsilon \rightarrow 1.0$; this agreement is to be anticipated since both theories then effectively consider a single spheroid in infinite space. The present predictions are also identical with Fricke's for the specific geometries defined by $e = 1.0$ (spheres) and $e \rightarrow 0$ (thin circular discs or cylinders). For all other values of eccentricity the present predictions (for all porosities $0 < \epsilon < 1$) are smaller than those of Fricke, considerably smaller for oblate spheroids.

These characteristics of the presented theory appear to be a direct consequence of the fact that the eccentricity of the outer surface of our model cell differs from the eccentricity of our reference spheroid (Appendix A, Figure 27) for all geometries excepting those defined by $e = 1.0$ and $e \rightarrow 0$; for these specific geometries (viz. spheres, thin circular discs and cylinders) the eccentricity of the outer surface of our model cell is identical with that of our reference spheroid, observations which follow directly from Equations (58) and (68).

Figure 14 displays the experimental conductivity data of De La Rue and Tobias⁴ for a dispersion of randomly orientated cylinders possessing a diameter to length ratio of 0.1. Now, such a cylinder is well approximated by a prolate spheroid possessing an eccentricity of 0.1; the results predicted by Equation (74) for randomly orientated prolate spheroids possessing this same eccentricity can be seen to

conform closely with the presented data.

It will be recalled that the predictions of Equation (74) for randomly orientated prolate spheroids lie within a *very* narrow band over the entire porosity range (Figure 13). That the data of De La Rue and Tobias for highly 'eccentric' cylinders lies within this band lends heavy support to the validity of the proposed theory.

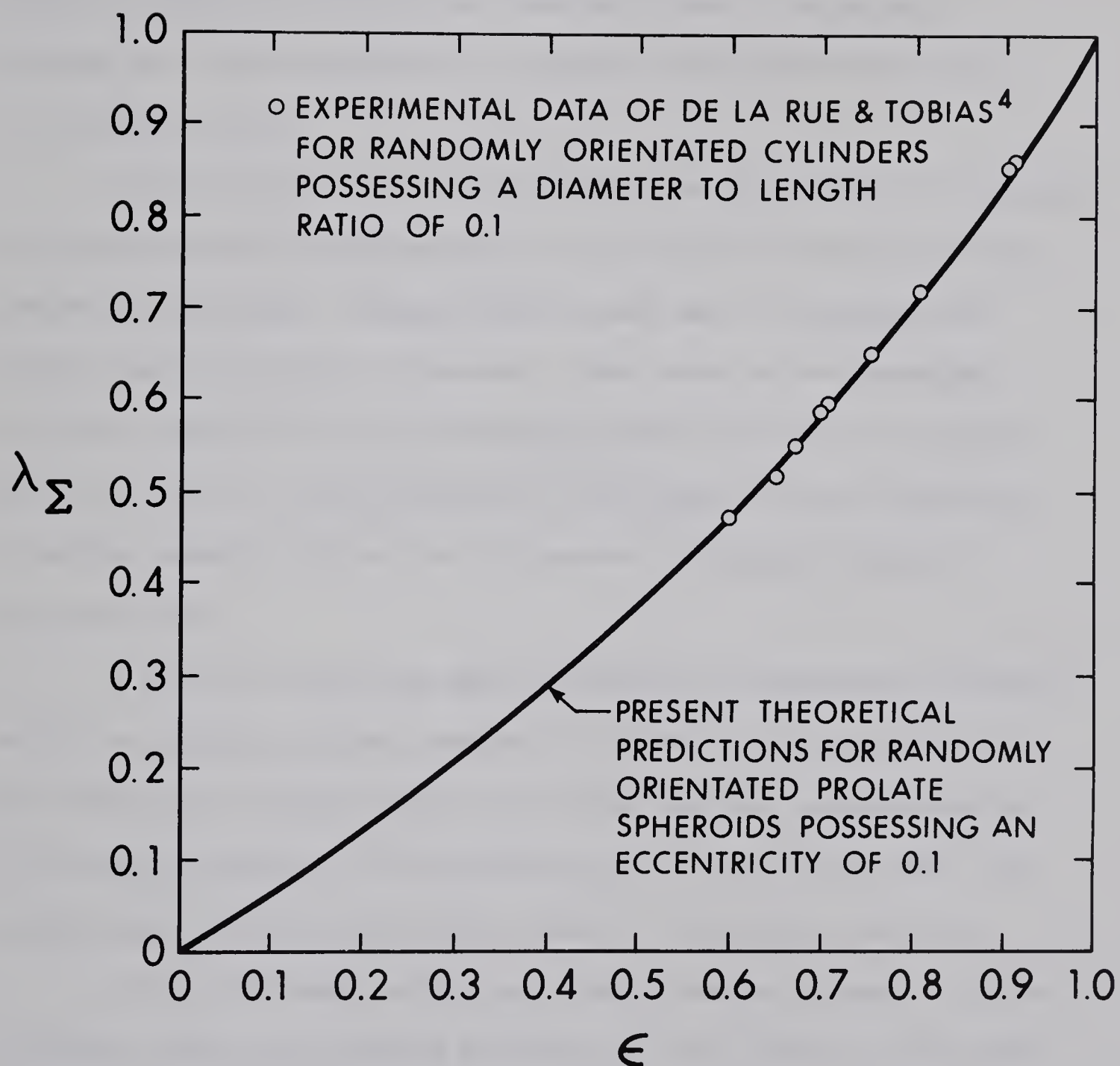


FIGURE 14. THE PREDICTED RESULTS FOR RANDOMLY ORIENTATED PROLATE SPHEROIDS: COMPARISON WITH EXPERIMENTAL DATA

I.13 SUMMARY

The presented results demonstrate that the proposed cell model offers a satisfactory representation not only of an isotropic swarm of spheres but also of an important class of anisotropic systems (viz. those composed of co-axially orientated disc-like or rod-like particles).

In particular, it has been demonstrated that swarms of co-axially orientated spheroids possessing an eccentricity of less than 0.5 are markedly anisotropic, although this is much more in evidence with oblate than with prolate spheroids. These results have important practical significance in those areas in which conductivity measurements are made on systems composed of flattish or fibrous particles, a notable example being on the deliberately deposited mudcakes in oil-well bores.

A study has also been made of diffusion (conduction) occurring within an isotropic system composed of randomly orientated spheroids. The diffusivity (conductivity) factor here has been demonstrated to be strongly dependent on the eccentricity for oblate spheroids, but surprisingly invariant with this parameter for prolate spheroids.

In view of these further encouraging results attempts will now be made to apply the proposed cell model to the study of a radically different, and far more complicated, transport process. This will involve incompressible creeping flow through an homogeneous swarm of spheres and will provide valuable insight into the nature of liquid flow through porous media in general.

PART II

STEADY STATE INCOMPRESSIBLE CREEPING FLOW
THROUGH AN HOMOGENEOUS
AND ISOTROPIC SWARM OF SPHERES

II.1 OBJECTIVES

The purpose of this investigation is to develop a fuller understanding of fluid flow occurring within an homogeneous and isotropic porous medium composed of spherical particles possessing an arbitrary size distribution; in particular, to evaluate the resistance offered by such a system to an incompressible fluid[†] in the creeping flow regime. In theory, the total resistance offered by such a system may be calculated by integrating the local shear stress over the entire surface thereof. However, so excessively complicated is the internal geometry of even the most regular array of spheres that resort must be made to a simplifying model.

On account of the encouraging results obtained during the preceding diffusion analyses, the proposed cell model will here be further employed to evaluate the *permeability* of an homogeneous swarm of spheres in the creeping flow regime. For liquid flow (with which this investigation will be exclusively concerned) through porous media it is generally acceptable to make this creeping flow assumption²⁸, namely that inertial forces may be neglected in comparison with viscous forces.

However, before proceeding further with the problem of interest it will firstly be elucidating to examine the nature of the equations which are normally employed to describe liquid flow through porous media, and which implicitly define the permeability thereof.

[†] Throughout this work attention will be confined to Newtonian fluids under isothermal conditions.

II.2 THE EQUATIONS GOVERNING INCOMPRESSIBLE CREEPING FLOW THROUGH POROUS MEDIA

There has been considerable dissension in the past concerning the nature of the differential equation which describes fluid flow through porous media. As a basis for further discussion it will here be convenient to consider the somewhat idealized system depicted in Figure 15, viz. an extent of homogeneous and isotropic porous material adjacent to a region of unobstructed fluid space.

Free Fluid Region

Throughout this region the validity of the Navier-Stokes Equation will be acknowledged. Thus, for the flow of a Newtonian fluid at a sufficiently low Reynolds number the hydrodynamic conditions within this region will be described by the equation²⁸:

$$\mu \nabla^2 \underline{u} = \underline{\nabla} p . \quad (80)$$

In this equation \underline{u} denotes the velocity vector, μ the absolute viscosity of the fluid and p the pressure referred to a datum plane.

Porous Medium Region

The following hypothetical differential form⁴², based on the pioneering experiments of Darcy in 1851, is generally quoted with confidence to describe incompressible creeping flow within an isotropic porous medium, viz.

$$-(\mu/\kappa) \underline{u}^* = \underline{\nabla} p^* . \quad (81)$$

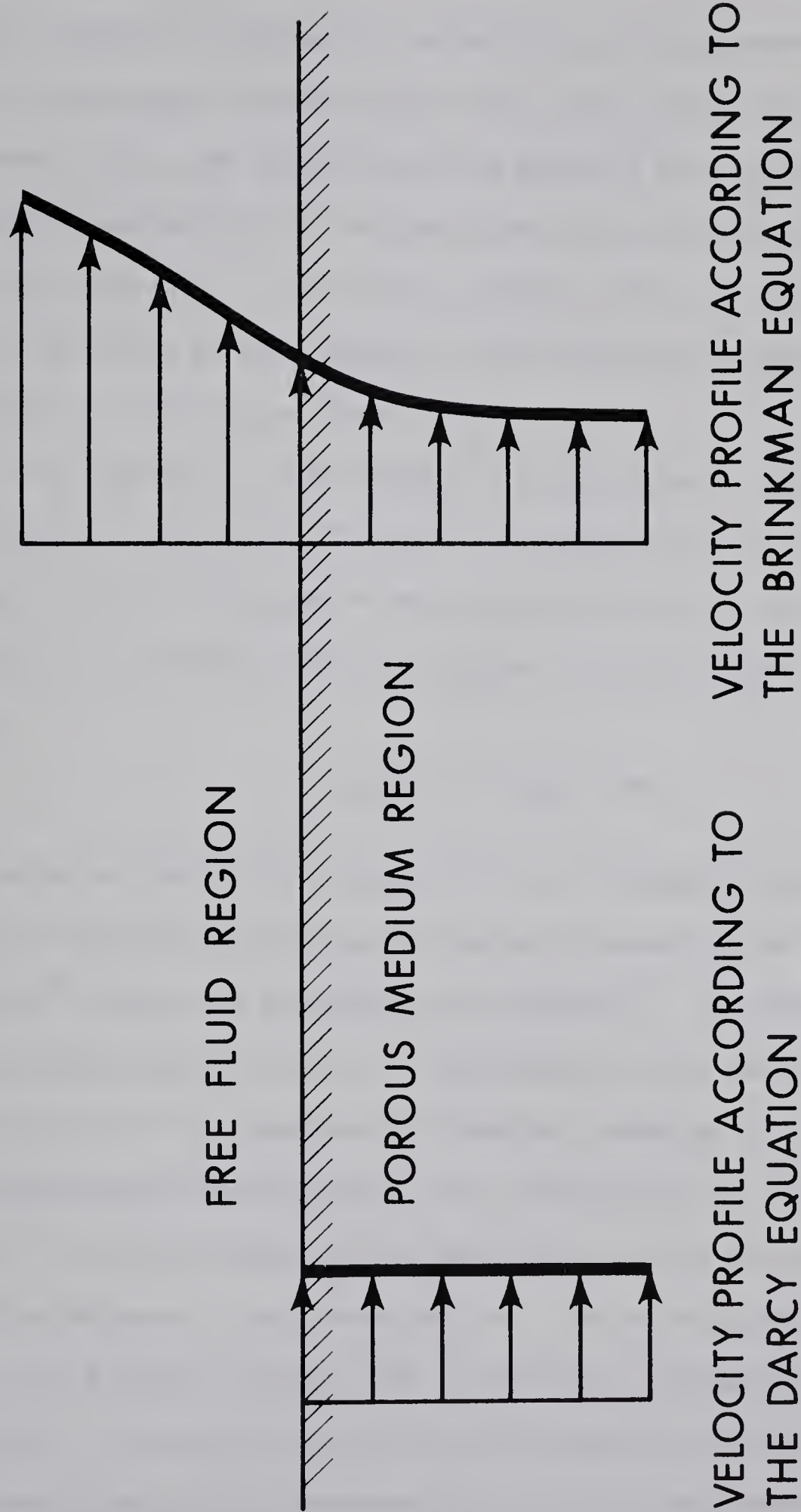


FIGURE 15. AN IDEALIZED TWO-REGION SYSTEM

In this equation κ denotes the *permeability* of the porous medium, \underline{u}^* the macroscopic velocity vector and p^* the local mean pressure referred to the same datum plane (the symbol $*$ will continue to designate macroscopically averaged quantities pertaining specifically to a porous medium). The velocity profile within the porous medium region according to this equation (now universally termed the Darcy Equation) is depicted in Figure 15.

As long ago as 1949 Brinkman³⁰ proposed that a viscous stress term need be incorporated in the Darcy Equation (81) in order to account for the distortion of macroscopic velocity profiles in the vicinity of containing walls and regions of unobstructed fluid space, thus:

$$-(\mu/\kappa)\underline{u}^* + \mu\nabla^2\underline{u}^* = \underline{\nabla}p^* . \quad (82)$$

This equation (hereafter referred to as the Brinkman Equation) has recently received encouraging theoretical substantiation from Slattery⁵⁴ and, quite independently, from Tam⁵⁵. For small values of κ the Brinkman Equation (82) is approximated by the Darcy Equation (81) whilst for $\kappa \rightarrow \infty$ it possesses the inherent advantage of developing into the Navier-Stokes Equation (80); this behaviour is to be anticipated because a non-porous mass and an unobstructed fluid represent the possible extremes of the porous medium. The velocity profile according to the Brinkman Equation (82) is displayed schematically in Figure 15. It should be noted that this equation further reduces to the Darcy Equation (81) whenever $\nabla^2\underline{u}^* = 0$, that is whenever the velocity vector \underline{u}^* is uniformly constant throughout the porous medium in question (as has been presumed in Darcy's pioneering experiments).

Considerations at the Interface

At the interface separating the two regions it is necessary that the limiting solution of the *micro*-flowfield associated with the free fluid region (as described by the Navier-Stokes Equation) must match correctly, when considered as a macro-flowfield, with the *macro*-flowfield associated with the porous medium region (as described by either the Darcy Equation or the Brinkman Equation), thereby reflecting physical consistency (Figure 15). This constitutes the principal reason as to why the Darcy Equation must be regarded as being incomplete and consequently inadequate, the explanation being that the Navier-Stokes Equation (80) is a differential equation of the second order whilst the Darcy Equation (81) is of the first order only; this makes it impossible to formulate physically rational boundary conditions at the interface using the Darcy representation within the porous region. However, this difficulty is not encountered when employing the Brinkman Equation (82), which is indeed of the second order by virtue of the presence of its viscous stress term; the inclusion of such a term is therefore imperative if physical consistency is to be maintained throughout the two region system depicted in Figure 15†.

† In order to demonstrate the consistency and effectiveness of the Brinkman Equation (82) three problems of considerable practical importance, which *cannot* be solved rigorously using the Darcy Equation (81), have been examined in some detail in Section II.9, Appendix D and Appendix E. These problems relate respectively to (1) sedimentation of an isolated *porous* sphere, (2) incompressible creeping flow parallel to a fracture within a petroleum reservoir, and (3) incompressible creeping flow through an isotropic porous medium containing a spherical cavity.

Having resolved matters concerning the nature of the differential equation which governs creeping flow through porous media it is now in order to return to the original problem of interest, viz. the application of the proposed cell model (Figures 1 and 2) to the study of incompressible creeping flow through an homogeneous swarm of spheres.

II.3 THE MODELLED SYSTEM FOR FLUID FLOW THROUGH AN HOMOGENEOUS SWARM OF SPHERES

The model representation for fluid flow through an homogeneous swarm of spheres is depicted in Figure 16; this may be compared with Figure 3 for the corresponding problem of diffusion. As before, it consists of a *reference sphere*, an *annular region* of void space and an *exterior region* of homogeneous and isotropic porous material. The radius of the unit cell (comprising the reference sphere and the annular region) must again be related according to Equation (1), viz.

$$S/R = (1-\epsilon)^{-1/3} \quad 0 \leq \epsilon < 1.0, \quad (83)$$

which ensures that the uniform porosity ϵ is not locally disturbed by the modelling procedure.

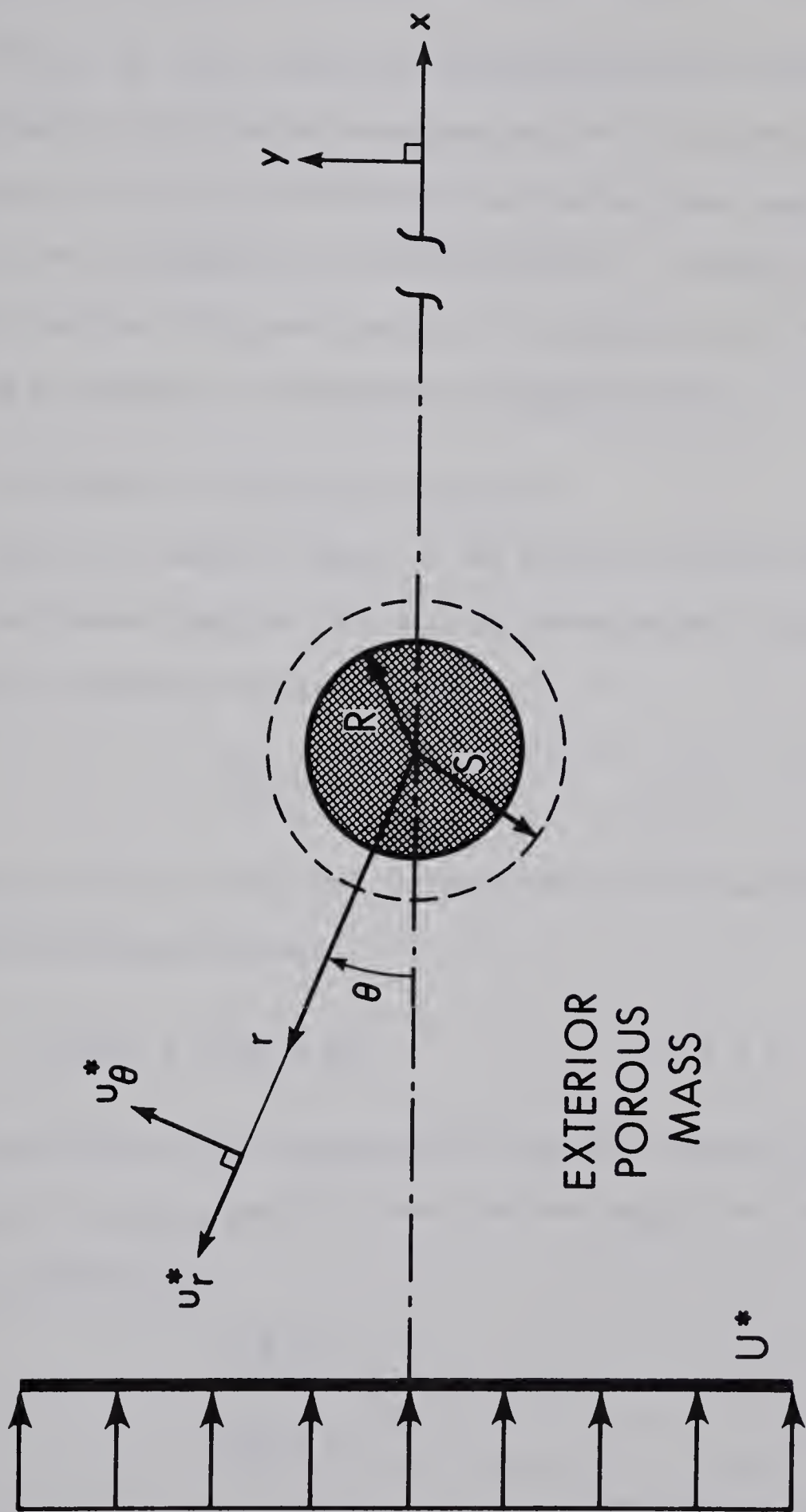


FIGURE 16. DESCRIPTION OF THE MODELLED SYSTEM FOR FLUID FLOW THROUGH AN HOMOGENEOUS SWARM OF SPHERES (Cross-Section Through Centre of Reference Sphere)

II.4 THE DEFINING EQUATIONS AND BOUNDARY CONDITIONS

It will be noted during the development which follows that the fundamental differential equations and the stipulated boundary conditions are radically different from, and far more complicated than, those for the corresponding diffusion problem. It should also be stressed that the subsequent analysis is rigorous in its entirety, requiring no physical or mathematical simplifications.

II.4.1 FUNDAMENTAL DIFFERENTIAL EQUATIONS

Within the annular region of the modelled system (Figure 16) the Navier-Stokes Equation (80) will be acknowledged to describe the prevailing creeping flowfield, thus:

$$\mu \nabla^2 \underline{u} = \underline{\nabla} p \quad R < r < S . \quad (84)$$

Within the exterior region the validity of the Brinkman Equation (82) will be proposed, thus:

$$-(\mu/\kappa) \underline{u}^* + \mu \nabla^2 \underline{u}^* = \underline{\nabla} p^* \quad S < r < \infty . \quad (85)$$

For steady state incompressible flow the continuity equation²⁸ assumes the following specific forms for the annular and exterior regions respectively:

$$\underline{\nabla} \cdot \underline{u} = 0 , \quad (86)$$

$$\underline{\nabla} \cdot \underline{u}^* = 0 . \quad (87)$$

The terms involving pressure in Equations (84) and (85) may be annihilated by performing the *curl* vector operation throughout.

By noting that pressure is a scalar quantity, and that μ and κ are independent of location, the following expressions are obtained, viz.

$$\mu[\nabla \times \nabla^2 \underline{u}] = [\nabla \times \nabla p] = 0 , \quad (88)$$

$$-(\mu/\kappa)[\nabla \times \underline{u}^*] + \mu[\nabla \times \nabla^2 \underline{u}^*] = [\nabla \times \nabla p^*] = 0 . \quad (89)$$

The system of Euler (stationary) coordinates convenient to this investigation will be spherical coordinates $[r, \theta, \phi]$, for which:

$$\underline{u} = [u_r, u_\theta, u_\phi] , \quad (90)$$

$$\underline{u}^* = [u_r^*, u_\theta^*, u_\phi^*] . \quad (91)$$

The expansions of the individual terms in Equations (88) and (89) in spherical coordinates are presented in numerous texts, notably Bird et al²⁸. On account of the specifications introduced so far the prevailing flowfield will exhibit axial symmetry. Thus, $u_\phi = 0$ and $u_\phi^* = 0$; hence, the ϕ variable may hereafter be suppressed. Consequently, streamfunctions ψ and ψ^* may now be introduced; these are defined in such a manner²⁸ as to automatically satisfy the continuity conditions implicit in Equations (86) and (87), viz.

$$u_r(r, \theta) = -(1/r^2 \sin \theta)(\partial \psi / \partial \theta) ; u_\theta(r, \theta) = (1/r \sin \theta)(\partial \psi / \partial r) , \quad (92)$$

$$u_r^*(r, \theta) = -(1/r^2 \sin \theta)(\partial \psi^* / \partial \theta) ; u_\theta^*(r, \theta) = (1/r \sin \theta)(\partial \psi^* / \partial r) . \quad (93)$$

On substituting these expressions into the expanded forms of Equations (88) and (89) the following partial differential equations can eventually be obtained:

annular region: $E^2(E^2\psi) = 0 \quad R < r < S , \quad (94)$

exterior region: $-(1/\kappa)E^2\psi^* + E^2(E^2\psi^*) = 0 \quad S < r < \infty . \quad (95)$

In these Equations E^2 denotes the Spherical Harmonic Operator^{28,42}, defined by:

$$E^2 \equiv (\partial^2/\partial r^2) + (1/r^2)(\partial^2/\partial \theta^2) - (\cot\theta/r^2)(\partial/\partial \theta) . \quad (96)$$

In order to describe the hydrodynamic conditions prevailing throughout the entire domain of the modelled system it will be necessary to determine respective solutions of Equations (94) and (95) which satisfy physically rational boundary conditions.

II.4.2 STIPULATED BOUNDARY CONDITIONS

Recognizing that the reference sphere is impermeable, and that there is no slip over the surface thereof, implies that:

$$u_r(R^+, \theta) = 0 , \quad (97)$$

$$u_\theta(R^+, \theta) = 0 . \quad (98)$$

From considerations of equilibrium and continuity at the interface separating the annular and exterior regions it is necessary that the pressure, the tangential shear stress and the velocity distributions within these regions match identically in the limit, viz.

$$p(S^-, \theta) = p^*(S^+, \theta) , \quad (99)$$

$$\tau(S^-, \theta) = \tau^*(S^+, \theta) , \quad (100)$$

$$u_r(S^-, \theta) = u_r^*(S^+, \theta) , \quad (101)$$

$$u_\theta(S^-, \theta) = u_\theta^*(S^+, \theta) . \quad (102)$$

Moreover, the velocity vector \underline{u}^* at any station sufficiently far removed from the reference sphere must approach that of the mainstream, \underline{U}^* , thus:

$$\lim_{r \rightarrow \infty} \underline{u}^*(r, \theta) = \underline{U}^* , \quad (103)$$

where $\underline{U}^* = [U^*, 0, 0]$ in Cartesian coordinates $[x, y, z]$.

II.5 SOLUTION OF THE DEFINING EQUATIONS

II.5.1 THE GLOBAL STREAMFUNCTION DISTRIBUTION

The flowfield throughout the modelled system will be completely defined by the respective solutions of Equations (94) and (95) which satisfy the boundary conditions stipulated in Equations (97)-(103). As detailed in Appendix C these solutions are found to be:

$$\psi(\chi, \theta) = (\kappa U^*/2)[A/\chi + B\chi + C\chi^2 + D\chi^4]\sin^2\theta \quad \alpha < \chi < \beta, \quad (104)$$

$$\psi^*(\chi, \theta) = (\kappa U^*/2)[E/\chi + \chi^2 + Ge^{-\chi}(1+\chi)/\chi]\sin^2\theta \quad \beta < \chi < \infty, \quad (105)$$

where χ denotes the normalized radial coordinate defined by:

$$\chi = r/\sqrt{\kappa}. \quad (106)$$

The parameters α and β denote the specific values of χ defined by:

$$\alpha = R/\sqrt{\kappa}, \quad (107)$$

$$\beta = S/\sqrt{\kappa}, \quad (108)$$

and A, B, C, D, E and G are expressed in terms of α and β as follows:

$$A = 6\alpha^3(-2\beta^6-7\beta^5-15\beta^4-15\beta^3+3\beta^4\alpha^2-\beta^3\alpha^3+3\beta^3\alpha^2+\beta^2\alpha^3)/J(\alpha, \beta), \quad (109)$$

$$B = 6\alpha(6\beta^6+21\beta^5+45\beta^4+45\beta^3-5\beta^4\alpha^2-5\beta^3\alpha^2-\beta\alpha^5-\alpha^5)/J(\alpha, \beta), \quad (110)$$

$$C = 3(-8\beta^6-28\beta^5-60\beta^4-60\beta^3+5\beta^3\alpha^3-5\beta^2\alpha^3+3\beta\alpha^5+3\alpha^5)/J(\alpha, \beta), \quad (111)$$

$$D = 3(4\beta^4+4\beta^3-3\beta^3\alpha+3\beta^2\alpha-\beta\alpha^3-\alpha^3)/J(\alpha, \beta), \quad (112)$$

$$\begin{aligned} E = 2(-4\beta^9-24\beta^8-60\beta^7-60\beta^6+9\beta^8\alpha+45\beta^7\alpha-10\beta^6\alpha^3+126\beta^6\alpha-30\beta^5\alpha^3 \\ +216\beta^5\alpha+9\beta^4\alpha^5-60\beta^4\alpha^3+270\beta^4\alpha-4\beta^3\alpha^6+9\beta^3\alpha^5 \\ -60\beta^3\alpha^3+270\beta^3\alpha-6\beta\alpha^6-6\alpha^6)/J(\alpha, \beta), \end{aligned} \quad (113)$$

$$G = 6e^\beta(20\beta^6-27\beta^5\alpha+5\beta^3\alpha^3-90\beta^3\alpha+2\alpha^6)/J(\alpha, \beta), \quad (114)$$

where:

$$J(\alpha, \beta) = (-4\beta^6 - 24\beta^5 - 180\beta^4 - 180\beta^3 + 9\beta^5\alpha + 45\beta^4\alpha - 10\beta^3\alpha^3 + 180\beta^3\alpha - 30\beta^2\alpha^3 + 9\beta\alpha^5 - 4\alpha^6 + 9\alpha^5) . \quad (115)$$

The parameters α and β appearing above are related according to Equations (107), (108) and (83), thus:

$$\beta = \alpha(S/R) = \alpha(1-\epsilon)^{-1/3} . \quad (116)$$

II.5.2 DISTURBANCE INTRODUCED BY THE MODELLING PROCEDURE

Typical streamlines, as computed from Equations (104) and (105), are displayed in Figure 17 for the modelled system possessing the representative porosity $\epsilon = 0.7$ (for which $S/R = 1.494$ from Equation (83), $\alpha = 3.708$ from Table 3 to follow, whence $\beta = 5.540$ from Equation (116)). The streamlines for other porosities are very similar in appearance.

The most important implication of Figure 17 is that the disturbance of the mainstream flowfield introduced by the modelling procedure diminishes rapidly with increasing distance from the unit cell: this disturbance is effectively confined to a region concentric with the unit cell and possessing twice its radius (it will be recalled that for the corresponding case of diffusion (Section I.3.4) this disturbance was wholly confined to within the unit cell). This observation counters any argument that the modelling procedure might cause anything more than an (inevitable) localized disturbance of the mainstream flowfield.

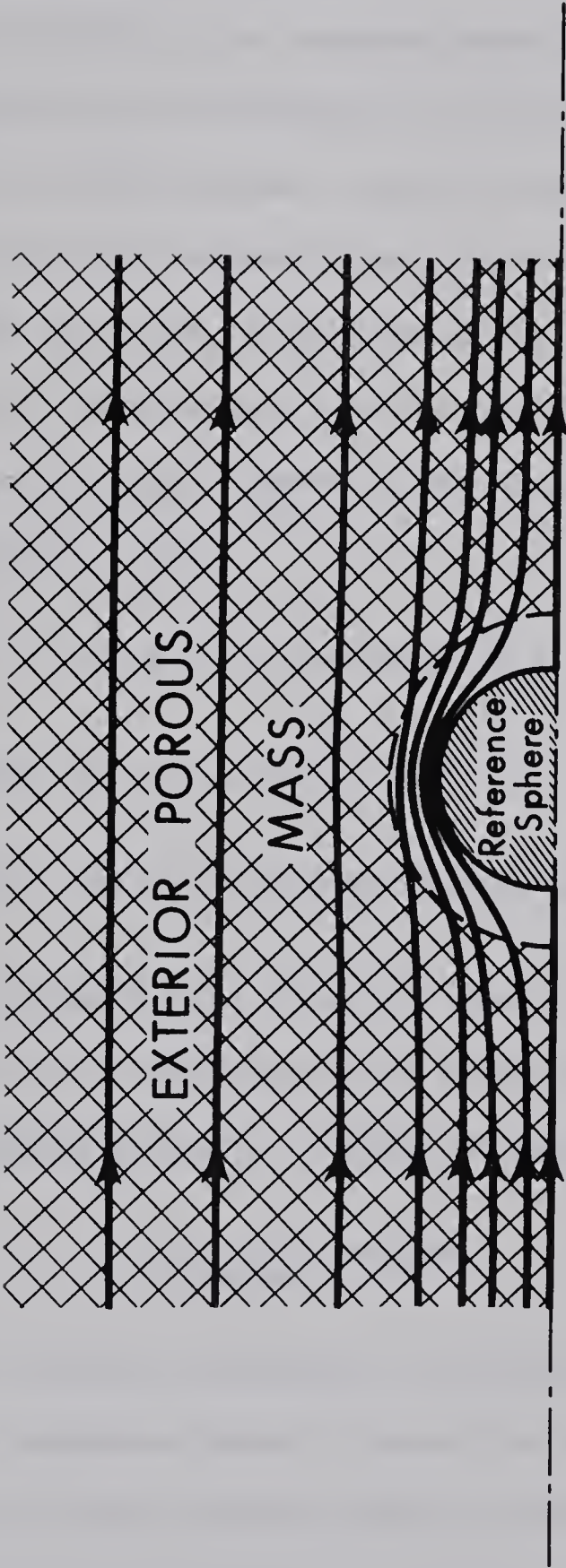


FIGURE 17. TYPICAL STREAMLINES FOR INCOMPRESSIBLE CREEPING FLOW THROUGH THE MODELLED SYSTEM (For The Representative Porosity $\epsilon = 0.7$)

II.5.3 THE RESISTANCE OFFERED BY THE REFERENCE SPHERE

Using the derived expression for the streamfunction within the annular region, $\psi(\chi, \theta)$, it is straightforward, although tedious, to develop expressions for the pressure and shear stress distributions over the surface of the reference sphere, $p(\alpha, \theta)$ and $\tau(\alpha, \theta)$ respectively. The normal and tangential resistance forces offered by the reference sphere (F_r and F_θ respectively) may then be calculated by integrating these distributions over the entire surface thereof. The total resistance force, F , offered by the reference sphere is so derived in Appendix C, viz.

$$F = F_r + F_\theta = 6\pi\mu U^* R \xi(\alpha, \beta) , \quad (117)$$

where the function $\xi(\alpha, \beta)$ is defined by:

$$\xi(\alpha, \beta) = 4(-6\beta^6 - 21\beta^5 - 45\beta^4 - 45\beta^3 + 5\beta^4\alpha^2 + 5\beta^3\alpha^2 + \beta\alpha^5 + \alpha^5) / J(\alpha, \beta) . \quad (118)$$

It will be demonstrated later (Table 3) that as $\varepsilon \rightarrow 1.0$, $\xi(\alpha, \beta) \rightarrow 1.0$ so that Equation (117) then approaches Stokes Law²⁸ for creeping flow past a single sphere in space, as would be expected, viz.

$$F_{\text{Stokes}} = 6\pi\mu U^* R . \quad (119)$$

The term $\xi(\alpha, \beta)$ therefore represents the extent to which the spheres surrounding the reference sphere increase the latter's resistance over that predicted by Stokes Law for a single isolated sphere.

II.5.4 THE TOTAL RESISTANCE OFFERED BY A SWARM OF MONOSIZED SPHERES

This analysis has heretofore been concerned with an *unbounded* homogeneous swarm of spheres. As noted earlier in Section II.2 the Darcy Equation (81) is valid for macroscopically uniform flow through such a system. According to this equation the total resistance offered by a swarm containing N *monosized* spheres of radius R will be (Equation (C71)):

$$F = 6\pi\mu U^* R N \{2\alpha^2/9(1-\epsilon)\} . \quad (120)$$

The total resistance offered by the *modelled* system may be evaluated by summing Equation (117) over all N spheres (since each individual sphere may be regarded as the reference sphere in turn), thus:

$$F = 6\pi\mu U^* R N \xi(\alpha, \beta) . \quad (121)$$

Since the modelled system is to be quantitatively representative of the original swarm of monosized spheres then the resistance forces predicted by Equations (120) and (121) must be identical. This generates the condition that:

$$2\alpha^2 - 9(1-\epsilon)\xi(\alpha, \beta) = 0 , \quad (122)$$

with the parameters α and β being related according to Equation (116), thus:

$$\beta = \alpha(1-\epsilon)^{-1/3} . \quad (123)$$

Consequently, Equation (122) may be re-expressed as the following implicit function of α and ϵ , viz.

$$2\alpha^2 - 9(1-\epsilon)\xi(\alpha, \alpha(1-\epsilon)^{-1/3}) = 0 . \quad (124)$$

This equation effectively defines the functional relationship existing between $\alpha = R/\sqrt{\kappa}$ and the porosity ϵ for any homogeneous swarm of mono-sized spheres.

II.5.5 COMPUTED RESULTS FOR MONOSIZED SPHERES

Recalling from Equation (118) the extremely complicated nature of the function $\xi(\alpha, \beta)$ it is apparent that α cannot be extracted from Equation (124) above as a function of ϵ in closed form. Resort must therefore be made to an iterative, and in consequence pointwise, technique of solution. As expected, Equation (124) constitutes a single valued function over the entire porosity range; the *regula falsi* technique provides a rapid iteration on α using a digital computer. Representative values of the $\alpha = \alpha(\epsilon)$ relationship, satisfying Equation (124) to within better than 10^{-10} , were obtained using this technique. These results are presented (to four significant figures) in Table 3 for reference; it will be noted that these predictions are physically consistent at both porosity limits, thus as $\epsilon \rightarrow 0$, $\alpha \rightarrow \infty$ and as $\epsilon \rightarrow 1.0$, $\alpha \rightarrow 0$.

It is particularly instructive to compare the resistance of the original system as predicted by Stokes Law, when assuming each sphere to be hydrodynamically independent of the remainder, with that predicted by the presented theory. This ratio, W , for monosized spheres is given by (Equation (C86)):

$$W = 9(1-\epsilon)/2\alpha^2 = 1/\xi(\alpha, \alpha(1-\epsilon)^{-1/3}) . \quad (125)$$

TABLE 3

THE PREDICTED DEPENDENCE OF α AND W
ON ϵ FOR HOMOGENEOUS SWARMS OF
MONOSIZED SPHERES

ϵ	α	$W = 1/\xi(\alpha, \beta)$
1.0	0.0	1.0
0.9999999999	0.2003×10^{-4}	0.9994
0.99999999	0.2124×10^{-3}	0.9968
0.999999	0.2137×10^{-2}	0.9850
0.9999	0.2200×10^{-1}	0.9300
0.999	0.7282×10^{-1}	0.8487
0.99	0.2584	0.6738
0.95	0.7071	0.4501
0.90	1.185	0.3207
0.85	1.684	0.2379
0.80	2.247	0.1782
0.75	2.908	0.1331
0.70	3.708	0.9819×10^{-1}
0.65	4.706	0.7112×10^{-1}
0.60	5.986	0.5023×10^{-1}
0.55	7.677	0.3436×10^{-1}
0.50	9.974	0.2262×10^{-1}
0.45	13.19	0.1423×10^{-1}
0.40	17.83	0.8496×10^{-2}
0.35	24.74	0.4780×10^{-2}
0.30	35.44	0.2508×10^{-2}
0.25	52.93	0.1205×10^{-2}
0.20	83.87	0.5118×10^{-3}
0.15	146.0	0.1794×10^{-3}
0.10	302.7	0.4419×10^{-4}
0.05	967.9	0.4564×10^{-5}
0.0	∞	0.0

The $W = W(\epsilon)$ relationship predicted by this equation is displayed in Table 3.

II.5.6 COMPARISON OF COMPUTED RESULTS WITH EXPERIMENTAL DATA

Figure 19 displays the $\alpha = \alpha(\epsilon)$ relationship for monosized spheres, as predicted by Equation (124), together with representative data from the literature^{25,43,47,48,53}. The overall agreement can be seen to be very satisfactory.

In keeping with literature trends the preceding results are presented in alternative form in Figure 20, which displays the $W = W(\epsilon)$ relationship predicted by Equation (125).

In connection with both Figures 19 and 20 it should be emphasized that the data of Happel and Epstein⁴³ and Martin et al⁴⁸ was obtained using regular assemblages⁴⁰ of spheres rather than using a random assemblage thereof³⁷. This is possibly the reason as to why their data points lie rather less close to the present predictions than do those of the other cited workers (who confined their attention to randomly arranged spheres).

Present Experimental Work

In order to confirm the validity of existing experimental data in the lower porosity range a number of permeability determinations were carried out using a cylindrical brass cell which was filled, under distilled water, with monosized stainless steel spheres (Figure 18). Distilled water at a constant temperature could be made to flow through the cell at a pre-selected constant flowrate (effected by means of a commercial constant-flow regulator). For each constant

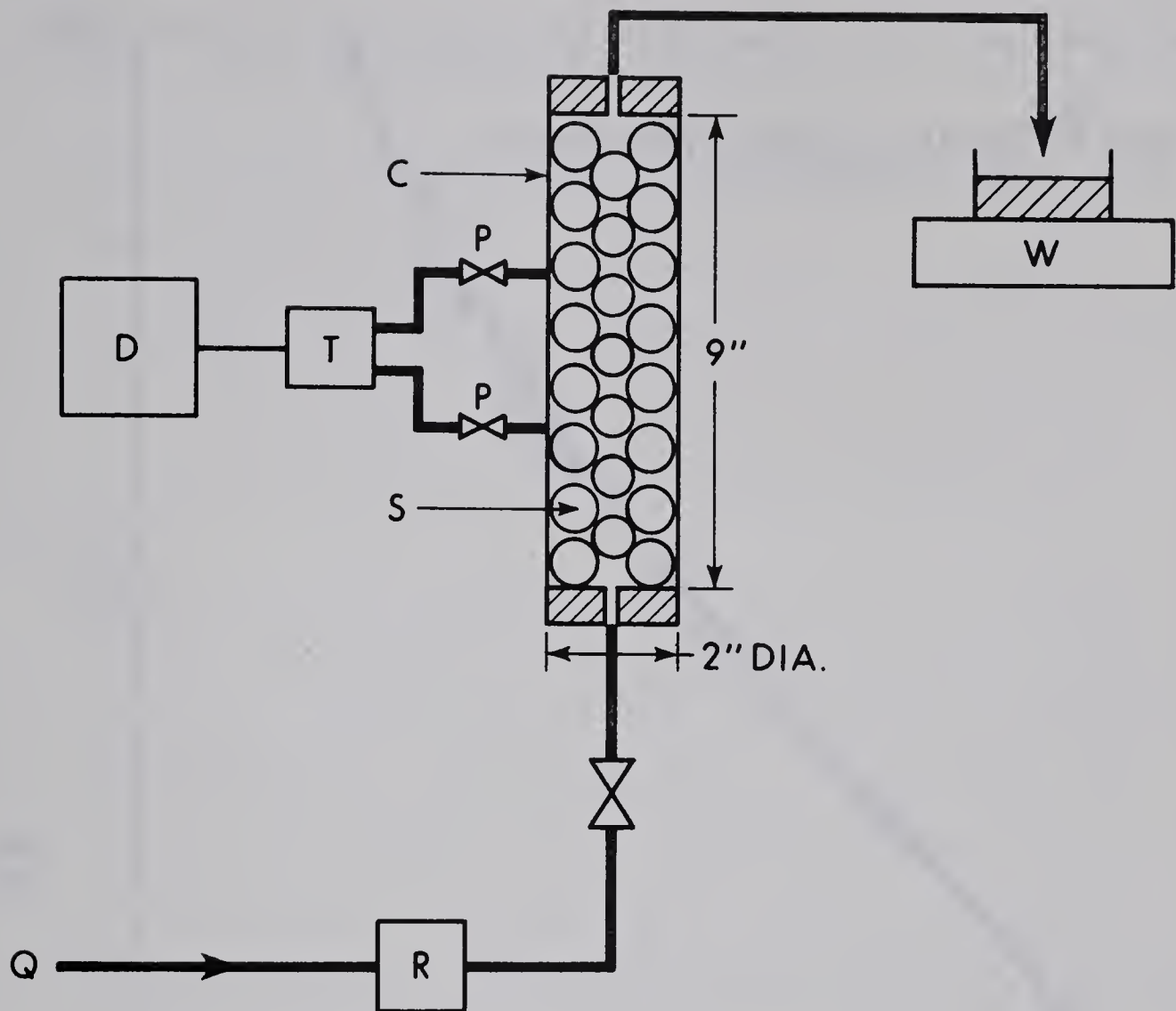
flowrate the pressure gradient in the direction of flow was ascertained by means of a pressure transducer (periodically calibrated against a high precision differential manometer). The permeability of the system was then calculated according to Equation (81). Finally, the porosity of the system was determined by a weighing technique (although the minimum porosity obtainable with monosized spheres is 0.2575, corresponding to a regular rhombohedral array⁴⁰, it is seldom possible to obtain a porosity lower than 0.37 with randomly arranged spheres).

Several measurements were carried out within the Reynolds number range $Re = 0.08 - 1.40$ (based on the superficial liquid velocity and the particle diameter). Within this range little discernible change in the measured permeability could be observed. This data is presented in normalized form in Table 4 below and in Figure 23 to follow. As displayed in Figures 19 and 20 this data conforms closely with previously reported experimental data.

TABLE 4

EXPERIMENTAL PERMEABILITY DATA FOR AN
HOMOGENEOUS SWARM OF MONOSIZED SPHERES

$\varepsilon = 0.379$		
Re	α	W
0.081	19.08	0.00768
0.093	19.12	0.00765
0.168	19.10	0.00766
0.192	19.09	0.00769
0.251	19.12	0.00765
0.290	19.10	0.00766
0.552	19.10	0.00766
0.670	19.13	0.00764
0.807	19.11	0.00765
0.932	19.14	0.00763
1.38	19.16	0.00762



KEY:

C CYLINDRICAL BRASS CELL

S STAINLESS STEEL SPHERES (1mm dia. bearing balls)

Q DISTILLED WATER SUPPLY (20-100 psig.)

P PRESSURE TAPS (spaced 3" apart)

W WEIGHING SCALE

R CONSTANT FLOW REGULATOR
(Moore Instrument Co. model 63BU)

T PRESSURE TRANSDUCER (Whittaker Corp. model KP15)

D DIGITAL VOLTMETER (Non-Linear Systems Inc. model X-3)

FIGURE 18. EQUIPMENT USED FOR THE EXPERIMENTAL DETERMINATION OF THE PERMEABILITY OF A PACK OF SPHERES

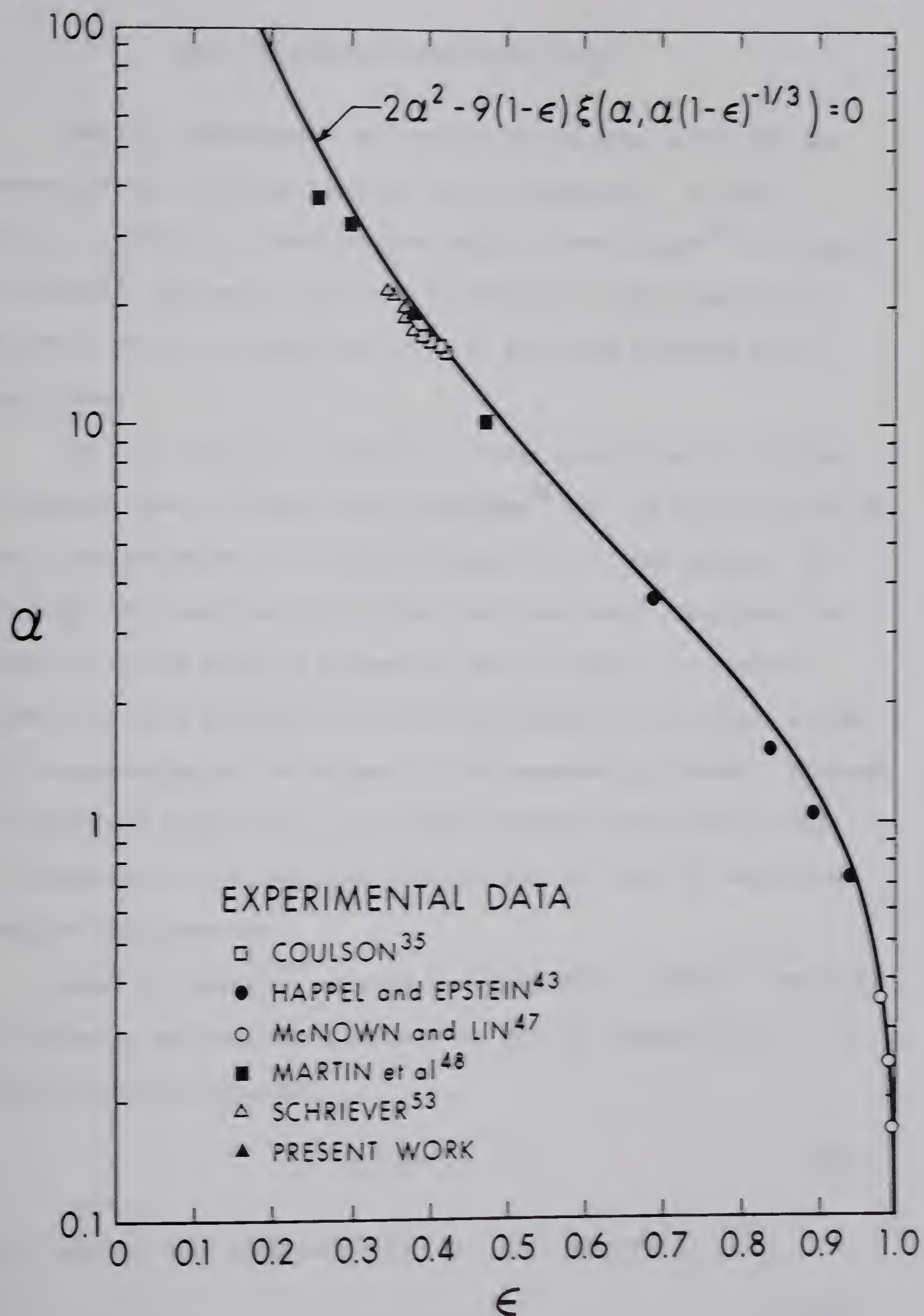


FIGURE 19. THE PREDICTED DEPENDENCE OF α ON ϵ FOR MONOSIZED SPHERES: COMPARISON WITH EXPERIMENTAL DATA

II.6 DISCUSSION OF PREVIOUS WORK

Numerous experimental and theoretical studies concerning the present problem have been reported in the literature. As these have been reviewed in conscientious detail by Scheidegger⁵² and Happel and Brenner⁴² discussion will here be limited to those theoretical treatments which are considered to be of principal interest and significance.

The first worker to establish a model concerning the problem of interest appears to have been Cunningham³⁶ who, in 1910, studied the rate of sedimentation of a cloud of spheres in a fluid medium. He postulated that each particle within the cloud would effectively be limited to motion within a concentric mass of fluid. He further assumed the outer boundary of this fluid envelope to be solid, presumably corresponding to the surface of the surrounding spheres. Although of fundamental significance, this model presents difficulty in that the dimensions of the spherical envelope must be fixed by additional empirical considerations.

Based on Kozeny's⁴⁵ classic capillary model, Carman³⁴ developed the following semi-empirical correlation for the permeability, κ , of a bed of monosized spheres:

$$\kappa = R^2 \epsilon^3 / \{9K_c (1-\epsilon)^2\} , \quad (126)$$

which together with Equations (107) and (125) becomes:

$$W = \epsilon^3 / \{2K_c (1-\epsilon)\} . \quad (127)$$

The parameter K_c denotes the so called 'Carman constant' which has to be determined by experiment. The universally acknowledged value of K_c for spheres is 5.0, for which Equation (127) becomes reasonably representative of a vast quantity of experimental data within the porosity range $0.26 < \epsilon < 0.7$ (Figure 20).

One of the more widely quoted theories concerning the present problem is that due to Brinkman²⁹. He extended the model proposed by Bruggemann³³ for electrical conduction (Section I.4) to the case of creeping flow, the representation underlying both treatments being that of a spherical particle embedded within a uniform porous mass. Brinkman obtained the following solution for an homogeneous swarm of monosized spheres:

$$W = 1 + \alpha + \alpha^2/3 = 1 - (3/4)(1-\epsilon) [\sqrt{8/(1-\epsilon)} - 3] . \quad (128)$$

However, this solution is entirely unsatisfactory for $\epsilon < 0.4$ and, in fact, predicts zero permeability for $\epsilon = 1/3$ (Figure 20)[†].

[†] Referring here to the predictions of the present theory it is elucidating to consider the limit of Equation (125) as $\beta \rightarrow \alpha$, that is as the thickness of the annular region in the proposed model tends to zero. Under these conditions the proposed model reduces to the simpler one employed by Brinkman; an inspection of Equation (125) in conjunction with Equation (118) ultimately yields:

$$\begin{aligned} \text{Limit } W &= \text{Limit } [1/\xi(\alpha, \beta)] = 1 + \alpha + \alpha^2/3 . \\ \beta &\rightarrow \alpha \qquad \beta \rightarrow \alpha \end{aligned}$$

This is identical with the Brinkman solution as would be expected.

Aiming to generalize his model to include porous spheres Brinkman³¹ made attempts to incorporate an annular region which could be varied in size so as to present the experimental facts throughout the entire porosity range. However, this valuable contribution has been neglected in the literature to date, probably on account of the fact that his revised solution was physically inconsistent and was presented without derivation.

Uchida⁵⁶ attempted a rigorous solution of the Navier-Stokes and continuity equations for incompressible creeping flow through an unbounded cubic assemblage of monosized spheres. However, the problem of simultaneously satisfying the appropriate boundary conditions on spherical as well as cubical surfaces proved to be intractable and he was only able to extract an approximate solution; this failure to solve exactly the specified boundary value problem resulted in very unsatisfactory predictions.

Happel⁴¹ proposed an interesting cell-type model which is now referred to as the 'free surface model'. It is apparently based on a refinement of Cunningham's³⁶ previously discussed cell model, the solid outer envelope thereof here being replaced by a free fluid surface on which both the normal velocity and the tangential shear stress vanish. Using this representation Happel derived the following expression for monosized spheres:

$$W = [6 - 9(1-\epsilon)^{1/3} + 9(1-\epsilon)^{5/3} - 6(1-\epsilon)^2] / [6 + 4(1-\epsilon)^{5/3}] . \quad (129)$$

Although the free surface model may be superficially unconvincing the agreement of its predictions with experimental data is undeniable. It is interesting to note that the predictions of the presented theory are in remarkably close agreement with those of Happel for $\epsilon > 0.7$, nowhere differing by more than 1% (Figure 20).

Kuwabara⁴⁶ modified the free surface model by replacing the zero shear stress condition at the outer envelope by one of zero vorticity. However, his predictions are far less satisfactory than those of Happel.

Various statistical models have been advanced to study fluid flow through porous media in general. A number of these have been reviewed by Scheidegger⁵² (who himself proposed a model in which the theory of Brownian motion is applied to the problem in question). Of significant interest amongst these is the approach of Yuhara who postulated an analogy between laminar flow in porous media and turbulent flow in bulk fluids. On a somewhat different theme Broadbent and Hammersley proposed a model in which any 'randomness' is attached to the medium rather than to the fluid (this is generally the case in practice). Although such approaches are extremely interesting they tend (at present) to be too qualitative in nature to permit any direct engineering application.

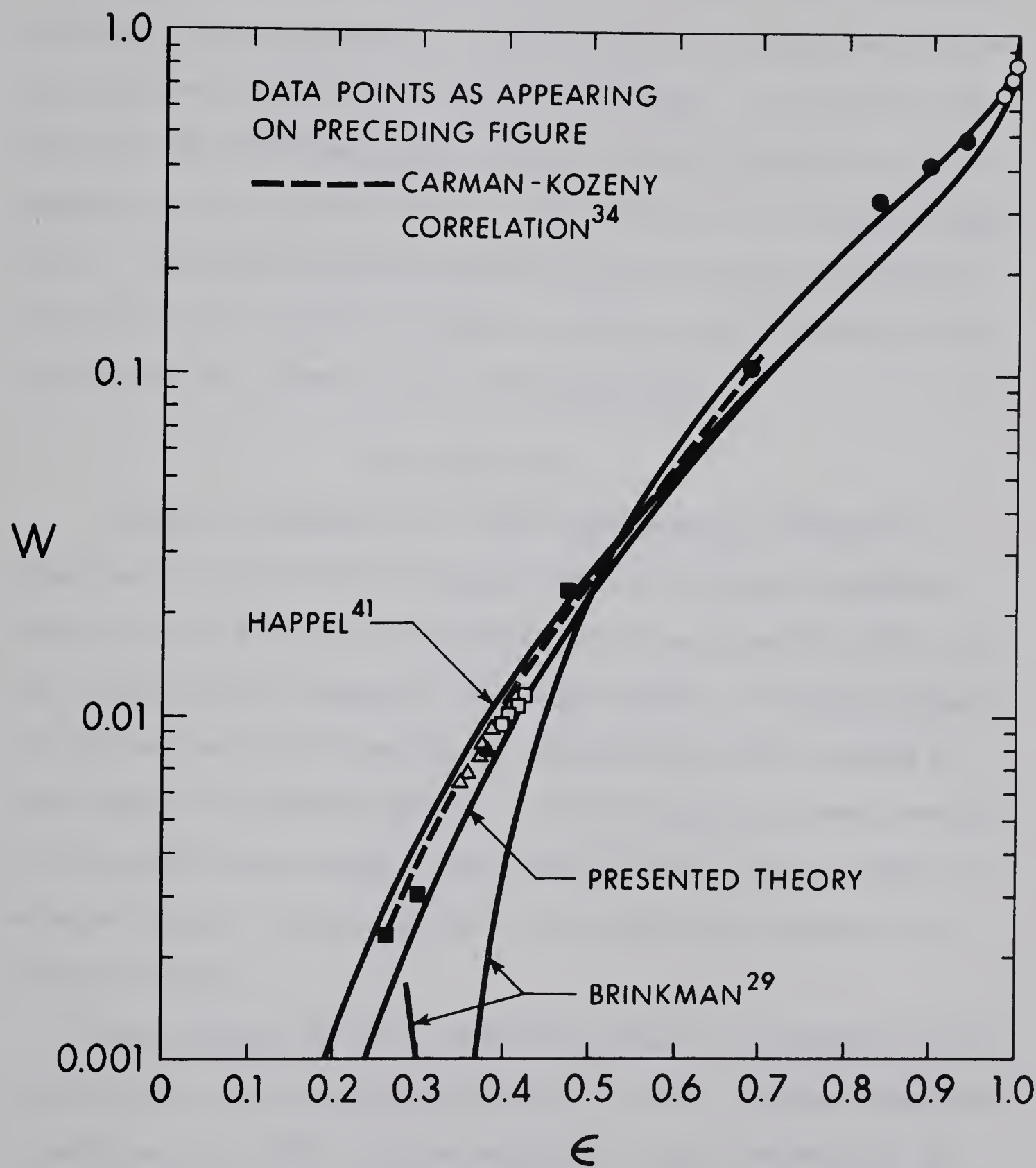


FIGURE 20. THE DEPENDENCE OF W ON ϵ FOR MONOSIZED SPHERES:
COMPARISON WITH PREVIOUS WORK

II.7 THE EFFECTS OF THE SIZE DISTRIBUTION

It was noted in Section I.3 that for *diffusive* flow processes occurring within an homogeneous swarm of spheres the size distribution had little or no effect on the diffusivity factor. In contrast, for fluid flow the presented theory predicts a definite dependence of the permeability on the prevailing size distribution of the spheres (Appendix C). The specific predictions which follow have been confined to binary mixtures of spheres in order to permit a more meaningful interpretation of the effects of the size distribution.

Size Ratio 5:1

Figure 21 displays the $W = W(\epsilon)$ relationships predicted by Equations (C84) and (C82) for binary mixtures of spheres possessing arbitrary radii R and $R/5$, in the relative proportions 100%, 50%, 25%, 10%, 1.74% and 0% by numbers of the larger species. As would be expected the results for 100% and 0% are identical since both systems are then composed of monosized spheres. Mixtures containing more than 50% of the larger species exhibit characteristics very close to those for monosized spheres and have therefore been omitted from Figure 21 to preserve clarity.

The solutions for 50%, 25% and 10% display an increasing departure from that for monosized spheres and, in fact, a maximum departure is predicted for 1.74%. As this proportion further decreases to 0% the solution rapidly re-approaches that for monosized spheres. Hence, the solution for any arbitrary mixture possessing a 5:1 size ratio will always lie between that for monosized spheres and that for the mixture

containing 1.74% of the larger species.

Size Ratio 2:1

Figure 22 displays the results predicted by Equations (C84) and (C82) for binary mixtures of spheres possessing arbitrary radii R and $R/2$. However, only the two limiting solutions (viz. that for monosized spheres and that exhibiting the maximum departure therefrom) have been included because, although the general trends are closely similar to those for the 5:1 size ratio, the corresponding departures are very much less pronounced. The maximum departure is here exhibited by the mixture containing 15.2% of the larger species.

The most important inference to be drawn from Figures 21 and 22 is that W , and hence the permeability of the system, do indeed depend on the prevailing size distribution of the spheres; this dependency increases rapidly with the size ratio. Equations (C84) and (C82) may likewise be employed to accomodate ternary, quaternary and higher order mixtures should the occasion arise.

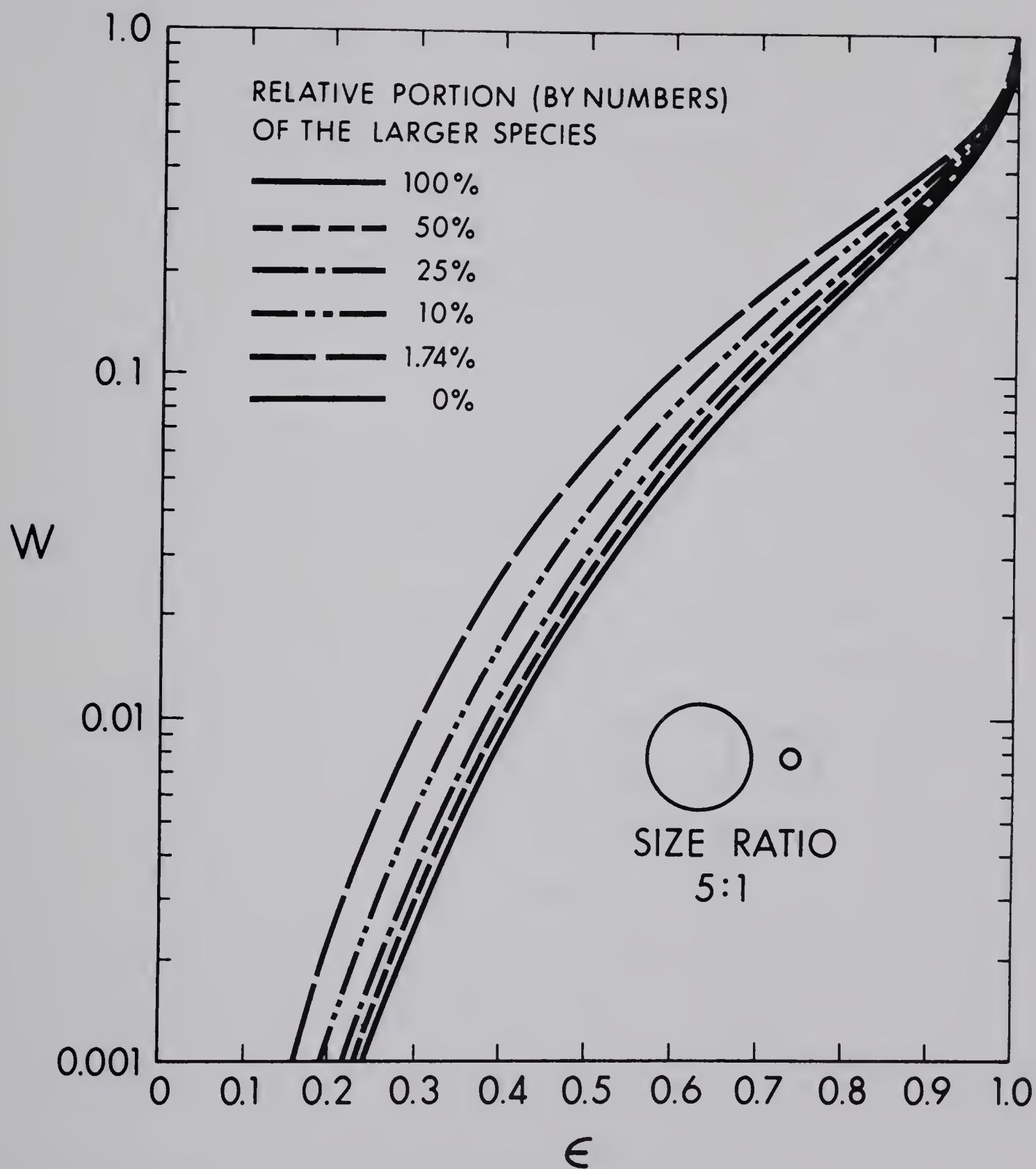


FIGURE 21. THE EFFECTS OF THE SIZE DISTRIBUTION IN BINARY MIXTURES OF SPHERES (SIZE RATIO 5:1)

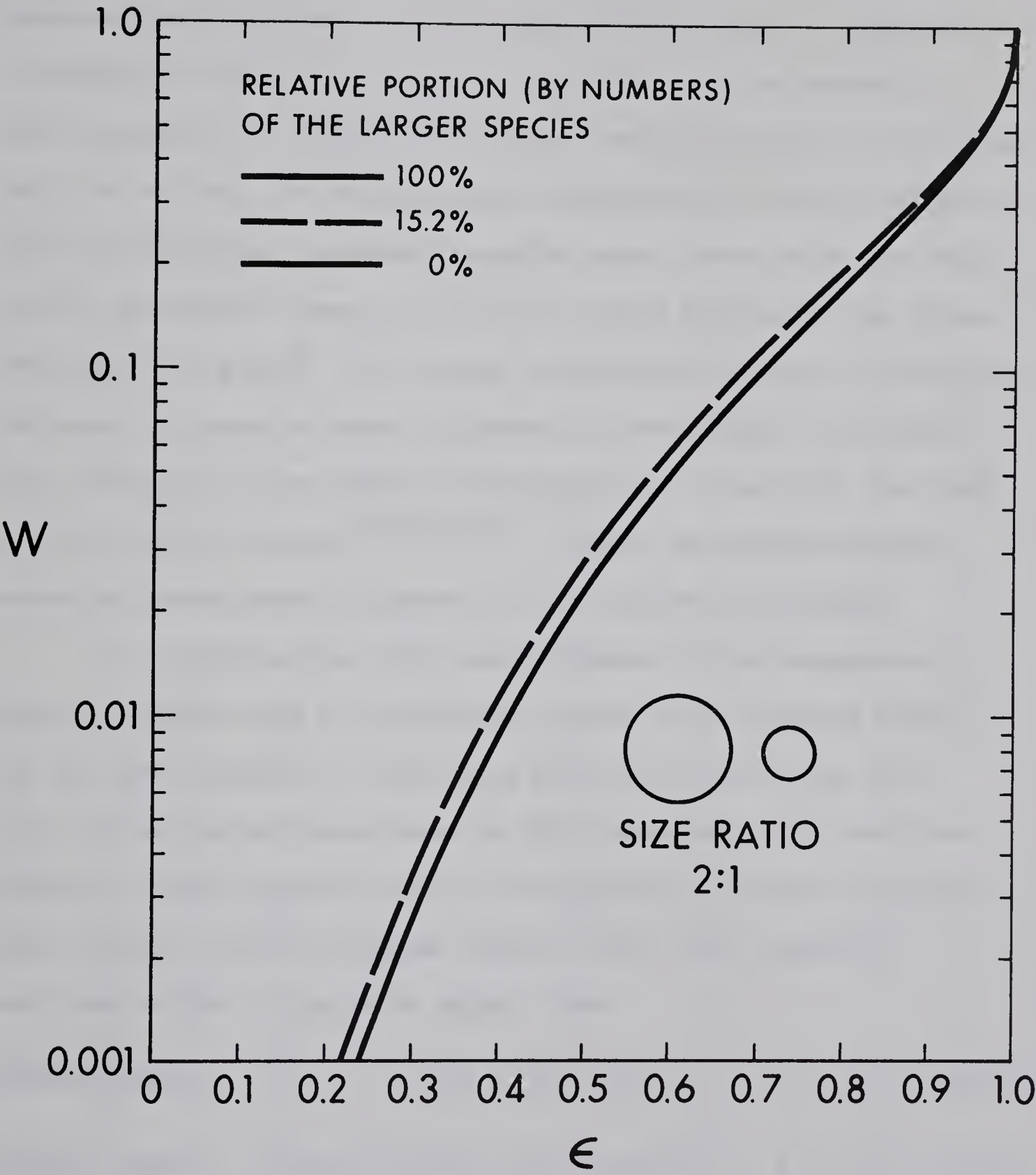


FIGURE 22. THE EFFECTS OF THE SIZE DISTRIBUTION IN
BINARY MIXTURES OF SPHERES (SIZE RATIO 2:1)

II.8 THE EFFECTS OF THE REYNOLDS NUMBER

The preceding theoretical results have all been based on the premise of creeping flow, viz. that inertial forces can be neglected in comparison with viscous forces. In practice this is generally a valid assumption for liquid flow; however, exceptions may be encountered from time to time. To this end, many investigations have been directed towards determining a universal Reynolds number, above which the creeping flow assumption ceases to be strictly valid for liquid flow through porous media in general. For swarms of monosized spheres, in particular, this specific Reynolds number is generally acknowledged to be about unity (Figure 23), when based on the superficial velocity of the fluid and the particle diameter^{32,38,49,51}. However, no universal result concerning porous media in general has so far been forthcoming.

It is possible that this specific number for an homogeneous swarm of spheres could be determined by means of the proposed model. This has been attempted by accounting for the inertial force term, $\rho \underline{u} \cdot \nabla \underline{u}$, in the Navier-Stokes Equation (84), which describes conditions within the annular region, and by introducing an equivalent macroscopic term, $\rho \underline{u}^* \cdot \nabla \underline{u}^*$, into the Brinkman Equation (85), which describes conditions within the exterior region, thus:

$$\text{annular region:} \quad \mu \nabla^2 \underline{u} = \nabla p + \rho \underline{u} \cdot \nabla \underline{u} \quad R < r < S, \quad (130)$$

$$\text{exterior region:} \quad -(\mu/\kappa) \underline{u}^* + \mu \nabla^2 \underline{u}^* = \nabla p^* + \rho \underline{u}^* \cdot \nabla \underline{u}^* \quad S < r < \infty. \quad (131)$$

The above equations have defied analytical attempts of solution. Perturbation techniques or numerical methods would appear to be inevitable.

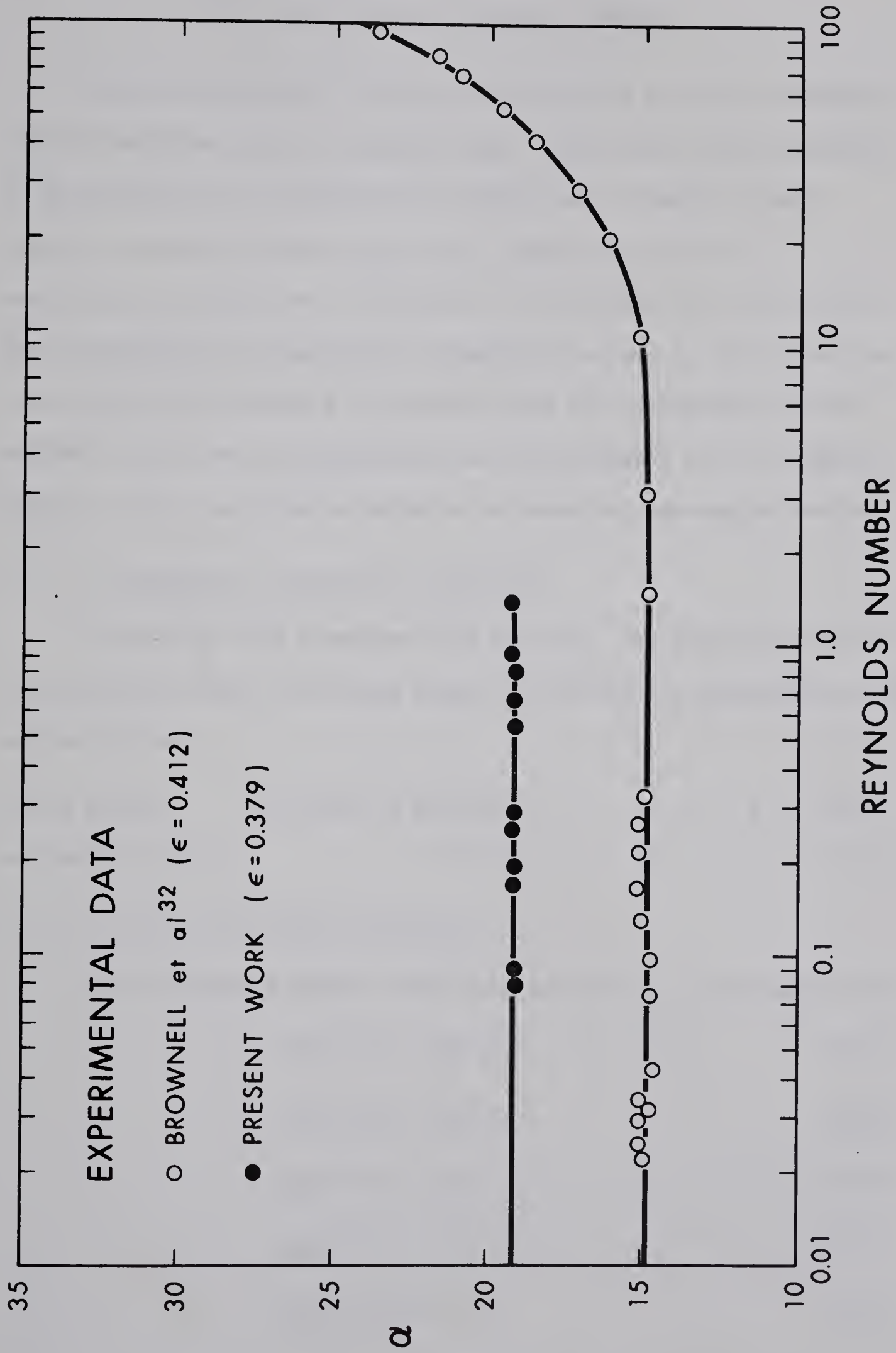


FIGURE 23. THE DEPENDENCE OF α ON THE REYNOLDS NUMBER FOR MONOSIZED SPHERES: EXPERIMENTAL DATA

II.9 THE EFFECTS OF PARTICLE POROSITY

As noted previously (Section I.3.6) porous particles frequently play an important role in catalyst beds. The problem often arises as to the fraction of a flowing fluid which passes through a single particle contained within such a bed. With this in mind it is particularly instructive to calculate the streamfunction distribution for incompressible creeping flow through and around a single isolated porous sphere (of radius R and permeability κ). Incidentally, this analysis will serve to demonstrate the effectiveness of the Brinkman Equation (82) in solving an hitherto intractable, two-region problem.

II.9.1 FUNDAMENTAL DIFFERENTIAL EQUATIONS

By analogy with Equations (94) and (95), the equations describing the flowfield within the porous sphere and within the surrounding fluid region will be:

$$\text{porous sphere:} \quad -(1/\kappa)E^2\psi^* + E^2(E^2\psi^*) = 0 \quad 0 < r < R, \quad (132)$$

$$\text{surrounding fluid:} \quad E^2(E^2\psi) = 0 \quad R < r < \infty. \quad (133)$$

II.9.2 STIPULATED BOUNDARY CONDITIONS

The following boundary conditions must here be stipulated, viz.

$$p^*(R^-, \theta) = p(R^+, \theta), \quad (134)$$

$$\tau^*(R^-, \theta) = \tau(R^+, \theta), \quad (135)$$

$$u_r^*(R^-, \theta) = u_r(R^+, \theta), \quad (136)$$

$$u_\theta^*(R^-, \theta) = u_\theta(R^+, \theta), \quad (137)$$

$$\text{Limit}_{r \rightarrow \infty} \underline{u}(r, \theta) = \underline{U}, \quad (138)$$

where $\underline{U} = [U, 0, 0]$ denotes the velocity vector of the undisturbed mainstream; the arguments on which the above boundary conditions are based are presented in Section II.4.2. In addition, a restriction demanding finiteness of the flowfield must be imposed, in particular that

$$u_r^*(0, \theta) \text{ must be finite.} \quad (139)$$

II.9.3 SOLUTION OF THE DEFINING EQUATIONS

The solutions of Equations (132) and (133) which satisfy the boundary conditions implicit in Equations (134)-(139) can be shown to be:

$$\psi^*(\chi, \theta) = (\kappa U/2) [M\chi^2 + N(\sinh\chi - \chi \cosh\chi)/\chi] \sin^2\theta \quad 0 < \chi < v, \quad (140)$$

$$\psi(\chi, \theta) = (\kappa U/2) [A/\chi + B\chi + \chi^2] \sin^2\theta \quad v < \chi < \infty, \quad (141)$$

where:

$$\chi = r/\sqrt{\kappa}, \quad (142)$$

$$v = R/\sqrt{\kappa}, \quad (143)$$

and:

$$M = (\tanh v - v)/(\tanh v - v - 2v^3/3), \quad (144)$$

$$N = (2v^3/\cosh v)/(\tanh v - v - 2v^3/3), \quad (145)$$

$$A = 2v^3(\tanh v\{1+v^2/2\} - v\{1+v^2/6\})/(\tanh v - v - 2v^3/3), \quad (146)$$

$$B = -v^3(\tanh v - v)/(\tanh v - v - 2v^3/3). \quad (147)$$

When the sphere ceases to exist ($R = 0$, $v = 0$), Equation (141) reduces to the limiting form $\psi = (1/2)Ur^2\sin^2\theta$. This is the familiar stream-function representation²⁸ of an undisturbed flowfield, \underline{U} , as would be expected.

II.9.4 THE RESISTANCE OFFERED BY AN ISOLATED POROUS SPHERE

The resistance force, F , offered by an isolated porous sphere may be calculated by means of Equation (C62), which here assumes the simpler form:

$$F = 6\pi\mu UR(12A - 2Bv^2)/9v^3 . \quad (148)$$

Substituting for A and B from Equations (146) and (147) ultimately yields *A Generalized Form of Stokes Law, for a Porous Sphere*, thus:

$$F = 6\pi\mu UR \zeta(v) , \quad (149)$$

where:

$$\zeta(v) = \frac{1 - (7/3v)\tanh v + (4/v^2) - (4/v^3)\tanh v}{1 + (3/2v^2) - (3/2v^3)\tanh v} \quad (150)$$

For solid spheres $v = \infty$, whence $\zeta(v) = 1.0$; Equation (149) then becomes identical with Stokes Law as would be expected.

For $v > 10$, $\zeta(v) \approx 1 - (7/3v)$. In general $v \gg 100$ for commercial porous spheres, whence $\zeta(v) \approx 1.0$ (Figure 24). The immediate inference is that for $v \gg 100$ an insignificant quantity of fluid actually passes *through* the particle itself; in other words the fluid prefers to flow around the porous sphere just as if it were solid (Figure 25). The implication of this for flow within a *swarm* of porous spheres is that most of the fluid will flow between the spheres; only a small fraction can be anticipated to flow through the individual spheres. In view of this a bed of catalyst pellets can be expected to function more efficiently when composed of a multitude of very small solid particles than when composed of a few much larger porous particles possessing

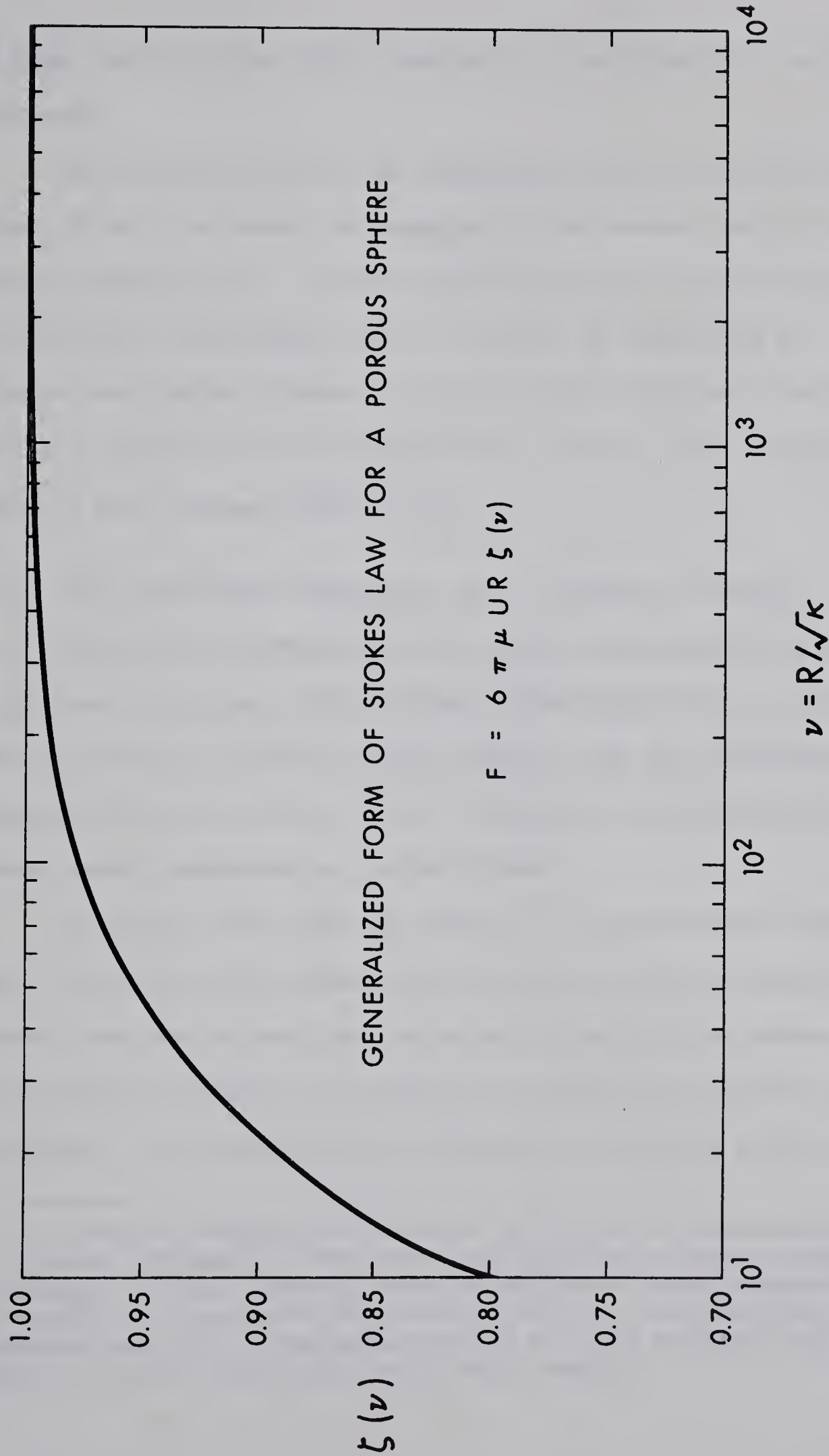


FIGURE 24. THE GENERALIZED FORM OF STOKES LAW FOR A POROUS SPHERE

the same overall volume (since catalysis is predominantly a surface phenomenon).

The proposed model for an homogeneous swarm of porous spheres (Figure 4) may, in theory, be extended to the present case of incompressible creeping flow. Unfortunately the algebra involved grows so excessively complicated that all attempts of completing the solution have failed. However, in view of the inferences drawn from the above analysis for an isolated porous sphere, such a solution would appear to have limited applicability.

II.9.5 THE RESISTANCE OFFERED BY A DENSE CLUSTER OF SPHERES

It should be stressed that the results developed above also apply to the case of a single porous sphere sedimenting within an unbounded extent of fluid. Of more interest, however, are the sedimentation characteristics of a dense cluster of spheres, particularly when the cluster itself approximates a porous sphere†.

At present there does not appear to be available any theoretical result relating to the sedimentation of such a cluster of spheres. However, the results developed above for a single porous sphere may be applied directly to the case of a sedimenting spherical cluster (of radius R_c and permeability κ) composed of monosized spheres (of

† Whilst studying the behaviour of biological macro-molecules in solution, Brinkman³⁰ noted that such particles showed a tendency to sediment in dense clusters which approximated porous spheres. (He attempted³¹ to incorporate this observation into his previously discussed model for an homogeneous swarm of solid spheres²⁹ but was unable to obtain a physically consistent solution).

radius R_s). The value of v for such a cluster will be:

$$\begin{aligned} v &= R_c / \sqrt{k} = (R_p / \sqrt{k}) (R_c / R_p) \\ &= \alpha (R_c / R_p) , \end{aligned} \tag{151}$$

with α being directly obtainable from Figure (19), or Table 3, if the porosity of the cluster is known (this will generally be between 0.40 and 0.44 for monosized spheres in contact). Hence, a knowledge of (R_c / R_p) and α for the cluster is sufficient to evaluate its sedimentation characteristics defined by Equations (149) and (150).

Inherent in the above discussion of an isolated cluster is the presumption that the cluster contains a sufficient number of spheres to approximate a sphere itself. For monosized spheres in contact this necessitates that $(R_c / R_p) > 5$ (from geometric considerations).

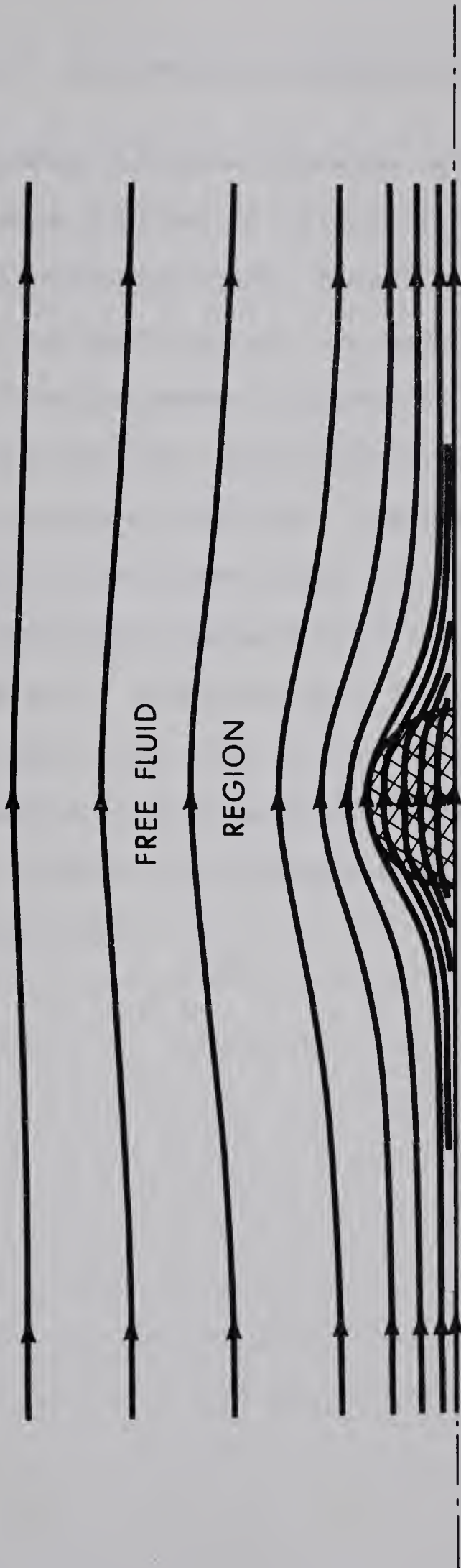


FIGURE 25. TYPICAL STREAMLINES FOR INCOMPRESSIBLE CREEPING FLOW THROUGH AN ISOLATED POROUS SPHERE (For The Representative Case $\nu = 20$)

II.10 THE EFFECTS OF PARTICLE SHAPE AND ORIENTATION

The effects of particle shape and orientation were considered in Part IB during the study of diffusion through certain arrangements of oblate and prolate spheroids. A similar analysis for incompressible creeping flow has been attempted. In essence, this problem constitutes one of obtaining general solutions of Equations (94) and (95) in spheroidal coordinates. Unfortunately, all attempts at determining an analytic solution of this latter equation have failed (although such a solution of the former equation *is* available⁴²). A numerical approach, as previously suggested in Section II.8 for the evaluation of inertial effects, therefore appears inevitable. However, it seems likely that the solution so obtained would suggest a permeability dependence on the eccentricity and mode of orientation of the spheroids similar to the diffusivity dependence on these parameters discussed in Part IB.

II.11 SUMMARY

The presented results demonstrate that the proposed model offers a satisfactory representation of, and provides valuable physical insight into, incompressible creeping flow occurring within an homogeneous swarm of spheres. For solid monosized spheres of known radius, the permeability may be evaluated by iteration of Equation (124) or by interpolation of Table 3. These predictions agree well with experimental data over the entire porosity range, lending heavy support to the realistic nature of the proposed model and to the acceptability of the assumptions implicit therein.

This analysis has demonstrated that, for spheres, the permeability is not invariant with the size distribution, inferring that fluid flow measurements *can* be expected to yield quantitative information relating to pore sizes, pore size distributions and specific surface areas of porous media in general; these conclusions are also in accord with experimental observations.

Although the presented results have been derived specifically for creeping flow, there exists a great deal of experimental data purporting to their validity up to a Reynolds number of at least unity. Since this is substantially higher than that usually encountered with liquid flow in porous media, the preceding results may, in such cases, be applied with confidence.

CONCLUSION

The nature of the results derived in this work serve to demonstrate that the proposed model satisfactorily fulfils the original objectives of (1) being able to predict successfully diffusive as well as hydrodynamic flow processes when occurring individually within an homogeneous swarm of spheres, and (2) providing valuable physical insight into these processes when occurring within unconsolidated porous media in general.

The diffusivity (conductivity) factor of an homogeneous swarm of spheres may be evaluated if the porosity is known. When the size distribution is known the permeability also may be evaluated. These predictions display similar trends to experimental data over the entire porosity range, observations which justify having resorted to the same mathematical model throughout this work.

The diffusivity (conductivity) factor has been demonstrated to be invariant with the size distribution of the spheres, thereby implying that such measurements cannot be expected to provide quantitative information relating to pore sizes, pore size distributions or specific surface areas of porous media in general. In contrast, however, the permeability has been demonstrated to be significantly dependent on the prevailing size distribution. Hence, caution is advisable when comparing theoretical or experimental permeability data, obtained for a given system, with experimental data obtained from systems having like porosities but different or unknown size distributions.

The important effects of particle shape and orientation were assessed during the study of diffusion (conduction) through systems of co-axially orientated oblate and prolate spheroids. The proposed model also yielded encouraging predictions for these fundamentally important anisotropic systems.

To summarize then, the proposed model provides valuable insight into the understanding of diffusion (conduction) as well as fluid flow when occurring individually within unconsolidated porous media. It is totally different in concept from the classical capillary model which, although widely utilized, remains rather unrealistic and restrictive in practice (its most serious limitation being that it is wholly unproductive in the study of diffusive flow processes); indeed, most unconsolidated porous media (and many consolidated ones) are more closely approximated by an homogeneous swarm of spheres or co-axially orientated spheroids than by a bundle of non-interconnected capillaries.

With reference to further work it is suggested that the proposed model be extended to the study of diffusive and hydrodynamic flow processes when occurring *simultaneously* within unconsolidated porous media. An important case in question would be the investigation of water evaporation from naturally occurring soils, sands and gravels, since this phenomenon, although of paramount importance in civil engineering, is poorly understood at present.

BIBLIOGRAPHY

I. REFERENCES PERTAINING TO DIFFUSIVE FLOW PROCESSES

1. ARCHIE, G.E., *Trans. AIME*, 146, 54-62, (1942).
2. BIRD, B.R., STEWART, W.E. and LIGHTFOOT, E.N., *Transport Phenomena*", Chapter 17, John Wiley, New York, 1960.
3. BRUGGEMANN, D.A.G., *Ann. Physik*, 24, 636-679, (1935).
4. DE LA RUE, R.E. and TOBIAS, C.W., *Jour. Electrochem. Soc.*, 106, 827-833, (1959).
5. FRICKE, H., *Phys. Rev.*, 24, 575-587, (1924).
6. FRICKE, H. and MORSE, S., *Phys. Rev.*, 25, 361-367, (1925).
7. FRICKE, H., *Physics*, 1, 106-115, (1931).
8. HASHIN, Z., *Jour. Composite Materials*, 2, 284-300, (1968).
9. HENRY, J.P., CUNNINGHAM, R.S. and GEANKOPLIS, C.J., *Chem. Eng. Sci.*, 22, 11-20, (1967).
10. KLINKENBERG, L.J., *Bull. Geol. Soc. Amer.*, 62, 559-564, (1951).
11. LAMB, H., *"Hydrodynamics"*, 6th Ed., Chapter 5, Cambridge Univ. Press, 1932.
12. MAXWELL, CLERK., *"Electricity and Magnetism"*, 3rd Ed., 435-441, The Clarendon Press, Oxford, 1892.
13. NADER, W., *"The Potential Distribution Near a Perforated Well"*, M.Sc. Thesis, The University of Texas, 1960.
14. PEARCE, C.A.R., *Brit. Jour. Appl. Phys.*, 6, 113-120, (1955).
15. PERKINS, T.K. and JOHNSTON, O.C., *Soc. Pet. Eng. Jour.*, 3, 70-84, (1963).
16. PRAGER, S., *Physica*, 29, 129-139, (1963).
17. RAYLEIGH, LORD., *Phil. Mag.*, 34, 481-502, (1892).

18. RICE, P.A., FONTUGNE, D.J., LATINI, R.G. and BARDUHN, A.J.,
Ind. Eng. Chem., 62, 23-31, (1970).
19. SCHOFIELD, R.K. and DAKSHINAMURTI, C., *Faraday Soc. Disc.*, 3,
56-61, (1948).
20. SKELLAND, A.H.P. and CORNISH, A.R.H., *AIChE Jour.*, 9, 73-76,
(1963).
21. SLAWINSKI, A.J., *Chim. Phys.*, 23, 710-727, (1926).
22. SNEDDON, I.N., "Elements of Partial Differential Equations",
Chapter 4, McGraw-Hill, New York, 1957.
23. VOLAROVICH, M.P. and MECKLER, Y.B., *Colloid Jour. of USSR*,
29, 483-485, (1967).
24. WINSAUER, W.O., SHEARIN, H.M., MASSON, P.H. and WILLIAMS, M.,
Bull. Amer. Assoc. Pet. Geol., 36, 253-277, (1952).
25. WYLLIE, M.R.J. and SPANGLER, M.B., *Bull. Amer. Assoc. Pet. Geol.*,
36, 359-403, (1952).
26. WYLLIE, M.R.J. and GREGORY, A.R., *Trans. AIME*, 198, 103-110,
(1953).
27. YOUNGQUIST, G.R., *Ind. Eng. Chem.*, 62, 52-63, (1970).

II. REFERENCES PERTAINING TO HYDRODYNAMIC FLOW PROCESSES

28. BIRD, B.R., STEWART, W.E. and LIGHTFOOT, E.N., "Transport
Phenomena", Chapter 4, John Wiley, New York, 1960.
29. BRINKMAN, H.C., *Appl. Sci. Res.*, A1, 27-34, (1949).
30. BRINKMAN, H.C., *Research*, 2, 190-194, (1949).
31. BRINKMAN, H.C., *Appl. Sci. Res.*, A1, 81-86, (1949).
32. BROWNELL, L.E., DOMBROWSKI, H.S. and DICKEY, C.A., *Chem. Eng.
Prog.*, 46, 415-422, (1950).

33. BRUGGEMANN, D.A.G., *Ann. Physik*, 24, 636-679, (1935).
34. CARMAN, P.C., *Trans. Inst. Chem. Eng.*, 15, 150-166, (1937).
35. COULSON, J.M., "*The Streamline Flow of Liquids through Beds Composed of Spherical Particles*", Ph.D. Thesis, The University of London, 1935.
36. CUNNINGHAM, E., *Proc. Roy. Soc.*, A83, 357-365, (1910).
37. DEBEAS, S. and RUMPF, H., *Chem. Eng. Sci.*, 21, 583-607, (1966).
38. FOX, J.W., *Proc. Phys. Soc.*, B62, 829-832, (1949).
39. GEERTSMA, J. and DE KERK, F., *Jour. Pet. Tech.*, 21, 1571-1581, (1969).
40. GRATON, L.C. and FRAZER, H.J., *Jour. Geol.*, 43, 785-909, (1935).
41. HAPPEL, J., *AIChE Jour.*, 4, 197-201, (1958).
42. HAPPEL, J. and BRENNER, H., "*Low Reynolds Number Hydrodynamics*", Chapters 4 and 7, Prentice-Hall Inc., N.J., 1965.
43. HAPPEL, J. and EPSTEIN, N., *Ind. Eng. Chem.*, 46, 1187-1194, (1954).
44. HUITT, J.L., *AIChE Jour.*, 2, 259-264, (1956).
45. KOZENY, J., *Akad. Wiss. Wien*, 136A, 271-306, (1927).
46. KUWABARA, S., *Jour. Phys. Soc. Japan*, 14, 527-532, (1959).
47. McNOWN, J.S. and LIN, P., *Proc. Second Midwestern Conf. Fluid Mech.*, Ohio State Univ., 1952.
48. MARTIN, J.J., McCABE, W.L. and MONRAD, C.C., *Chem. Eng. Prog.*, 47, 91-94, (1951).
49. MERTES, T.S. and RHODES, H.B., *Chem. Eng. Prog.*, 51, 429-432, 517-522, (1955).
50. PARSONS, R.W., *Soc. Pet. Eng. Jour.*, 6, 126-136, (1966).
51. PLAIN, G.J. and MORRISON, M.L., *Amer. Jour. Phys.*, 22, 143-146, (1954).

52. SCHEIDEGGER, A.E., *"The Physics of Flow Through Porous Media"*, Chapters 6 and 7, Univ. of Toronto Press, 1960.
53. SCHRIEVER, W., *Trans. AIME*, 86, 329-336, (1930).
54. SLATTERY, J.C., *AIChE Jour.*, 15, 866-872, (1969).
55. TAM, C.K.W., *Jour. Fluid Mech.*, 38, 537-546, (1969).
56. UCHIDA, S., *Ind. Eng. Chem.*, 46, 1194-1195, (1954).

APPENDIX A

THE CALCULATION OF λ_x AND λ_y
FOR CO-AXIALLY ORIENTATED
OBLATE SPHEROIDS

A.1 ESSENTIAL GEOMETRY OF THE OBLATE SPHEROID

An oblate spheroid is generated when an ellipse is rotated about its minor axis (Figure 26). The system of coordinates convenient to this investigation will be oblate spheroidal coordinates $[\xi, \eta, \phi]$, which constitute the special case of ellipsoidal coordinates in which, of the three principal axes of the general ellipsoid, the two largest are of equal length. If a Cartesian frame of reference $[x, y, z]$ is chosen to be collinear with these three principal axes then it can be shown¹¹ that:

$$x = a \sinh \xi \sin \eta , \quad (A1)$$

$$y = a \cosh \xi \cos \eta \cos \phi , \quad (A2)$$

$$z = a \cosh \xi \cos \eta \sin \phi , \quad (A3)$$

where: $\xi \geq 0$; $-\pi/2 \leq \eta \leq \pi/2$; $0 \leq \phi < 2\pi$.

In these equations a denotes the distance between the trajectory of the focus, $F(0, a)$, and the geometric centre, O . The coordinate surfaces of constant ξ comprise a family of confocal oblate spheroids; those of constant η comprise a family of confocal hyperboloids of revolution. The third orthogonal coordinate, ϕ , denotes the azimuthal angle measured out of the plane of the paper of Figure 26. Typical unit vectors \underline{i}_ξ and \underline{i}_η are depicted in this figure; the unit vector \underline{i}_ϕ is orthogonal to the paper.

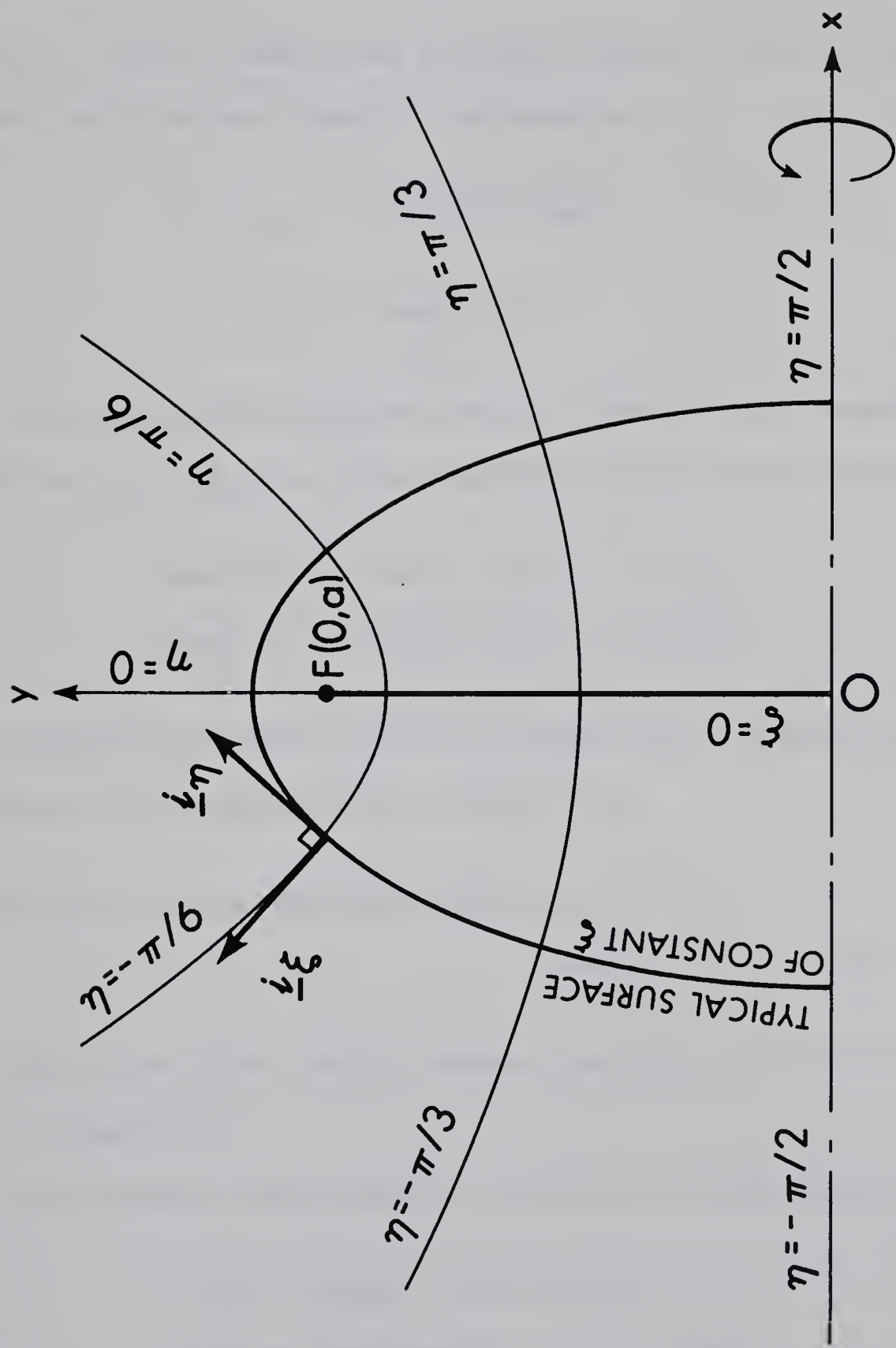


FIGURE 26. OBLATE SPHEROIDAL COORDINATES IN A MERIDIAN PLANE

An element of distance in space, dL , may be represented by:

$$(dL)^2 = (dx)^2 + (dy)^2 + (dz)^2 = (h_\xi d\xi)^2 + (h_\eta d\eta)^2 + (h_\phi d\phi)^2, \quad (A4)$$

where h_ξ , h_η and h_ϕ denote the so-called metrical coefficients (scale factors) which follow directly from Equations (A1) - (A4), viz.

$$h_\xi = h_\eta = a \sqrt{\sinh^2 \xi + \sin^2 \eta}, \quad (A5)$$

$$h_\phi = a \cosh \xi \cos \eta. \quad (A6)$$

The particular spheroidal shape of interest will henceforth be identified by $\xi = \xi_0$; for this geometry it may be noted that:

$$\text{length of semi-minor axis} = a \sinh \xi_0, \quad (A7)$$

$$\text{length of semi-major axis} = a \cosh \xi_0. \quad (A8)$$

When designating specific spheroidal shapes it is customary to do so by means of their *eccentricity*, defined by:

$$\begin{aligned} \text{eccentricity} &= \text{minor axis} / \text{major axis} = e \\ &= \tanh \xi_0 \quad 0 < e < 1.0. \end{aligned} \quad (A9)$$

This definition holds also for prolate spheroids, and will be used as such in Appendix B.

For future convenience the following functions will be defined:

$$f(\xi) = 1/\sinh \xi - \operatorname{arccot}(\sinh \xi), \quad (A10)$$

$$g(\xi) = \sinh \xi / \cosh^2 \xi - \operatorname{arccot}(\sinh \xi), \quad (A11)$$

$$h(\xi) = 2f(\xi) - g(\xi). \quad (A12)$$

A.2 THE PROPOSED MODEL FOR CO-AXIALLY ORIENTATED OBLATE SPHEROIDS

Attention will here be confined to an homogeneous swarm of oblate spheroids of identical eccentricity, e , possessing an arbitrary size distribution and orientated such that the axis of revolution of each particle is collinear with the x -direction.

The proposed model for this system (Figure 27) is closely related to that for spheres (Figure 3). It here consists of a reference spheroid ($\xi = \xi_0$), an annular region of void space (bounded by the two confocal spheroidal surfaces $\xi = \xi_0$ and $\xi = \xi_1$) and an exterior region of homogeneous porous material possessing the same macroscopically *anisotropic* characteristics as the original system.

In order that the porosity of the unit cell (comprising the reference spheroid and the annular region) remains equal to that of the original system, ϵ , it is necessary that

$$\{ (4\pi/3) (\text{acosh}\xi_0)^2 (\text{asinh}\xi_0) \} / \{ (4\pi/3) (\text{acosh}\xi_1)^2 (\text{asinh}\xi_1) \} = (1-\epsilon) . \quad (\text{A13})$$

After re-arrangement, this expression yields the condition:

$$\sinh^3 \xi_1 + \sinh \xi_1 - (\cosh^2 \xi_0 \sinh \xi_0) / (1-\epsilon) = 0 . \quad (\text{A14})$$

It should be noted that the eccentricity of the outer surface of the unit cell will, in general, be different from that of the reference spheroid.

This model possesses the distinct advantage that the macroscopically homogeneous and anisotropic characteristics of the original

system of spheroids remain unaffected by the modelling procedure, i.e. the modelled system is macroscopically indistinguishable from the original system when viewed from the outside.

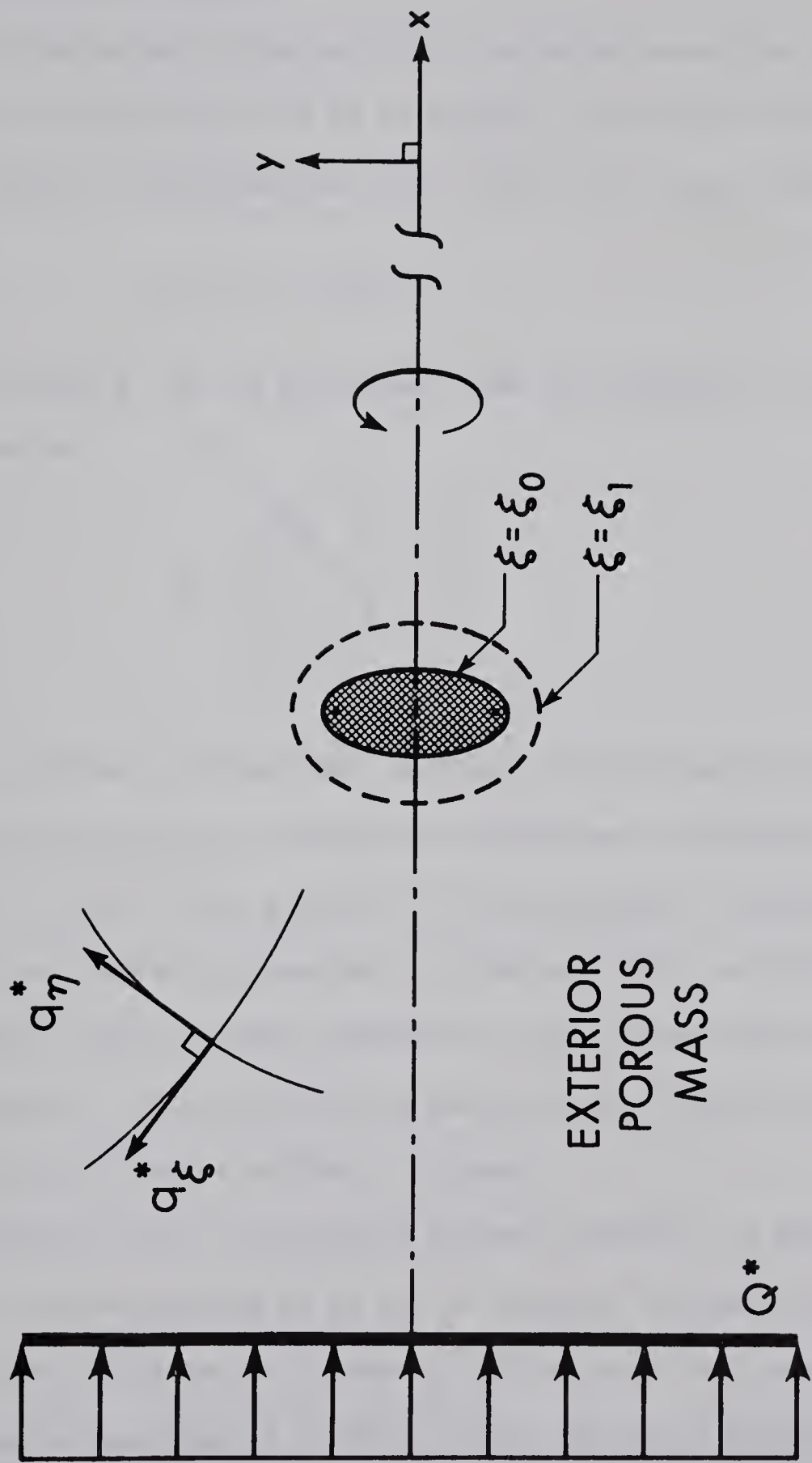


FIGURE 27. THE PROPOSED MODEL FOR AN HOMOGENEOUS SWARM OF CO-AXIALLY ORIENTATED OBLATE SPHEROIDS (Cross-Section Through Centre of Reference Spheroid)

A.3 THE DEFINING EQUATIONS AND BOUNDARY CONDITIONS

A.3.1 GENERAL DISCUSSION

The macroscopic form of Fick's Law which describes diffusion through an homogeneous swarm of co-axially orientated oblate spheroids may be recalled from Equations (45) - (51) of the main text as being:

$$\underline{q}^* = -D \underline{\lambda} \underline{\nabla} c^* , \quad (\text{A15})$$

with the tensor $\underline{\lambda}$, in the preferred frame of reference $[x,y,z]$, being represented by

$$\underline{\lambda} = \begin{bmatrix} \lambda_x & 0 & 0 \\ 0 & \lambda_y & 0 \\ 0 & 0 & \lambda_y \end{bmatrix} . \quad (\text{A16})$$

It may be further recalled that in order to fully describe diffusion occurring in an arbitrary direction it suffices to possess a knowledge of λ_x and λ_y , since this provides *all* the necessary information to construct the tensor $\underline{\lambda}$ appearing in Equations (A15) and (A16) above. Consequently, the principal objective of this investigation must be to so evaluate λ_x (the diffusivity factor in the x-direction) and λ_y (the diffusivity factor in the y-z plane).

Intrinsically, the modelled system possesses the same macroscopic anisotropy (characterized by $\underline{\lambda}$) as the original system of spheroids. However, the evaluation of λ_x and λ_y for the modelled system implicitly presupposes a knowledge of $\underline{\lambda}$ (which itself *implies* a knowledge of λ_x and λ_y). The problem, as it stands, is therefore intractable.

However, this difficulty may be averted for diffusion occurring specifically in a characteristic direction. In general, the mainstream flux, Q^* , within the original system will not be collinear with its inducing concentration gradient on account of the anisotropy of the system. Only for diffusion occurring specifically in a characteristic direction will Q^* be collinear with its inducing concentration gradient. In other words, for flow in a characteristic direction the macroscopic flowfield will remain totally unaware of any anisotropy in the system. Therefore, the previously mentioned difficulty within the modelled system may be averted for diffusion occurring *specifically* in a characteristic direction by treating the macroscopic flowfield within the exterior region of this system as if it, too, is unaware of any anisotropy of the system as a whole[†]. Thus, Fick's Law for the exterior region ($\xi_1 \leq \xi < \infty$) may be written in the form:

$$\begin{aligned} \underline{q^*(\xi, \eta, \phi)} &= [q_{\xi}^*, q_{\eta}^*, q_{\phi}^*] \\ &= [-D^*(1/h_{\xi})(\partial c^*/\partial \xi), -D^*(1/h_{\eta})(\partial c^*/\partial \eta), -D^*(1/h_{\phi})(\partial c^*/\partial \phi)], \end{aligned} \tag{A17}$$

where:

$D^* = D_x^*$ for diffusion collinear with the x-direction;

$D^* = D_y^*$ for diffusion collinear with the y-z plane.

[†] It will be recalled from Section I.3.4 that for *spheres* the exterior flowfield is *everywhere* collinear with the mainstream flowfield. Observations made in Section A.4 to follow demonstrate that this also holds true for spheroids.

Fick's Law for the isotropic annular region ($\xi_0 \leq \xi \leq \xi_1$) is:

$$\begin{aligned} \underline{q}(\xi, \eta, \phi) &= [q_\xi, q_\eta, q_\phi] \\ &= [-D(1/h_\xi)(\partial c/\partial \xi), -D(1/h_\eta)(\partial c/\partial \eta), -D(1/h_\phi)(\partial c/\partial \phi)] . \end{aligned} \quad (A18)$$

A.3.2 FUNDAMENTAL DIFFERENTIAL EQUATIONS

By direct analogy with Equations (7) and (8) of the main text (for an homogeneous swarm of spheres) the describing equations for the corresponding case of co-axially orientated oblate spheroids will be:

$$\text{annular region:} \quad \nabla^2 c = 0 \quad \xi_0 < \xi < \xi_1 , \quad (A19)$$

$$\text{exterior region:} \quad \nabla^2 c^* = 0 \quad \xi_1 < \xi < \infty . \quad (A20)$$

The Laplacian operator, ∇^2 , here assumes the form¹¹:

$$\begin{aligned} \nabla^2 \equiv (\partial/\partial \sin \eta)(\cos^2 \eta \{\partial/\partial \sin \eta\}) + (\partial/\partial \sinh \xi)(\cosh^2 \xi \{\partial/\partial \sinh \xi\}) \\ + (h_\xi^2/h_\phi^2)(\partial^2/\partial \phi^2) . \end{aligned} \quad (A21)$$

A.3.3 STIPULATED BOUNDARY CONDITIONS

Again, by direct analogy with Equations (12)-(15) for spheres, the following boundary conditions respectively must be stipulated for co-axially orientated oblate spheroids, viz.

$$q_\xi(\xi_0^+, \eta, \phi) = 0 , \quad (A22)$$

$$c(\xi_1^-, \eta, \phi) = c^*(\xi_1^+, \eta, \phi) , \quad (A23)$$

$$q_\xi(\xi_1^-, \eta, \phi) = q_\xi^*(\xi_1^+, \eta, \phi) , \quad (A24)$$

$$\text{Limit}_{\xi \rightarrow \infty} \underline{q}^*(\xi, \eta, \phi) = \underline{Q}^* , \quad (A25)$$

where:

$\underline{Q^*} = [Q^*, 0, 0]$ for diffusion in the characteristic x-direction;

$\underline{Q^*} = [0, Q^*, 0]$ for diffusion in the characteristic y-direction;

$\underline{Q^*} = [0, 0, Q^*]$ for diffusion in the characteristic z-direction,

these latter three expressions referring to the preferred Cartesian frame of reference $[x, y, z]$.

A.4 SOLUTION OF THE DEFINING EQUATIONS

A.4.1 CASE 1: DIFFUSION COLLINEAR WITH THE AXES OF REVOLUTION OF THE SPHEROIDS

The flowfield in this case will be collinear with the characteristic x-direction and will therefore exhibit axial symmetry; this implies that $q_\phi^* = 0$ and $q_\phi = 0$ in Equations (A17) and (A18) respectively. Consequently, the ϕ variable may hereafter be suppressed.

Sufficiently general solutions of Laplace's Equations (A19) and (A20) for diffusion in the x-direction can be extracted from fundamental series solutions developed by Lamb¹¹, viz.

$$c(\xi, \eta) = [A_1 + A_2 \operatorname{arccot}(\sinh \xi)] + [A_3 + A_4 f(\xi)] \sinh \xi \sin \eta \quad \xi_0 < \xi < \xi_1, \quad (\text{A26})$$

$$c^*(\xi, \eta) = [A_1^* + A_2^* \operatorname{arccot}(\sinh \xi)] + [A_3^* + A_4^* f(\xi)] \sinh \xi \sin \eta \quad \xi_1 < \xi < \infty, \quad (\text{A27})$$

where A_i and A_i^* ($i = 1, 2, 3, 4$) denote arbitrary constants. The particular solutions which satisfy the boundary conditions stipulated in Equations (A22)-(A25) transpire to be:

$$c(\xi, \eta) = c^*(\xi, 0) - A(aQ^*/D_x^*)[1 - f(\xi)/g(\xi_0)] \sinh \xi \sin \eta, \quad (\text{A28})$$

$$c^*(\xi, \eta) = c^*(\xi, 0) - (aQ^*/D_x^*)[1 - A^* f(\xi)] \sinh \xi \sin \eta, \quad (\text{A29})$$

in which A and A^* are defined by

$$A = \frac{\lambda_x g(\xi_0) \{f(\xi_1) - g(\xi_1)\}}{f(\xi_1) \{g(\xi_0) - g(\xi_1)\} - \lambda_x g(\xi_1) \{g(\xi_0) - f(\xi_1)\}}, \quad (\text{A30})$$

$$A^* = \frac{\{g(\xi_0) - g(\xi_1)\} - \lambda_x \{g(\xi_0) - f(\xi_1)\}}{f(\xi_1) \{g(\xi_0) - g(\xi_1)\} - \lambda_x g(\xi_1) \{g(\xi_0) - f(\xi_1)\}}, \quad (A31)$$

the functions $f(\xi)$ and $g(\xi)$ being defined by Equations (A10) and (A11) respectively.

Since the modelled system is to be quantitatively representative of the original system then it is necessary that within the unit cell the average flux in the mainstream direction be equal to that of the mainstream itself. This necessitates that

$$\{1/\pi(\text{acosh}\xi_1)^2\} \int_{\xi_0}^{\xi_1} q_\eta(\xi, 0) 2\pi(\text{acosh}\xi) d(\text{acosh}\xi) = Q^* . \quad (A32)$$

This equation is analagous to Equation (22) of the main text for spheres. The flux component $q_\eta(\xi, 0)$ appearing in Equation (A32) may be evaluated by means of Equations (A18) and (A26), thus:

$$q_\eta(\xi, 0) = \{-D(1/h_\eta)(\partial c/\partial \eta)\}_{\eta=0} = (AQ^*/\lambda_x) \{1 - f(\xi)/g(\xi_0)\} . \quad (A33)$$

The substitution of this expression into Equation (A32) can be shown to yield:

$$\int_{\xi_0}^{\xi_1} \sinh\xi \{1 - f(\xi)/g(\xi_0)\} d(\sinh\xi) = (\lambda_x/2A) \cosh^2\xi_1 . \quad (A34)$$

After integration and manipulation this equation yields:

$$1 - g(\xi_1)/g(\xi_0) = \lambda_x/A . \quad (A35)$$

Following substitution for A from Equation (A30) the ultimate expression for the diffusivity factor in the characteristic x -direction can be obtained, viz.

$$\lambda_x = \{g(\xi_0) - g(\xi_1)\} / \{g(\xi_0) - f(\xi_1)\} . \quad (\text{A36})$$

The parameters ξ_0 and ξ_1 are defined by Equations (A9) and (A14) respectively.

The substitution of the above expression for λ_x into Equation (A31) serves to illustrate that, in fact, $A^* = 0$; this implies that the flowfield within the exterior region of the modelled system is *everywhere* totally undisturbed by the modelling procedure (compare with the like conclusions of Section I.3.4 for spheres).

A.4.2 CASE 2: DIFFUSION ORTHOGONAL TO THE AXES OF REVOLUTION OF THE SPHEROIDS

Although the following analysis relates specifically to diffusion occurring in the characteristic z-direction (for which the calculations are simplest) the final results will be valid for diffusion occurring in *any* direction collinear with the y-z plane (from considerations of symmetry). As already noted in Equation (50) of the main text this implies, in particular, that:

$$\lambda_z = \lambda_y . \quad (\text{A37})$$

However, in such cases the flowfield will no longer be axi-symmetric but will be ϕ -dependent. Sufficiently general solutions of Laplace's Equations (A19) and (A20) for diffusion in the z-direction can be shown¹¹ to be:

$$c(\xi, \eta, \phi) = [B_1 + B_2 \operatorname{arccot}(\sinh \xi)] + [B_3 + B_4 g(\xi)] \cosh \xi \cos \eta \sin \phi$$

$$\xi_0 < \xi < \xi_1 , \quad (\text{A38})$$

$$c^*(\xi, \eta, \phi) = [B_1^* + B_2^* \operatorname{arccot}(\sinh \xi)] + [B_3^* + B_4^* g(\xi)] \cosh \xi \cos \eta \sin \phi$$

$$\xi_1 < \xi < \infty, \quad (\text{A39})$$

where B_i and B_i^* ($i = 1, 2, 3, 4$) denote arbitrary constants. The particular solutions which satisfy the boundary conditions stipulated in Equations (A22)-(A25) transpire to be:

$$c(\xi, \eta, \phi) = c^*(\xi, \eta, 0) - B(aQ^*/D_y^*)[1 - g(\xi)/h(\xi_0)] \cosh \xi \cos \eta \sin \phi, \quad (\text{A40})$$

$$c^*(\xi, \eta, \phi) = c^*(\xi, \eta, 0) - (aQ^*/D_y^*)[1 - B^*g(\xi)] \cosh \xi \cos \eta \sin \phi, \quad (\text{A41})$$

in which B and B^* are defined by

$$B = \frac{\lambda_y h(\xi_0) \{g(\xi_1) - h(\xi_1)\}}{g(\xi_1) \{h(\xi_0) - h(\xi_1)\} - \lambda_y h(\xi_1) \{h(\xi_0) - g(\xi_1)\}}, \quad (\text{A42})$$

$$B^* = \frac{\{h(\xi_0) - h(\xi_1)\} - \lambda_y \{h(\xi_0) - g(\xi_1)\}}{g(\xi_1) \{h(\xi_0) - h(\xi_1)\} - \lambda_y h(\xi_1) \{h(\xi_0) - g(\xi_1)\}}, \quad (\text{A43})$$

the functions $g(\xi)$ and $h(\xi)$ being defined by Equations (A11) and (A12) respectively.

Again, since the modelled system is to be quantitatively representative of the original system then it is necessary that within the unit cell the average flux in the mainstream direction be equal to that of the mainstream itself. This here necessitates that

$$\{1/\pi(a \sinh \xi_1)(a \cosh \xi_1)\} \int_{\xi_0}^{\xi_1} q_\phi(\xi, \eta, 0) dA = Q^*, \quad (\text{A44})$$

where dA denotes an annular element of area in the plane $\phi = 0$, viz.

$$dA = \pi a^2 (\sinh^2 \xi + \cosh^2 \xi) d\xi . \quad (A45)$$

The flux component $q_\phi(\xi, \eta, 0)$ appearing in this equation may be evaluated by means of Equations (A18) and (A38), thus:

$$q_\phi(\xi, \eta, 0) = \left\{ -D(1/h_\phi) (\partial c / \partial \phi) \right\}_{\phi=0} = (BQ^*/\lambda_y) \{1 - g(\xi)/h(\xi_0)\} . \quad (A46)$$

The substitution of Equations (A46) and (A45) into Equation (A44) can be shown to yield:

$$\int_{\xi_0}^{\xi_1} (\cosh^2 \xi + \sinh^2 \xi) \{1 - g(\xi)/h(\xi_0)\} d\xi = (\lambda_y/B) \sinh \xi_1 \cosh \xi_1 . \quad (A47)$$

After integration and manipulation this equation reduces to:

$$1 - h(\xi_1)/h(\xi_0) = \lambda_y/B . \quad (A48)$$

Following substitution for B from Equation (A42) the ultimate expression for the diffusivity factor in any direction collinear with the y-z plane can be obtained, viz.

$$\lambda_y = \{h(\xi_0) - h(\xi_1)\} / \{h(\xi_0) - g(\xi_1)\} . \quad (A49)$$

The parameters ξ_0 and ξ_1 are again defined by Equations (A9) and (A14) respectively.

The substitution of the above expression for λ_y into Equation (A43) shows that, in fact, $B^* = 0$; this implies (once again) that the exterior flowfield within the modelled system is everywhere totally undisturbed by the modelling procedure (compare again with the like conclusions reached in Section I.3.4 for spheres).

APPENDIX B

THE CALCULATION OF λ_x AND λ_y
FOR CO-AXIALLY ORIENTATED
PROLATE SPHEROIDS

B.1 ESSENTIAL GEOMETRY OF THE PROLATE SPHEROID

A prolate spheroid is generated when an ellipse is rotated about its major axis. The system of coordinates appropriate to this investigation will be prolate spheroidal coordinates $[\xi, \eta, \phi]$. This coordinate system constitutes the special case of ellipsoidal coordinates in which, of the three principal axes of the general ellipsoid, the two smallest are of equal length. If a Cartesian frame of reference $[x, y, z]$ is chosen to be collinear with these three principal axes, then it can be shown¹¹ that:

$$x = a \cosh \xi \sin \eta, \quad (B1)$$

$$y = a \sinh \xi \cos \eta \cos \phi, \quad (B2)$$

$$z = a \sinh \xi \cos \eta \sin \phi, \quad (B3)$$

where: $\xi \geq 0$; $-\pi/2 \leq \eta \leq \pi/2$; $0 \leq \phi < 2\pi$.

B.2 THE SOLUTION FOR PROLATE SPHEROIDS

Attention will here be confined to an homogeneous swarm of prolate spheroids of identical eccentricity, e , possessing an arbitrary size distribution and orientated such that the axis of revolution of each particle is collinear with the x -direction.

However, rather than solving this problem anew, it is possible to proceed more directly by making avail of the preceding results developed for oblate spheroids together with a standard mathematical transformation⁴². Thus, as may readily be verified, if a is replaced by $-ia$ and $\sinh\xi$ by $i\cosh\xi$ in the expressions developed in Appendix A for oblate spheroids then the solutions of the corresponding problems involving prolate spheroids will be obtained. Execution of this transformation on Equations (A36), (A49) and (A10)-(A12) ultimately yields the following expressions:

$$\lambda_x = \{G(\xi_0) - G(\xi_1)\} / \{G(\xi_0) - F(\xi_1)\} \quad , \quad (B4)$$

$$\lambda_y = \{H(\xi_0) - H(\xi_1)\} / \{H(\xi_0) - G(\xi_1)\} \quad , \quad (B5)$$

in which the functions $F(\xi)$, $G(\xi)$ and $H(\xi)$ are defined by

$$F(\xi) = 1/\cosh\xi - \operatorname{arccoth}(\cosh\xi) \quad , \quad (B6)$$

$$G(\xi) = \cosh\xi/\sinh^2\xi - \operatorname{arccoth}(\cosh\xi) \quad , \quad (B7)$$

$$H(\xi) = 2F(\xi) - G(\xi) \quad . \quad (B8)$$

The parameter ξ_0 is again related to the eccentricity, e , according to Equation (A9), viz.

$$\xi_0 = \operatorname{arctanh}(e) \quad 0 < e < 1.0 \quad . \quad (B9)$$

However, the parameter ξ_1 is here defined by:

$$\cosh^3 \xi_1 - \cosh \xi_1 - (\sinh^2 \xi_0 \cosh \xi_0) / (1-e) = 0 \quad . \quad (B10)$$

This equation ensures that the porosity of the unit cell for prolate spheroids is equal to that of the original system; it corresponds to Equation (A14) for oblate spheroids and could, in fact, have been derived from this equation by application thereon of the above specified mathematical transformation.

APPENDIX C

THE CALCULATION OF α AND W
FOR AN HOMOGENEOUS SWARM
OF SPHERES

C.1 REVIEW OF THE DEFINING EQUATIONS AND BOUNDARY CONDITIONS

C.1.1 FUNDAMENTAL DIFFERENTIAL EQUATIONS

The differential equations describing steady, incompressible creeping flow through the modelled system (Figure 16) have been presented and developed in Section II.4 of the main text. Solutions are there sought of Equations (94) and (95) within the annular and exterior regions respectively, viz.

$$\text{annular region:} \quad E^2(E^2\psi) = 0 \quad R < r < S, \quad (C1)$$

$$\text{exterior region:} \quad -(1/\kappa)E^2\psi^* + E^2(E^2\psi^*) = 0 \quad S < r < \infty. \quad (C2)$$

In these equations ψ and ψ^* denote the streamfunctions in the annular and exterior regions respectively, and E^2 denotes the Spherical Harmonic Operator^{28, 42}, defined by:

$$E^2 \equiv (\partial^2/\partial r^2) + (1/r^2)(\partial^2/\partial \theta^2) - (\cot\theta/r^2)(\partial/\partial \theta). \quad (C3)$$

C.1.2 STIPULATED BOUNDARY CONDITIONS

The boundary conditions which must be satisfied have been stipulated in Equations (97)-(103), viz.

$$u_r(R^+, \theta) = 0, \quad (C4)$$

$$u_\theta(R^+, \theta) = 0, \quad (C5)$$

$$u_r(S^-, \theta) = u_r^*(S^+, \theta), \quad (C6)$$

$$u_\theta(S^-, \theta) = u_\theta^*(S^+, \theta), \quad (C7)$$

$$\tau(S^-, \theta) = \tau^*(S^+, \theta), \quad (C8)$$

$$p(S^-, \theta) = p^*(S^+, \theta), \quad (C9)$$

$$\lim_{r \rightarrow \infty} \underline{u}^*(r, \theta) = \underline{U}^* , \quad (C10)$$

where $\underline{U}^* = [U^*, 0, 0]$ in Cartesian coordinates $[x, y, z]$. The velocity components u_r , u_θ , u_r^* and u_θ^* appearing above are defined in terms of their respective streamfunctions by Equations (92) and (93), viz.

$$u_r(r, \theta) = -(1/r^2 \sin \theta) (\partial \psi / \partial \theta) , \quad (C11)$$

$$u_\theta(r, \theta) = (1/r \sin \theta) (\partial \psi / \partial r) , \quad (C12)$$

$$u_r^*(r, \theta) = -(1/r^2 \sin \theta) (\partial \psi^* / \partial \theta) , \quad (C13)$$

$$u_\theta^*(r, \theta) = (1/r \sin \theta) (\partial \psi^* / \partial r) . \quad (C14)$$

For the present case of axial symmetry, τ and τ^* denote the non-zero shear stress components, $\tau_{r\theta}$ and $\tau_{r\theta}^*$, of their respective stress tensors²⁸, viz.

$$\tau(r, \theta) = -\mu [r \partial (u_\theta / r) / \partial r + (1/r) (\partial u_r / \partial \theta)] , \quad (C15)$$

$$\tau^*(r, \theta) = -\mu [r \partial (u_\theta^* / r) / \partial r + (1/r) (\partial u_r^* / \partial \theta)] . \quad (C16)$$

The pressures p and p^* are defined respectively by the Navier-Stokes Equation (84) and the Brinkman Equation (85). These equations yield, on expansion²⁸, the following expressions for the radial pressure gradients $\partial p / \partial r$ and $\partial p^* / \partial r$:

$$\begin{aligned} \partial p / \partial r = \mu [& (\partial^2 u_r / \partial r^2) + (2/r) (\partial u_r / \partial r) + (1/r^2) (\partial^2 u_r / \partial \theta^2) + (\cot \theta / r^2) (\partial u_r / \partial \theta) \\ & - (2u_r / r^2) - (2/r^2) (\partial u_\theta / \partial \theta) - (2u_\theta \cot \theta / r^2)] , \end{aligned} \quad (C17)$$

$$\begin{aligned} \partial p^*/\partial r = \mu [& (\partial^2 u_r^*/\partial r^2) + (2/r) (\partial u_r^*/\partial r) + (1/r^2) (\partial^2 u_r^*/\partial \theta^2) + (\cot \theta / r^2) (\partial u_r^*/\partial \theta) \\ & - (2u_r^*/r^2) - (2/r^2) (\partial u_\theta^*/\partial \theta) - (2u_\theta^* \cot \theta / r^2) - (u_r^*/\kappa)] . \end{aligned}$$

(C18)

The pressures p and p^* may be obtained by integration of these equations with respect to r .

C.2 SOLUTION OF THE DEFINING EQUATIONS

C.2.1 THE GENERAL SOLUTIONS

The following analysis derives in detail the results presented and utilized in Sections II.5 and II.7 of the main text.

The Exterior Region

The boundary condition implicit in Equation (C10) may be rewritten in component form as follows, viz.

$$\lim_{r \rightarrow \infty} u_r^*(r, \theta) = -U^* \cos \theta, \quad (C19)$$

$$\lim_{r \rightarrow \infty} u_\theta^*(r, \theta) = U^* \sin \theta. \quad (C20)$$

These equations, in connection with Equations (C13) and (C14), imply that:

$$\lim_{r \rightarrow \infty} \psi^*(r, \theta) = (1/2)U^*r^2 \sin^2 \theta. \quad (C21)$$

Observing the nature of this limiting solution for ψ^* a general solution of Equation (C2) is sought in the separable form:

$$\psi^*(r, \theta) = [\omega_1(r) + \omega_2(r) + \omega_3(r) + \omega_4(r)] \sin^2 \theta, \quad (C22)$$

where $\omega_i(r)$ denotes any function of r such that $\omega_i(r) \sin^2 \theta$ constitutes a particular solution of Equation (C2).

It transpires that a general solution of the above form is:

$$\psi^*(\chi, \theta) = (\kappa U^*/2) [E/\chi + F\chi^2 + Ge^{-\chi}(1+\chi)/\chi + He^{\chi}(1-\chi)/\chi] \sin^2 \theta, \quad (C23)$$

where E, F, G and H denote arbitrary constants and χ represents the

normalized radial coordinate defined by:

$$\chi(r) = r/\sqrt{\kappa} . \quad (C24)$$

From a closer inspection of Equations (C21) and (C23) it follows necessarily that $H = 0$ and $F = 1$, whence Equation (C23) becomes:

$$\psi^*(\chi, \theta) = (\kappa U^*/2) [E/\chi + \chi^2 + Ge^{-\chi}(1+\chi)/\chi] \sin^2 \theta . \quad (C25)$$

The Annular Region

A general solution of Equation (C1), possessing the same separable form as Equation (C22), can be shown to be²⁸:

$$\psi(\chi, \theta) = (\kappa U^*/2) [A/\chi + B\chi + C\chi^2 + D\chi^4] \sin^2 \theta, \quad (C26)$$

where A, B, C and D denote arbitrary constants.

The Global Streamfunction Distribution

The entire flowfield around the reference sphere is completely defined by the streamfunctions presented in Equations (C25) and (C26), viz.

$$\psi(\chi, \theta) = (\kappa U^*/2) [A/\chi + B\chi + C\chi^2 + D\chi^4] \sin^2 \theta \quad \alpha < \chi < \beta , \quad (C27)$$

$$\psi^*(\chi, \theta) = (\kappa U^*/2) [E/\chi + \chi^2 + Ge^{-\chi}(1+\chi)/\chi] \sin^2 \theta \quad \beta < \chi < \infty . \quad (C28)$$

The parameters α and β represent the particular values of χ defined by:

$$\alpha = \chi(R) = R/\sqrt{\kappa} , \quad (C29)$$

$$\beta = \chi(S) = S/\sqrt{\kappa} . \quad (C30)$$

Now that the general form of the global streamfunction has been ascertained the global velocity, shear stress and pressure distributions may be determined directly, as follows.

The Global Velocity Distribution

The radial and tangential components of the prevailing flow-field follow at once from Equations (C11)-(C14) and Equations (C27)-(C28), thus:

$$u_r(\chi, \theta) = -U^*[A/\chi^3 + B/\chi + C + D\chi^2]\cos\theta, \quad (C31)$$

$$u_r^*(\chi, \theta) = -U^*[1 + E/\chi^3 + Ge^{-\chi}(1+\chi)/\chi^3]\cos\theta, \quad (C32)$$

$$u_\theta(\chi, \theta) = U^*[-A/2\chi^3 + B/2\chi + C + 2D\chi^2]\sin\theta, \quad (C33)$$

$$u_\theta^*(\chi, \theta) = U^*[1 - E/2\chi^3 - Ge^{-\chi}(1+\chi+\chi^2)/2\chi^3]\sin\theta. \quad (C34)$$

The Global Shear Stress Distribution

From Equations (C15)-(C16) and Equations (C31)-(C34) above it may be shown that:

$$\tau(\chi, \theta) = -(\mu U^*/\sqrt{\kappa})[3A/\chi^4 + 3D\chi]\sin\theta, \quad (C35)$$

$$\tau^*(\chi, \theta) = -(\mu U^*/\sqrt{\kappa})[3E/\chi^4 + Ge^{-\chi}(6+6\chi+3\chi^2+\chi^3)/2\chi^4]\sin\theta. \quad (C36)$$

The Global Pressure Distribution

From Equations (C17)-(C18) and Equations (C31)-(C34) it is possible to show that:

$$p(\chi, \theta) = p^*(\chi, \pi/2) - (\mu U^*/\sqrt{\kappa})[B/\chi^2 + 10D\chi]\cos\theta, \quad (C37)$$

$$p^*(\chi, \theta) = p^*(\chi, \pi/2) - (\mu U^*/\sqrt{\kappa})[E/2\chi^2 - \chi]\cos\theta. \quad (C38)$$

C.2.2 EVALUATION OF THE ARBITRARY CONSTANTS

The stipulated boundary conditions presented in Equations (C4)-(C9) may be re-expressed in terms of the normalized parameters α and β , as follows:

$$u_r(\alpha^+, \theta) = 0 , \quad (C39)$$

$$u_\theta(\alpha^+, \theta) = 0 , \quad (C40)$$

$$u_r(\beta^-, \theta) = u_r^*(\beta^+, \theta) , \quad (C41)$$

$$u_\theta(\beta^-, \theta) = u_\theta^*(\beta^+, \theta) , \quad (C42)$$

$$\tau(\beta^-, \theta) = \tau^*(\beta^+, \theta) , \quad (C43)$$

$$p(\beta^-, \theta) = p^*(\beta^+, \theta) . \quad (C44)$$

It transpires that these six conditions contain sufficient information to permit the determination of the six unknown arbitrary constants A,B,C,D,E and G. Thus, by applying these conditions to the respective global distributions presented in Equations (C31)-(C38) the following six *independent* equations may be generated:

$$A + B\alpha^2 + C\alpha^3 + D\alpha^5 = 0 , \quad (C45)$$

$$A - B\alpha^2 - 2C\alpha^3 - 4D\alpha^5 = 0 , \quad (C46)$$

$$A + B\beta^2 + C\beta^3 + D\beta^5 = \beta^3 + E + Ge^{-\beta}(1+\beta) , \quad (C47)$$

$$A - B\beta^2 - 2C\beta^3 - 4D\beta^5 = -2\beta^3 + E + Ge^{-\beta}(1+\beta+\beta^2) , \quad (C48)$$

$$6A + 6D\beta^5 = 6E + Ge^{-\beta}(6+6\beta+3\beta^2+\beta^3) , \quad (C49)$$

$$2B + 20D\beta^3 = -2\beta^3 + E . \quad (C50)$$

Equations (C45)-(C50) constitute six simultaneous equations in the six unknowns A,B,C,D,E and G; the solution of these equations can be shown to be:

$$A = 6\alpha^3(-2\beta^6-7\beta^5-15\beta^4-15\beta^3+3\beta^4\alpha^2-\beta^3\alpha^3+3\beta^3\alpha^2+\beta^2\alpha^3)/J(\alpha,\beta) , \quad (C51)$$

$$B = 6\alpha(6\beta^6+21\beta^5+45\beta^4+45\beta^3-5\beta^4\alpha^2-5\beta^3\alpha^2-\beta\alpha^5-\alpha^5)/J(\alpha,\beta) , \quad (C52)$$

$$C = 3(-8\beta^6-28\beta^5-60\beta^4-60\beta^3+5\beta^3\alpha^3-5\beta^2\alpha^3+3\beta\alpha^5+3\alpha^5)/J(\alpha,\beta) , \quad (C53)$$

$$D = 3(4\beta^4+4\beta^3-3\beta^3\alpha+3\beta^2\alpha-\beta\alpha^3-\alpha^3)/J(\alpha,\beta) , \quad (C54)$$

$$E = 2(-4\beta^9-24\beta^8-60\beta^7-60\beta^6+9\beta^8\alpha+45\beta^7\alpha-10\beta^6\alpha^3+126\beta^6\alpha-30\beta^5\alpha^3 \\ +216\beta^5\alpha+9\beta^4\alpha^5-60\beta^4\alpha^3+270\beta^4\alpha-4\beta^3\alpha^6+9\beta^3\alpha^5 \\ -60\beta^3\alpha^3+270\beta^3\alpha-6\beta\alpha^6-6\alpha^6)/J(\alpha,\beta) , \quad (C55)$$

$$G = 6e^\beta(20\beta^6-27\beta^5\alpha+5\beta^3\alpha^3-90\beta^3\alpha+2\alpha^6)/J(\alpha,\beta) , \quad (C56)$$

where:

$$J(\alpha,\beta) = (-4\beta^6-24\beta^5-180\beta^4-180\beta^3+9\beta^5\alpha+45\beta^4\alpha-10\beta^3\alpha^3+180\beta^3\alpha \\ -30\beta^2\alpha^3+9\beta\alpha^5-4\alpha^6+9\alpha^5) . \quad (C57)$$

C.2.3 THE RESISTANCE OFFERED BY THE REFERENCE SPHERE

The normal resistance force, F_r , and the tangential resistance force, F_θ , offered by the reference sphere may be calculated by integrating the local pressure $p(\alpha,\theta)$ and the local shear stress $\tau(\alpha,\theta)$ respectively over the entire surface thereof²⁸, thus:

$$F_r = 2\pi R^2 \int_0^\pi [p(\alpha,\theta)\cos\theta] \sin\theta \, d\theta , \quad (C58)$$

$$F_\theta = 2\pi R^2 \int_0^\pi [-\tau(\alpha,\theta)\sin\theta] \sin\theta \, d\theta . \quad (C59)$$

After substituting for $p(\alpha, \theta)$ and $\tau(\alpha, \theta)$ from Equations (C37) and (C35) respectively, it is found that:

$$F_r = 6\pi\mu U^* R (-2B - 20D\alpha^3) / 9\alpha , \quad (C60)$$

$$F_\theta = 6\pi\mu U^* R (4A + 4D\alpha^5) / 3\alpha^3 . \quad (C61)$$

The total resistance force, F , offered by the reference sphere will therefore be:

$$F = F_r + F_\theta = 6\pi\mu U^* R (12A - 2B\alpha^2 - 8D\alpha^5) / 9\alpha^3 . \quad (C62)$$

After substituting for A, B and D from Equations (C51), (C52) and (C54) respectively the ultimate expression for F is obtained, viz:

$$F = 6\pi\mu U^* R \xi(\alpha, \beta) , \quad (C63)$$

where:

$$\xi(\alpha, \beta) = 4(-6\beta^6 - 21\beta^5 - 45\beta^4 - 45\beta^3 + 5\beta^4\alpha^2 + 5\beta^3\alpha^2 + \beta\alpha^5 + \alpha^5) / J(\alpha, \beta) . \quad (C64)$$

It has been demonstrated in the main text (Table 3) that as $\epsilon \rightarrow 1.0$, $\xi(\alpha, \beta) \rightarrow 1.0$ so that Equation (C63) then approaches Stokes Law²⁸ for creeping flow past a single isolated sphere, viz.

$$F_{\text{Stokes}} = 6\pi\mu U^* R . \quad (C65)$$

C.2.4 THE TOTAL RESISTANCE OFFERED BY AN ARBITRARY SWARM OF SPHERES

A randomly textured swarm of spheres possessing the following size distribution will be considered:

Total number of spheres : N ,

Number of spheres having radius R_i : N_i ($i = 1, 2, 3, \dots, n$),

Fraction of spheres having radius R_i : $f_i = N_i/N$,

Size Ratio : $y_i = R_i/R_0$,

where R_0 denotes the radius of any chosen species of sphere present, for example the radius of the most prolific.

The Original System

This analysis has heretofore considered an unbounded swarm of spheres. This implies an absence of all wall and end effects so that \underline{U}^* will be uniformly constant throughout and, in consequence, $\nabla^2 \underline{U}^* = 0$. Under these circumstances the Brinkman Equation (82) reduces to the familiar Darcy Equation (81) as previously noted in Section II.2 of the main text. This means that:

$$(\mu/\kappa)U^* = \Delta p^*/\Delta x \quad , \quad (C66)$$

where Δp^* denotes the pressure differential across the system and Δx its overall length. Letting A denote the cross-sectional area of the system orthogonal to the flowfield, the total resistance offered by the swarm of spheres will be:

$$F_{\text{swarm}} = \Delta p^* A \quad . \quad (C67)$$

Substituting for Δp^* from Equation (C66) then yields:

$$F_{\text{swarm}} = \mu U^* A \Delta x / \kappa = \mu U^* V \alpha_0^2 / R_0^2 \quad . \quad (C68)$$

In this equation V denotes the total volume of the system ($A\Delta x$) and κ

has been replaced according to Equation (C29), viz.

$$\kappa = R_0^2 / \alpha_0^2 . \quad (C69)$$

The total volume of the system may be expressed in terms of the total particle volume and the porosity as follows:

$$V = \sum_i (4\pi/3) R_i^3 N_i / (1-\epsilon) = (4\pi/3) R_0^3 N \sum_i y_i^3 f_i / (1-\epsilon) . \quad (C70)$$

Substituting this expression for V into Equation (C68) then yields the following expression for the total resistance offered by the original swarm of spheres, viz.

$$F_{\text{swarm}} = 6\pi\mu U R_0 N \{ 2\alpha_0^2 / 9 (1-\epsilon) \} \sum_i y_i^3 f_i . \quad (C71)$$

The Modelled System

According to Equation (C63) the resistance force, F_i , offered by a reference sphere of radius R_i will be:

$$F_i = 6\pi\mu U R_i \xi(\alpha_i, \beta_i) = 6\pi\mu U R_0 y_i \xi(\alpha_i, \beta_i) , \quad (C72)$$

where:

$$\alpha_i = R_i / \sqrt{\kappa} , \quad (C73)$$

$$\beta_i = S_i / \sqrt{\kappa} . \quad (C74)$$

There still exists a constant ratio between β_i and α_i according to Equation (116) of the main text, since each sphere within the swarm may be considered to be the reference sphere in turn, thus:

$$\beta_i = \alpha_i (1-\epsilon)^{-1/3} . \quad (C75)$$

The total resistance offered by the swarm of N spheres according to the proposed model may therefore be expressed by:

$$F_{\text{model}} = \sum_i F_i N_i = N \sum_i F_i f_i . \quad (C76)$$

Combining Equations (C76) and (C72) then yields the ultimate expression:

$$F_{\text{model}} = 6\pi\mu U^* R_0 N \sum_i y_i f_i \xi(\alpha_i, \beta_i) . \quad (C77)$$

C.2.5 QUANTITATIVE CONSISTENCY OF THE MODELLED SYSTEM

Since the modelled system is to be quantitatively representative of the original system (as regards hydrodynamic resistance) then the total resistances as predicted by Equations (C71) and (C77) must be identical, i.e.

$$F_{\text{model}} = F_{\text{swarm}} . \quad (C78)$$

Equating these expressions finally generates the identity:

$$2\alpha_0^2 \sum_i y_i^3 f_i - 9(1-\epsilon) \sum_i y_i f_i \xi(\alpha_i, \beta_i) = 0 . \quad (C79)$$

The parameters α_i and β_i may be expressed in terms of y_i , α_0 and ϵ as follows, thus:

$$\alpha_i = R_i / \sqrt{\kappa} = (R_0 / \sqrt{\kappa}) (R_i / R_0) = \alpha_0 y_i , \quad (C80)$$

$$\beta_i = \alpha_i (1-\epsilon)^{-1/3} = \alpha_0 y_i (1-\epsilon)^{-1/3} . \quad (C81)$$

After introducing these expressions into Equation (C79) it becomes apparent that α_0 and ϵ are related by an exceedingly complicated function, viz.

$$2\alpha_0^2 \sum_i y_i^3 f_i - 9(1-\epsilon) \sum_i y_i f_i \xi(\alpha_0 y_i, \alpha_0 y_i (1-\epsilon)^{-1/3}) = 0 . \quad (C82)$$

Provided the size distribution (f_i, y_i) of the spheres is known then α_0 may be extracted from Equation (C82) as a function of ϵ by an iterative procedure.

C.2.6 COMPARISON OF THE TOTAL RESISTANCE WITH THAT PREDICTED BY STOKES LAW

The total resistance of the original swarm of N spheres, assuming each sphere to be hydrodynamically independent of the remainder, would be given by Stokes Equation (C65) as:

$$F_{\text{Stokes}} = \sum_i 6\pi\mu U^* R_i N_i = 6\pi\mu U^* R_0 N \sum_i y_i f_i . \quad (C83)$$

It is instructive to compare this expression with the resistance predicted by the presented theory. Thus, from Equations (C71) and (C83) it follows that:

$$W = F_{\text{Stokes}} / F_{\text{swarm}} = \{9(1-\epsilon)/2\alpha_0^2\} [\sum_i y_i f_i] / [\sum_i y_i^3 f_i] . \quad (C84)$$

Hence, for a specified porosity ϵ and a known size distribution (f_i, y_i) , a knowledge of α_0 is sufficient to evaluate W .

Monosized Spheres

For a system composed exclusively of monosized spheres

($n = 1$, $i = 1$, $f_i = 1$, $y_i = 1$ and $\alpha_0 \equiv \alpha$) Equations (C82) and (C84)

reduce to:

$$2\alpha^2 - 9(1-\varepsilon)\xi(\alpha, \alpha(1-\varepsilon)^{-1/3}) = 0 , \quad (\text{C85})$$

$$W = 9(1-\varepsilon)/2\alpha^2 = 1/\xi(\alpha, \alpha(1-\varepsilon)^{-1/3}) . \quad (\text{C86})$$

Therefore, for a specified porosity ε the corresponding value of α may be obtained from Equation (C85) by an iterative procedure; W may then be computed directly from Equation (C86).

APPENDIX D

INCOMPRESSIBLE CREEPING FLOW THROUGH

A FRACTURED POROUS MEDIUM

D.1 DISCUSSION OF THE SYSTEM

Fractures in petroleum reservoirs often play an important role in the production of fluid from the pay formation⁴⁴. In fact, in some instances the oil or gas could not be produced economically in the absence of fractures functioning as arteries for transporting the fluids from the reservoir rock formation to the well-bore. Indeed, deliberate attempts are often made to induce fractures and to widen existing fractures during oil-field production³⁹.

The idealized system depicted in Figure 28 may be considered representative of a fractured petroleum reservoir. This system comprises two semi-infinite extents of isotropic porous medium, possessing permeabilities κ_1 and κ_2 (which may or may not be equal), separated by a uniform fracture (channel) of width $2h$. The flowfield will here be presumed to be collinear with the fracture.

The analysis which follows seeks to calculate the velocity profile prevailing throughout the idealized system described above and, in doing so, to demonstrate the inadequacy of the Darcy Equation for describing fluid flow in porous media.

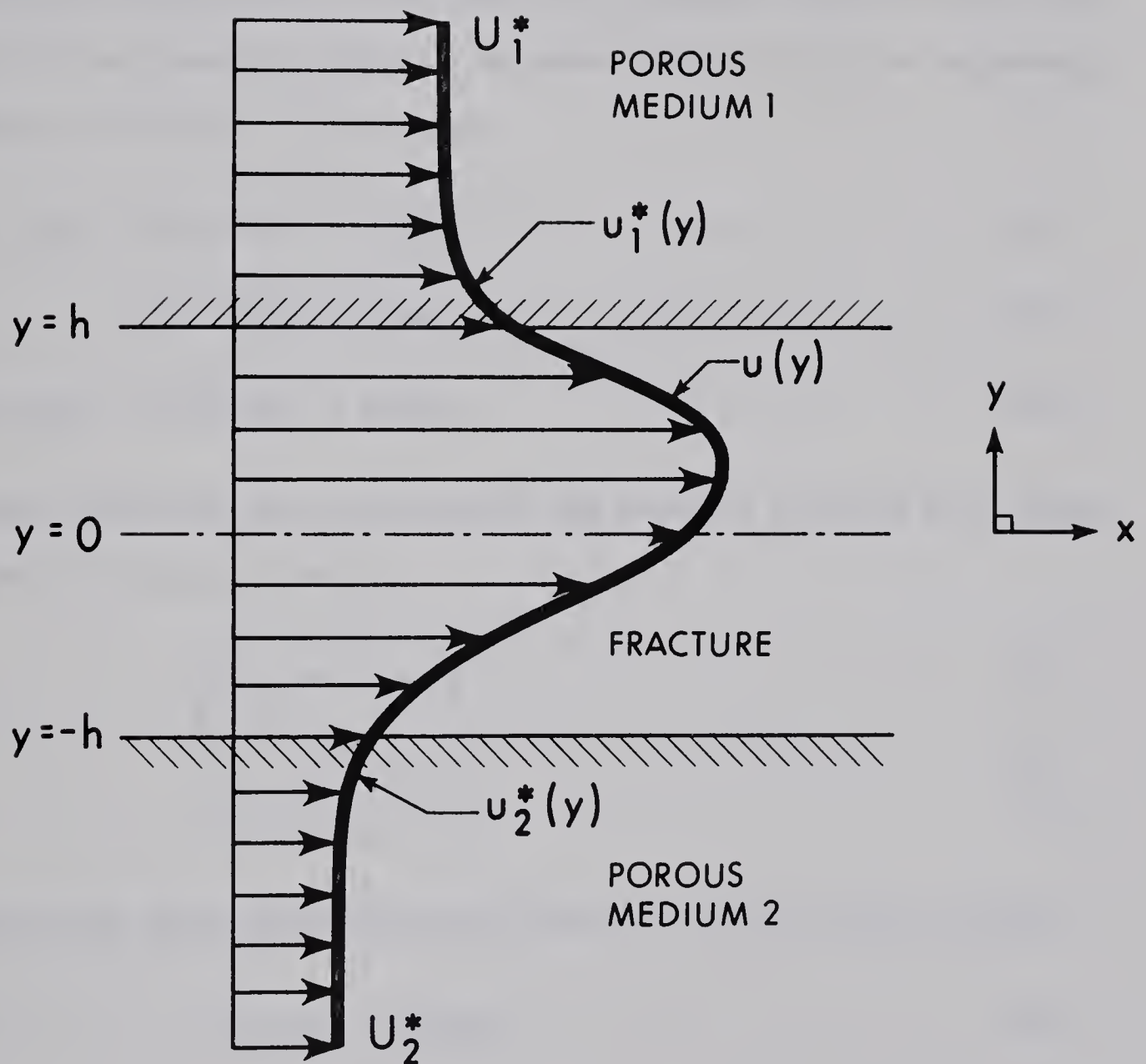


FIGURE 28. AN IDEALIZED FRACTURE WITHIN A PETROLEUM RESERVOIR

D.2 THE DEFINING EQUATIONS AND BOUNDARY CONDITIONS

D.2.1 FUNDAMENTAL DIFFERENTIAL EQUATIONS

The Brinkman Equation (82) will be employed to describe the hydrodynamic conditions within each of the porous regions, whilst the Navier-Stokes Equation (80) will be acknowledged within the separating channel of free fluid space, thus:

$$-(\mu/\kappa_1)u_1^* + \mu(d^2u_1^*/dy^2) = dp_1^*/dx \quad h < y < \infty, \quad (D1)$$

$$\mu(d^2u/dy^2) = dp/dx \quad -h < y < h, \quad (D2)$$

$$-(\mu/\kappa_2)u_2^* + \mu(d^2u_2^*/dy^2) = dp_2^*/dx \quad -\infty < y < -h. \quad (D3)$$

At great distances from the fracture the velocity profiles will become uniformly constant, that is:

$$\text{Limit}_{y \rightarrow \infty} u_1^*(y) = U_1^*, \quad (D4)$$

$$\text{Limit}_{y \rightarrow -\infty} u_2^*(y) = U_2^*. \quad (D5)$$

Substituting these expressions into Equations (D1) and (D3) yields:

$$-(\mu/\kappa_1)U_1^* = dp_1^*/dx, \quad (D6)$$

$$-(\mu/\kappa_2)U_2^* = dp_2^*/dx. \quad (D7)$$

However, from considerations of equilibrium it is necessary that

$$dp_1^*/dx = dp/dx = dp_2^*/dx = \text{constant}. \quad (D8)$$

In view of these equalities the substitution of Equations (D6) and (D7) into Equations (D1)-(D3) ultimately yields:

$$-u_1^*/\kappa_1 + d^2u_1^*/dy^2 = -U_1^*/\kappa_1 \quad h < y < \infty , \quad (D9)$$

$$d^2u/dy^2 = -U_1^*/\kappa_1 \quad -h < y < h , \quad (D10)$$

$$-u_2^*/\kappa_2 + d^2u_2^*/dy^2 = -U_2^*/\kappa_2 \quad -\infty < y < -h . \quad (D11)$$

D.2.2 STIPULATED BOUNDARY CONDITIONS

From considerations of continuity and equilibrium at the extrema of the channel the following boundary conditions must be stipulated:

$$u_1^*(h^+) = u(h^-) , \quad (D12)$$

$$\tau_1^*(h^+) = \tau(h^-) , \quad (D13)$$

$$u(-h^+) = u_2^*(-h^-) , \quad (D14)$$

$$\tau(-h^+) = \tau_2^*(-h^-) . \quad (D15)$$

In these equations τ_1^* , τ and τ_2^* denote the tangential shear stresses, defined by:

$$\tau_1^* = -\mu(du_1^*/dy) , \quad (D16)$$

$$\tau = -\mu(du/dy) , \quad (D17)$$

$$\tau_2^* = -\mu(du_2^*/dy) . \quad (D18)$$

D.3 SOLUTION OF THE DEFINING EQUATIONS

The solutions of Equations (D9) - (D11) which satisfy the boundary conditions stipulated in Equations (D12)-(D15) transpire to be:

$$u_1^*(\eta) = U_1^*(1+A_1^*e^{-\eta}) \quad \delta < \eta < \infty, \quad (D19)$$

$$u(\eta) = U_1^*(B+C\eta-\eta^2/2) \quad -\delta < \eta < \delta, \quad (D20)$$

$$u_2^*(\eta) = U_2^*(1+A_2^*e^{\gamma\eta}) \quad -\infty < \eta < -\delta, \quad (D21)$$

$$U_2^* = U_1^*/\gamma^2. \quad (D22)$$

In these equations η denotes the normalized variable defined by:

$$\eta = y/\sqrt{\kappa_1}. \quad (D23)$$

The parameters δ and γ are defined by:

$$\delta = h/\sqrt{\kappa_1}, \quad (D24)$$

$$\gamma = \sqrt{\kappa_1/\kappa_2}, \quad (D25)$$

and A_1^* , B , C and A_2^* possess the specific forms:

$$A_1^* = e^{\delta}(1-\gamma^2+2\delta\gamma+2\delta^2\gamma^2)/M(\delta,\gamma), \quad (D26)$$

$$B = (1+\gamma+\delta+2\delta\gamma+\delta\gamma^2+3\delta^2\gamma/2+3\delta^2\gamma^2/2+\delta^3\gamma^2)/M(\delta,\gamma), \quad (D27)$$

$$C = -(1-\gamma^2+\delta\gamma-\delta\gamma^2)/M(\delta,\gamma), \quad (D28)$$

$$A_2^* = -\gamma e^{\delta\gamma}(1-\gamma^2-2\delta\gamma^2-2\delta^2\gamma^2)/M(\delta,\gamma), \quad (D29)$$

where:

$$M(\delta, \gamma) = \gamma(1 + \gamma + 2\delta\gamma) . \quad (D30)$$

Equations (D19) - (D30), being of a rather general nature, are capable of several interesting specializations, as follows.

One Medium Impermeable

Supposing that medium 2 is impermeable ($\kappa_2 = 0$, $\gamma = \infty$) then the prevailing flowfield will be described by:

$$u_1^*(\eta) = U_1^*(1 + A_1^* e^{-\eta}) , \quad (D31)$$

$$u(\eta) = U_1^*(B + C\eta - \eta^2/2) , \quad (D32)$$

$$u_2^*(\eta) = 0 , \quad (D33)$$

where:

$$A_1^* = -e^\delta (1 - 2\delta^2) / (1 + 2\delta) , \quad (D34)$$

$$B = \delta (1 + 3\delta/2 + \delta^2) / (1 + 2\delta) , \quad (D35)$$

$$C = (1 + \delta) / (1 + 2\delta) . \quad (D36)$$

From these equations it is clear that $u(-\delta) = 0$, as required for non-slip fluid flow past a solid surface.

Both Media Possessing an Equal Permeability

Under these conditions ($\kappa_2 = \kappa_1$, $\gamma = 1$) the flowfield will be described by:

$$u_1^*(\eta) = U_1^*(1 + \delta e^{\delta - \eta}) , \quad (D37)$$

$$u(\eta) = U_1^*(1 + \delta + \delta^2/2 - \eta^2/2) , \quad (D38)$$

$$u_2^*(\eta) = U_1^*(1 + \delta e^{\delta + \eta}) . \quad (D39)$$

The flowfield is therefore symmetric about $\eta = 0$, as would be expected.

Both Media in Contact

In this case ($h = 0$, $\delta = 0$) the channel separating the two media ceases to exist and, in effect, constitutes a discontinuity between them. The flowfield will then be described by:

$$u_1^*(\eta) = U_1^*(1 + A_1^* e^{-\eta}) , \quad (D40)$$

$$u_2^*(\eta) = (U_1^*/\gamma^2)(1 + A_2^* e^{\gamma\eta}) , \quad (D41)$$

where:

$$A_1^* = (1 - \gamma)/\gamma , \quad (D42)$$

$$A_2^* = (\gamma - 1) . \quad (D43)$$

Furthermore, when the permeabilities of the two media become equal the flowfield will become uniformly constant. Under these conditions ($\gamma = 1$) Equations (D40) and (D41) reduce to the necessary forms, viz.

$$u_1^*(\eta) = u_2^*(\eta) = U_1^* . \quad (D44)$$

D.4 COMPARISON OF THE PRESENTED SOLUTION WITH THE APPROXIMATE REPRESENTATION OBTAINED USING THE DARCY EQUATION

When estimating liquid flow through fractured porous media it has been customary⁴⁴ in the past to adopt the Darcy Equation (81) within the porous regions and the Poiseuille Equation²⁸ within the separating channel. Thus, when both media possess equal permeabilities (which is usually the case in practice) the flowfield would be approximated by:

$$u_1^*(\eta) = U_1^* \quad \delta < \eta < \infty, \quad (D45)$$

$$u(\eta) = U_1^*(\delta^2/2 - \eta^2/2) \quad -\delta < \eta < \delta, \quad (D46)$$

$$u_2^*(\eta) = U_1^* \quad -\infty < \eta < -\delta. \quad (D47)$$

These profiles are depicted schematically in Figure 29. It is immediately apparent that the above equations do not satisfy the continuity boundary conditions implicit in Equations (D12) and (D14), viz.

$$u_1^*(\delta) = u(\delta), \quad (D48)$$

$$u(-\delta) = u_2^*(-\delta). \quad (D49)$$

Moreover, they are also unable to satisfy the equilibrium conditions implicit in Equations (D13) and (D15), viz.

$$\tau_1^*(\delta) = \tau(\delta), \quad (D50)$$

$$\tau(-\delta) = \tau_2^*(-\delta). \quad (D51)$$

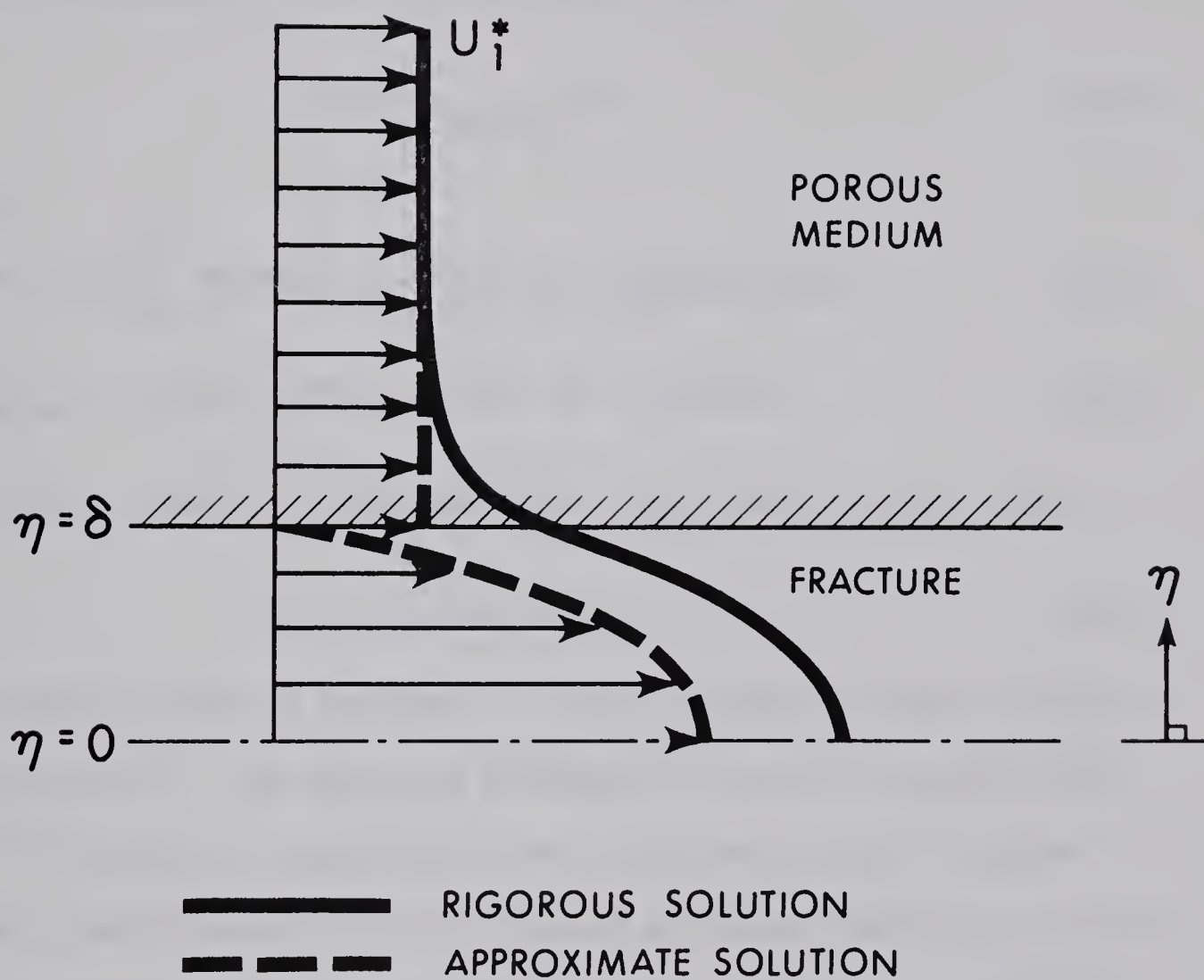


FIGURE 29. THE APPROXIMATE AND RIGOROUS VELOCITY PROFILES FOR THE FRACTURED SYSTEM (Schematic)

In order to obtain an estimate of the relative error, Δ , incurred by adopting this approximate representation of the flowfield it will be instructive to compare the mean velocity, \bar{u} , within the channel as predicted rigorously from Equation (D38) with that predicted approximately from Equation (D46), viz.

$$\Delta = (\bar{u} - \bar{u}_{\text{approx}})/\bar{u} , \quad (\text{D52})$$

where:

$$\bar{u} = (1/2\delta) \int_{-\delta}^{+\delta} U_1^* (1 + \delta + \delta^2/2 - \eta^2/2) d\eta = U_1^* (1 + \delta + \delta^2/3) , \quad (\text{D53})$$

$$\bar{u}_{\text{approx}} = (1/2\delta) \int_{-\delta}^{+\delta} U_1^* (\delta^2/2 - \eta^2/2) d\eta = U_1^* (\delta^2/3) . \quad (\text{D54})$$

Substituting Equations (D53) and (D54) into Equation (D52) yields

$$\Delta = (1 + \delta)/(1 + \delta + \delta^2/3) . \quad (\text{D55})$$

This equation predicts that for $\delta < 300$ the relative error Δ will be greater than 1%. The immediate inference is that the incurred error will be of practical significance for sufficiently thin fractures. However, the thickness ($2h$) of a typical petroleum reservoir fracture would be of the order of 1 mm., with δ being in the range 500-5000. In practice, therefore, the *quantitative* error incurred by employing the Darcy Equation (81) rather than the Brinkman Equation (82) will usually be negligible.

This analysis has indeed served to demonstrate that the Brinkman Equation permits a mathematically consistent solution to a realistic problem involving adjacent regions of porous medium and fluid space; a problem, in fact, which could not otherwise be treated rigorously.

APPENDIX E

INCOMPRESSIBLE CREEPING FLOW THROUGH
AN ISOTROPIC POROUS MEDIUM
CONTAINING A SPHERICAL CAVITY

E.1 DISCUSSION OF THE SYSTEM

In many naturally occurring rock formations there occur distinct cavities of various shapes and sizes. Having particular significance in Canada are those encountered in oilfields formed within dolomite reefs. An understanding of liquid flow through such two-porosity systems is therefore desirable. In order to gain physical insight into this problem it will be instructive to consider incompressible creeping flow through the idealized system consisting of an unbounded, isotropic porous medium which contains an isolated spherical cavity. As yet, there does not appear to be available a solution to this important problem.

This analysis will also serve to demonstrate the necessity and effectiveness of the Brinkman Equation (82) in solving another, hitherto intractable, two-region problem.

E.2 THE DEFINING EQUATIONS AND BOUNDARY CONDITIONS

E.2.1 FUNDAMENTAL DIFFERENTIAL EQUATIONS

The Navier-Stokes Equation (80) will describe the flowfield within the cavity (of radius S); this equation may be expressed in terms of the streamfunction ψ as per Equation (94), viz.

$$E^2(E^2\psi) = 0 \quad 0 < r < S . \quad (E1)$$

The Brinkman Equation (82) will be acknowledged to describe the flowfield within the isotropic porous medium (of permeability κ); in terms of the streamfunction ψ^* this equation assumes the following form (Equation (95)):

$$-(1/\kappa)E^2\psi^* + E^2(E^2\psi^*) = 0 \quad S < r < \infty . \quad (E2)$$

E.2.2 STIPULATED BOUNDARY CONDITIONS

The following boundary conditions must be stipulated for this physically realistic problem:

$$p(S^-, \theta) = p^*(S^+, \theta) , \quad (E3)$$

$$\tau(S^-, \theta) = \tau^*(S^+, \theta) , \quad (E4)$$

$$u_r(S^-, \theta) = u_r^*(S^+, \theta) , \quad (E5)$$

$$u_\theta(S^-, \theta) = u_\theta^*(S^+, \theta) , \quad (E6)$$

$$\text{Limit}_{r \rightarrow \infty} \underline{u}^*(r, \theta) = \underline{U}^* . \quad (E7)$$

The arguments on which the above boundary conditions are based are presented in Section II.4.2 of the main text. In addition, a restriction demanding finiteness of the flowfield must be imposed,

in particular that

$$u_r(0,\theta) \text{ must be finite .} \quad (\text{E8})$$

E.3 SOLUTION OF THE DEFINING EQUATIONS

E.3.1 THE GLOBAL STREAMFUNCTION DISTRIBUTION

The solutions of Equations (E1) and (E2) which satisfy the boundary conditions implicit in Equations (E3)-(E8) can be shown to be:

$$\psi(\chi, \theta) = (\kappa U^*/2)[C\chi^2 + D\chi^4]\sin^2\theta \quad 0 < \chi < \beta, \quad (E9)$$

$$\psi^*(\chi, \theta) = (\kappa U^*/2)[E/\chi + \chi^2 + Ge^{-\chi}(1+\chi)/\chi]\sin^2\theta \quad \beta < \chi < \infty, \quad (E10)$$

where:

$$\chi = r/\sqrt{\kappa}, \quad (E11)$$

$$\beta = S/\sqrt{\kappa}, \quad (E12)$$

and:

$$C = (6\beta^3 + 21\beta^2 + 45\beta + 45)/(\beta^3 + 6\beta^2 + 45\beta + 45), \quad (E13)$$

$$D = -3(\beta + 1)/(\beta^3 + 6\beta^2 + 45\beta + 45), \quad (E14)$$

$$E = 2\beta^3(\beta^3 + 6\beta^2 + 15\beta + 15)/(\beta^3 + 6\beta^2 + 45\beta + 45), \quad (E15)$$

$$G = -30\beta^3 e^{\beta}/(\beta^3 + 6\beta^2 + 45\beta + 45). \quad (E16)$$

When the cavity ceases to exist ($S = 0$, $\beta = 0$), Equation (E10) reduces to the limiting form $\psi^* = (1/2)U^*r^2\sin^2\theta$. This is the familiar streamfunction representation²⁸ of an undisturbed flowfield, \underline{U}^* , as would be expected.

E.3.2 GENERAL APPEARANCE OF THE STREAMLINES

Typical streamlines, as computed from Equations (E9)-(E16) above, are depicted in Figure 30 for the representative case $\beta = 1000$. The most important inference to be drawn therefrom is that the disturbance created by the cavity on the mainstream flow is effectively localized to a region concentric with the cavity and possessing thrice its radius.

It is evident, therefore, that the Brinkman Equation (82) permits the solution of a realistic hydrodynamic problem which has not hitherto been solved.

E.3.3 THE PRESENTED SOLUTION AS A LIMITING SPECIALIZATION

The geometric model proposed in Section II.3 of the main text for an homogeneous swarm of spheres (Figure 16) is fundamentally related in structure to the spherical cavity system here investigated. The modelled system may, in fact, be constructed *from* this cavity system by suspending a sphere (of radius R) concentrically within the cavity.

As might be expected, the presented solution for the spherical cavity system agrees identically with the limiting solution for the modelled system (Equations (104)-(115)) for the limiting specialization in which the radius, R , of the reference sphere becomes equal to zero.

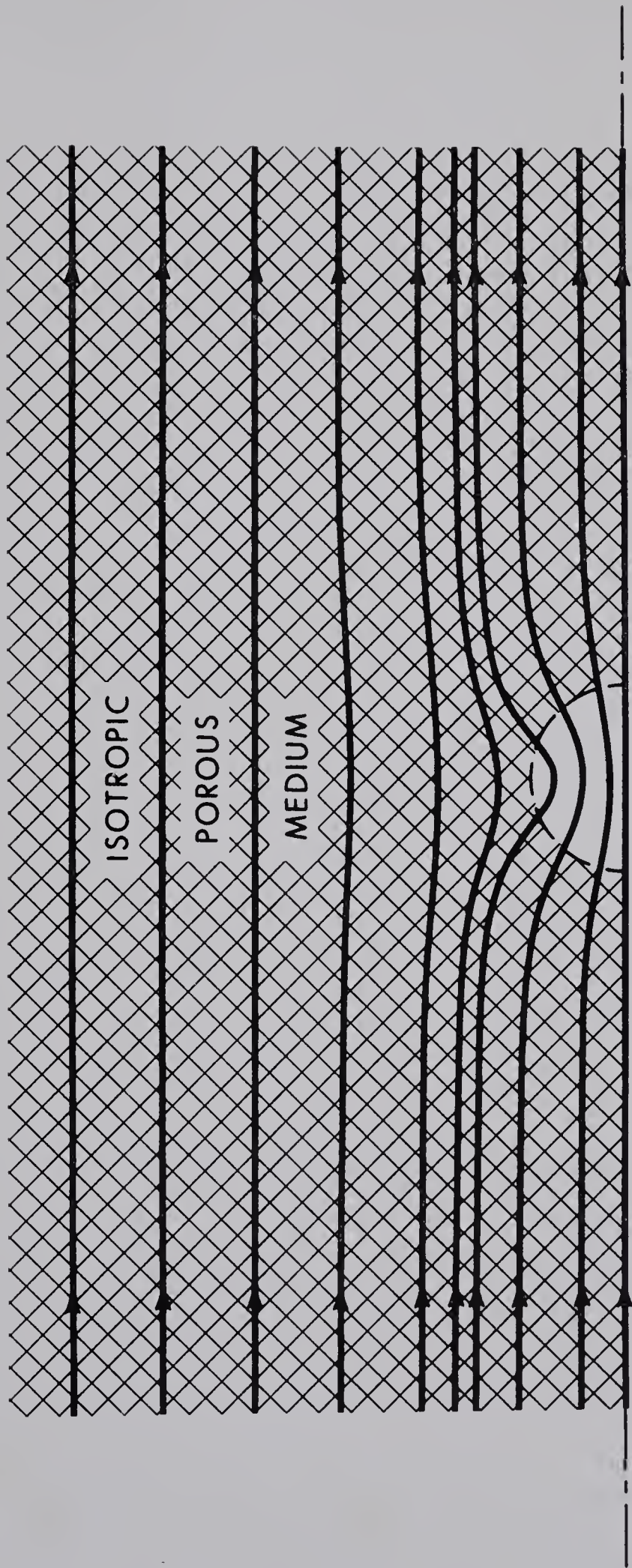


FIGURE 30. TYPICAL STREAMLINES FOR INCOMPRESSIBLE CREEPING FLOW THROUGH AN ISOTROPIC POROUS MEDIUM CONTAINING AN ISOLATED SPHERICAL CAVITY (For The Representative Case $\beta = 1000$)

B30021